Symmetries and Bifurcations in Timed Continuous Petri Nets

Von der Fakultät für Elektrotechnik,
Informatik und Mathematik
der Universität Paderborn
zur Erlangung des akademischen Grades
Doktor der Naturwissenschaften
– Dr. rer. nat. –
genehmigte Dissertation

von

Anna-Lena Meyer

Paderborn, 2012

Gutachter: Prof. Dr. Michael Dellnitz
Universität Paderborn

Prof. Dr. Manuel Silva
Universidad de Zaragoza

Acknowledgments

I would like to thank the numerous people who, during the last years, made this work possible or more enjoyable. First and foremost, I would like to thank my supervisor Prof. Dr. Michael Dellnitz who brought me in contact with this interesting field of research and who gave me the opportunity to write this thesis at the Institute for Industrial Mathematics. I'm indebted to him for his support and the encouragement to go my own way in the scientific world.

I would like to thank Prof. Dr. Manuel Silva from the University of Zaragoza for giving me the chance to stay with his group in 2010 and for pointing interesting examples to me. I remember many fruitful discussions where he shared the "engineer's view" on the topic with me. I also thank him for serving as a reviewer for this thesis. Thanks also to Prof. Dr. Cristian Mahulea and Prof. Dr. Jorge Júlvez and their colleagues for scientific discussions and for receiving me warmly at the University of Zaragoza.

I enjoy working at the Chair of Applied Mathematics, being surrounded by a lot of people that I admire for their brains as well as for their hearts. In particular Dr. Mirko Hessel-von Molo, Sebastian Hage-Packhäuser, and Kathrin Flaßkamp helped me to overcome many mathematical difficulties. I thank them and all my colleagues and former colleagues for discussions on scientific and nonscientific topics and for technical and administrative support, including Tanja Bürger, Dr. Roberto Castelli, Dr. Alessandro Dell'Aere, Dr. Laura Di Gregorio, Christian Horenkamp, Marianne Kalle, Dr. Stefan Klus, Dr. Giorgio Mingotti, Jun.-Prof. Dr. Sina Ober-Blöbaum, Dr. Pierpaolo Pergola, Dr. Marcus Post, Prof. Dr. Robert Preis, Maik Ringkamp, Marcel Schwalb, Stefan Sertl, Mariusz Slonina, Simon Sonntag, Bianca Thiere, Robert Timmermann, Dr. Katrin Witting, and Anna Zanzottera. I furthermore want to express my gratitude to my friends who read this manuscript and helped me to improve it.

This list would not be complete without special thanks to my parents and my sister. I could always rely on their support and motivation, in particular in phases of doubt. I am grateful for their love and their encouragement. Finally, I thank Philipp — for a number of things.

Abstract

Petri nets are a popular modeling paradigm for discrete event dynamic systems, that allow to model concurrency and synchronization. Continuous Petri nets have been introduced as a relaxation in order to deal with the state explosion problem that typically appears in discrete systems. In this thesis, timed continuous Petri nets under infinite server semantics (TCPN) are analyzed. They are represented by a continuous piecewise linear system with polyhedral regions. A special focus is on the relation between the structure of the underlying net and the system's dynamics, in particular with respect to symmetries and bifurcations.

Symmetries in timed continuous Petri nets are defined as graph automorphisms of the underlying directed, vertex- and edge-labeled graph. These symmetries are shown to appear also in the associated piecewise linear system which turns out to be equivariant with respect to the action of a symmetry on the marking space. It is furthermore shown that symmetries in any continuous piecewise linear system come with a permutation of the regions with linear dynamics, which is induced by the corresponding group action, and similar system matrices for equivalent regions, just as in the case of TCPNs. Symmetries imply the existence of flow-invariant fixed-point subspaces. A reduction technique is proposed that reduces the associated piecewise linear system making use of these and other flow invariant (affine) subspaces. This idea is then taken further in order to obtain a reduction technique which generates a smaller TCPN from the original one by removing symmetries.

In addition, parameter-dependent TCPNs are investigated. It has been observed that performance indicators of TCPNs may decrease discontinuously if firing rates of transitions are increased. This phenomenon is explained by discontinuity-induced bifurcations, which may occur when a steady state hits a boundary between regions upon variation of a bifurcation parameter.

Keywords: continuous Petri net, piecewise linear system, symmetry, equivariant dynamics, reduction technique, discontinuity-induced bifurcation

Zusammenfassung

Petrinetze sind ein beliebter Formalismus für ereignisdiskrete Dynamische Systeme, die die Modellierung von Nebenläufigkeit und Synchronisation ermöglichen. Kontinuierliche Petrinetze stellen eine Relaxierung dar, um dem Problem der Zustandsraumexplosion zu begegnen, das typischerweise in diskreten Systemen auftritt. In dieser Arbeit werden kontinuierliche, zeitbehaftete Petrinetze, sogenannte „timed continuous Petri nets under infinite server semantics“ (TCPN) analysiert. Sie sind durch ein kontinuierliches, stückweise lineares System mit polyedrischen Regionen gegeben. Das Hauptaugenmerk liegt auf der Beziehung zwischen der Struktur des zu Grunde liegenden Netzes und der Systemdynamik, insbesondere in Bezug auf Symmetrien und Verzweigungen.

Symmetrien in kontinuierlichen, zeitbehafteten Petrinetzen werden durch Graphautomorphismen des gerichteten Graphen mit gewichteten Knoten und Kanten beschrieben. Es wird gezeigt, dass sich diese Symmetrien im zugehörigen stückweise linearen System widerspiegeln, das äquivariant bezüglich der Gruppenwirkung einer Symmetrie auf den Markierungsraum ist. Es wird außerdem gezeigt, dass Symmetrien in beliebigen kontinuierlichen stückweise linearen Systemen mit einer von ihrer Gruppenwirkung induzierten Permutation ihrer Regionen und ähnlichen Systemmatrizen für äquivalente Regionen einhergehen, ebenso wie im Fall von TCPNs. Symmetrien implizieren die Existenz flussinvarianter Fixpunktunterräume. Eine Reduktionstechnik wird entwickelt, die das zugehörige stückweise lineare System reduziert, indem sie diese und andere invariante (affine) Unterräume nutzt. Darauf basierend wird eine Reduktionstechnik entwickelt, die ein kleineres kontinuierliches Petrinetz vom ursprünglichen großen Netz erzeugt, in dem Symmetrien beseitigt sind.

Zudem werden parameterabhängige TCPNs untersucht. Es ist bekannt, dass Leistungsindikatoren für TCPNs diskontinuierlich abfallen können, wenn die Feuerraten von Transitionen erhöht werden. Dieses Phänomen wird mit Hilfe von diskontinuierlichen Verzweigungen erklärt, die auftreten können, wenn ein Gleichgewichtspunkt unter Variation des Verzweigungsparameters auf den Rand einer Region trifft.

Stichworte: Kontinuierliches Petrinetz, stückweise lineares System, Symmetrie, äquivariante Dynamik, Reduktionstechnik, diskontinuierliche Verzweigung

Contents

List of Figures

1

Introduction

Petri nets are a popular modeling paradigm for discrete event systems. Areas of application range from hardware systems and communication protocols to manufacturing systems. This thesis studies dynamical properties of timed continuous Petri nets with infinite server semantics which are mathematically described by continuous piecewise linear systems. A lot is known about their analysis and control. However, there remain many open questions concerning their dynamics. Among those, this work focuses on symmetries and bifurcations. It is illustrated how symmetries affect the dynamics of timed continuous Petri nets with infinite server semantics and how this knowledge can be used to obtain reduced models. Reductions are performed both in order to reduce the computational effort and to have smaller, more manageable models. Moreover, discontinuities of performance indicators upon variation of a parameter are explained in terms of discontinuity-induced bifurcations that occur at points where the vector field is nonsmooth. This chapter introduces the central ideas and concepts this thesis is based upon, followed by a description of the thesis outline together with a short summary of the contributions of each chapter.

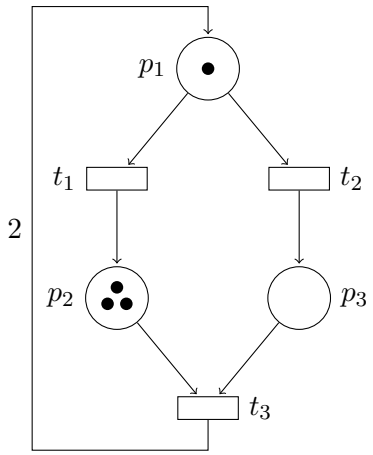

Figure 1.1: A simple Petri net with three nodes p_1, p_2, p_3 and transitions t_1, t_2, t_3. The weight of the arc (t_3, p_1) is equal to 2. All other arc weights are 1. Place p_1 contains one token and place p_2 contains three tokens.

Discrete, Continuous, and Hybrid Petri Nets

Petri nets provide a uniform environment for modeling, formal analysis, and design of discrete event systems [ZZ94]. They allow to model how events can occur concurrently, conflict with each other and depend on each other. They go back to the work of Carl Adam Petri [Pet62] and have been an active area of research since with a considerable number of applications to real-world problems in various areas. With the great variety of applications came different requirements on the formalism. For this reason, numerous variants of Petri nets have been developed. They all have in common that they provide a graphical representation of the modeled system by a graph with two types of nodes, namely places and transitions, and directed arcs between them. An example can be seen in Figure 1.1 where circles represent places and rectangles represent transitions.

A number of tokens is assigned to each place. This is called a *marking* of the net and describes the current state of the system. In high-level Petri nets, e.g., colored Petri nets, generalizations of tokens are used. A change of the marking occurs if a transition fires, i.e., tokens are removed from its input places and at the same time new tokens are added to its output places. Even though this formalism is originally not equipped with any notion of time, over the last decades time has been included

in various Petri net formalisms. This has turned out to be particularly useful, e.g., for the computation of performance indicators such as the throughput or average usage of a device.

The analysis of a Petri net traditionally requires the enumeration of markings that can be reached from an initial marking by firing of transitions (respecting the firing rules of the chosen Petri net formalism). A typical problem is that the number of reachable discrete markings can be extremely high even for small nets. The number may even be exponential in the number of nodes of the net [Val98]. For this reason, continuous Petri nets have been introduced by David and Alla [DA87]. The idea is that in systems with large markings, these can be approximated by nonnegative real numbers. An example is a manufacturing system where places represent buffers of material or semifinished products and transitions represent the machines in between which process the goods. If the amount of material in the system is large, it may be acceptable to use real markings as an approximation.

In fact, there exist many systems where timed continuous Petri nets provide an excellent approximation of performance indicators of timed discrete Petri nets even if the number of tokens in the system is small or even restricted to 0 and 1. Hybrid Petri nets have been suggested for systems in which not all integrality conditions can be relaxed. They contain discrete and continuous nodes and combine discrete and continuous dynamics [DA05, DFGS08b].

In this thesis, *timed continuous Petri nets with infinite server semantics* are studied. The marking is given by a vector $m \in \mathbb{R}_{\geq 0}^{|\mathcal{P}|}$ where $|\mathcal{P}|$ is the number of places. Its evolution over time is described by

$$\dot{m} = F(m), \quad m(0) = m_0$$

where F is a piecewise linear continuous vector field with polyhedral regions [SR02, SJMV11]. The partition into polyhedral regions is due to the fact that a transition may have more than one input place and its throughput is restricted by the smallest weighted marking of its input places. The focus of this work is on obtaining a deeper insight into the dynamic behavior of such a timed continuous Petri net with respect to the structure of the underlying directed, vertex- and edge-labeled graph.

Symmetries in Petri Nets and Differential Equations

Many systems to be modeled exhibit some kind of symmetry such as identical components or subprocesses coupled symmetrically. Such symmetries will usually also be present in the resulting Petri nets. Examples from the literature on discrete Petri nets are, for example,

- parallel production lines that share common resources like robots or buffers (see [Abe90, p. 24] and [MRRS08, p. 12]),
- protocols with symmetrically coupled agents (see [Sch00a, p. 586]), a famous example being the classic dining philosophers system (e.g., in [Val94]),
- transport by a container crane where loading and unloading correspond to identical abstract processes (see [Abe90, p. 108]),
- a multiprocessor computer system that consists of multiple copies of components which are coupled symmetrically (see [ACB84, p. 196]).

Formally, a symmetry of a Petri net is a permutation of its nodes that respects the node type and arcs. Depending on the chosen Petri net formalism, arc weights and inscriptions to nodes might also have to be preserved by the permutation [Sch00a]. Symmetries are graph automorphisms of the underlying directed graph. They have been used in discrete Petri nets to work with a reduced set of reachable markings in the analysis by considering only equivalence classes of markings [Sta91].

For continuous Petri nets, symmetries have not been studied prior to this work. However, it is not surprising that such symmetries are also reflected in the associated piecewise linear system. We prove that F is equivariant with respect to the action of the symmetries, i.e., if S_σ is the permutation matrix associated with the permutation of places of a symmetry, then

$$F(S_\sigma m) = S_\sigma F(m).$$

Equivariant dynamics are well known in the area of nonlinear smooth dynamical systems [GSS88, GS03]. Symmetries appear in many dynamical systems modeling real world phenomena. They can appear due to the system geometry or simplifying modeling assumptions. It is well known that in systems with symmetries, the action

of any element of the symmetry group maps trajectories to trajectories. All states along a trajectory have the same isotropy subgroup, i.e., a solution may not "lose" or "gain" symmetry over time. This implies the existence of flow-invariant sets. Symmetric systems often exhibit dynamical phenomena which are nongeneric in systems without these symmetries. Therefore, the knowledge of a system's symmetry is vital in order to obtain a profound understanding of its dynamical properties.

Reduction Techniques for Petri Nets

Various reduction and transformation rules for Petri nets have been developed over the last decades. Since firing in Petri nets follows rules which are local to the transitions, the rules usually consist in the identification of local structures and local transformations. Modifications of the net comprise, for example, the fusion of nodes or the removal of entire subnets such that relevant properties (liveness, boundedness, etc.) are preserved. Unfortunately, these rules are usually restricted to a specific Petri net formalism or net class (e.g., nets where all arc weights are equal to one). In particular, it is rarely possible to apply rules for untimed Petri nets to those which explicitly model time.

In discrete Petri nets, symmetries have been used to reduce the complexity of the analysis. They have also been used in [ADFN99] for a reduction of the net in the way that if a net contains several identical subnets, all but one can be removed. However, the restrictions both on the structural properties of the subnet and on the coupling of the subnets to the remaining net are very strict. In this work, a novel structured procedure for (i) the reduction of the piecewise linear system associated to a timed continuous Petri net with infinite server semantics to flow-invariant fixed-point sets and (ii) a reduction of the net itself by removing redundancies induced by the symmetries are presented. Since symmetries in these nets haven not been studied before, neither of the two approaches can be found in the literature. However, for the reduction of the net itself some examples are known. Consider, for example, the two nets in Figure 1.2 modeling a multi-computer programmable logic controller from [ŽS10]. The three identical subnets in the net on the left hand side, which correspond to three identical computers, are replaced by a single subnet. Furthermore, the weight of the output arc of $\tilde{t}_2$ is adapted. In this thesis, a general procedure for such

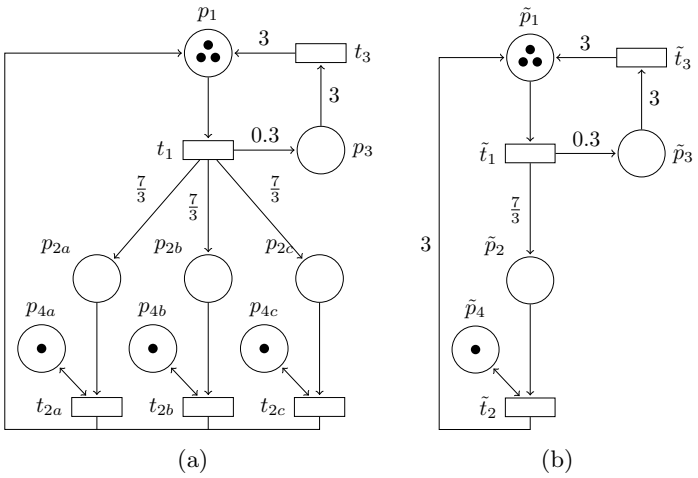

Figure 1.2: Original and reduced model of a multi-computer programmable logic controller (adapted from [ŽS10]).

a reduction is developed and its correctness is proved. The reduction to fixed-point sets is embedded in a more general reduction procedure to flow-invariant (affine) subspaces.

Bifurcations in Piecewise Smooth Systems and Parameter-Dependent Petri Nets

Many dynamical systems in physics, engineering, social sciences, etc. depend on some parameters which can either change or are not known precisely. Roughly speaking, if the character of a system's solutions suddenly changes as a parameter is varied, we call this a bifurcation. Well-known examples that occur in smooth systems are saddle-node, pitchfork, and Hopf bifurcations [GH83, Wig90, GSS88]. In systems where the evolution is not everywhere smooth, new types of bifurcations may arise if invariant sets interact with subsets of the phase space where the system is nonsmooth. Such bifurcations are called discontinuity-induced.

Discontinuity-induced bifurcations have been studied in the context of piecewise smooth dynamical systems [BCBK08]. These are systems with a partition of the

phase space such that the system is smooth in each region but nonsmooth on some manifolds separating the regions. Many examples of such systems can be found in electrical and mechanical systems where discontinuities are introduced by saturation, backlash, or impact but also in mathematical biology and systems in the social and financial sciences.

One of the simplest examples of piecewise smooth dynamical systems are piecewise linear systems such as those describing the dynamics of timed continuous Petri nets with infinite server semantics. In these nets the performance (in terms of the throughput of the transitions) usually increases when the firing rates, which are associated to the transitions, are increased. As an example, consider a Petri net modeling a manufacturing system such that its places correspond to buffers of material and the transitions to machines processing it. The replacement of a machine by a faster one is modeled by an increase of a firing rate and, intuitively, the performance of the system should increase. However, there exist continuous Petri nets where, for specific values of the firing rates, the throughput of the transitions suddenly drops. This phenomenon has not been explained yet. In this thesis, such jumps in the throughput are identified with discontinuity-induced bifurcations. They occur when the steady state marking, which depends on the firing rate, hits a boundary between regions of the piecewise linear system and loses hyperbolicity. Such bifurcations affect the robustness of the system with respect to a variation of firing rates and can be critical for control issues.

Contributions and Structure of this Thesis

In this thesis, the dynamics of timed continuous Petri nets with infinite server semantics is studied with respect to the net topology. After an introduction to the model, this is done with a special focus on symmetries and bifurcations. It has to be mentioned that parts of this thesis grew out of the publications [MD09, MDH11, MS12, Mey12], for each of which the author has given a substantial contribution.

The thesis is structured as follows.

Chapter 2 introduces the Petri net model that is used throughout this thesis. As in the historical development, it starts with a description of the components and

discrete dynamics of place/transition nets and stochastic Petri nets. Thereafter, the state explosion problem, which is typical for such discrete event systems, is illustrated. This motivates the introduction of timed continuous Petri nets that relax integrality constraints on the markings and firings. In particular, timed continuous Petri nets with infinite server semantics (cf. [SR02]) are introduced. They are identified to be piecewise linear systems with polyhedral regions as observed in [MRRS08]. It is well-known that some of these regions which are naturally deduced from the underlying Petri net are redundant. It is proved that such redundant configurations are always due to choices in the net structure. The chapter ends with a summary of results on the dynamics of such continuous Petri nets from the literature.

In **Chapter 3** a definition of symmetry in timed continuous Petri nets is established and compared with symmetries in place/transition nets. For the discrete case algorithms for the computation of such symmetries have been developed. These can also be used for timed extensions and are therefore briefly described. Symmetries in the net structure and timing are shown to be reflected in the induced piecewise linear system. More precisely, symmetries bring about a permutation of configurations and, what is more, equivariant dynamics. The piecewise linear system is equivariant with respect to the group action of certain permutations of nodes on the marking space. This allows to apply well-known results on properties of general equivariant dynamical systems such as the existence of flow-invariant fixed-point sets which are also summarized in this chapter. Finally, general equivariant piecewise linear systems are studied. The permutations of regions observed for symmetric Petri nets appear here as well.

Chapter 4 illustrates several reduction techniques for timed continuous Petri nets. First, a summary of traditional reduction approaches is given. They concentrate on local graph transformations that preserve certain properties like liveness or boundedness. Second, an algebraic reduction technique for the piecewise linear system associated with a Petri net system is developed. It makes use of the fact that invariants of the Petri net and symmetries induce invariant (affine) subspaces, fixed-point subspaces in the latter case. This reduction consists in an (affine) linear transformation of the system that reduces the dimension of the associated dynamical system. It is demonstrated for $\mathcal{P}$-invariants, symmetries, and the joint case. A proof is provided that the original system and the reduced system are equivalent in the sense

that trajectories of one system can be transformed into trajectories of the other by a simple linear transformation.

The reduction with respect to fixed-point sets is then taken a step further. Not only the corresponding piecewise linear system is reduced but also the net itself is reduced by removing redundancies introduced by symmetries. More precisely, a smaller net is constructed whose nodes represent equivalence classes of nodes of the original net. The procedure includes the construction of the new net structure, the choice of arc weights, and an adaption of firing rates associated with the transitions of the reduced net. The method works under mild restrictions on unequal conflicts. In contrast to the reduction that affects only the piecewise linear system, a reduction of the net itself is beneficial during the modeling process and allows to apply further transformations which are known for Petri nets.

Parameter-dependent timed continuous Petri nets are the topic of research that **Chapter 5** deals with. Here, the steady states and throughput of timed continuous Petri nets are studied in dependence on the firing rate of one transition. For four examples, discontinuities in these values are explained in terms of discontinuity-induced bifurcations. These bifurcations are introduced and characterized for the case of nonsmooth but continuous systems following the works of [BCBK08, Sim10]. However, the bifurcations observed in timed continuous Petri nets are not generic in general piecewise smooth systems as they involve more than two regions of smooth dynamics and involve nonhyperbolic equilibria. Finally, the special role of so-called critical regions, which appear together with conflicts, is explained in terms of their sensitivity towards variations of firing rates.

The thesis closes with a summary of the results and a discussion about open problems and possible future directions of research in **Chapter 6**.

2

From Discrete to Continuous Petri Nets

Petri nets have been used successfully to model and analyze systems that exhibit concurrency, synchronization, or conflicts. Their name goes back to the thesis "Kommunikation mit Automaten" of Carl Adam Petri [Pet62]. Since then, hundreds of different definitions and extensions with numerous features and analysis methods for different purposes and application areas have been proposed in the literature [DJ01, PE01]. In this thesis, *timed continuous Petri nets with infinite server semantics* as defined in [SR02] are considered. They have been introduced to overcome the state explosion problem which typically appears in highly populated models. The structure of continuous Petri nets is the same as that of discrete nets and they can — under some assumptions — be used as approximations for the performance analysis of discrete systems. This chapter starts with an introduction to discrete Petri nets. In Section 2.2, timed continuous Petri nets with infinite server semantics (TCPNs) are introduced, followed by their representation as piecewise linear systems in Section 2.3, where also the existence of redundant regions is discussed. The chapter ends with a summary of known facts about the dynamics of TCPNs.

2.1 Discrete Petri Nets

2.1.1 The Petri Net Modeling Paradigm

In their paper "What Is a Petri Net? Informal Answers for the Informed Reader" [DJ01], Desel and Juhás worked out those aspects of Petri nets which are common to at least most models.[1] According to this work, Petri nets are characterized by being a graphical notion and at the same time a precise mathematical notion. They are bipartite graphs with two kinds of nodes interpreted as places and transitions. Graphically, places are represented as circles and transitions as boxes or bars. A global state of the net is constituted by the discrete local states of all places. A behavior is then assigned to the net by enabling and firing rules that depend on and affect the places in the vicinity of a transition. In this section place/transition nets are defined.

Formally, the structure of a place/transition net[2] can be described by a tuple

$$\mathcal{N} = \langle \mathcal{P}, \mathcal{T}, F, W \rangle \tag{2.1}$$

where $\mathcal{P} = \{p_1, \ldots, p_{|\mathcal{P}|}\}$ and $\mathcal{T} = \{t_1, \ldots, t_{|\mathcal{T}|}\}$ are disjoint, finite[3] sets of *places* and *transitions*, respectively. $F \subset (\mathcal{P} \times \mathcal{T}) \cup (\mathcal{T} \times \mathcal{P})$ is the set of directed arcs. The weight function $W : F \to \mathbb{N}$ assigns a weight to the arcs. We call $\langle \mathcal{P}, \mathcal{T}, F \rangle$ the underlying *net graph* (cf. [ISO04]). For a node $v \in \mathcal{P} \cup \mathcal{T}$ we denote by ${}^\bullet v = \{u : (u, v) \in F\}$ and $v^\bullet = \{u : (v, u) \in F\}$ the set of its *input nodes* and *output nodes*, respectively.

[1] Due to the significant number of different Petri net classes, there are attempts to scientifically unify the different concepts and approaches. Suggestions on how this could be done can be found in [EJPR01]. In terms of formal definitions, the standard *ISO/IEC 15909-1:2004 Software and system engineering - High-level Petri nets - Part 1: Concepts, definitions and graphical notation* has been developed as a basis for the development of a transfer format for High-level Petri nets. This thesis follows this standard to a great extent. The main difference is that in this thesis, there is a strict distinction between the net structure and the marking evolution. This is done in order to interpret Petri nets as dynamical systems. In contrast, the ISO/IEC 15909-1:2004 standard considers the initial marking to be part of the net.

[2] With such a 4-tuple most low-level Petri nets can be described, not only place/transition nets. If nets without arc weights are considered, W is omitted. Some Petri net formalisms use inhibitor arcs as an additional type of arcs. Such nets are not considered in this thesis.

[3] In general, it is not necessary to restrict to finite sets of places and transitions, respectively. It is usual though to say that the number of arcs from or to a node is finite. In this thesis, only nets with finitely many nodes are considered. This allows to describe the arcs by matrices which is the notation primarily used in this work.

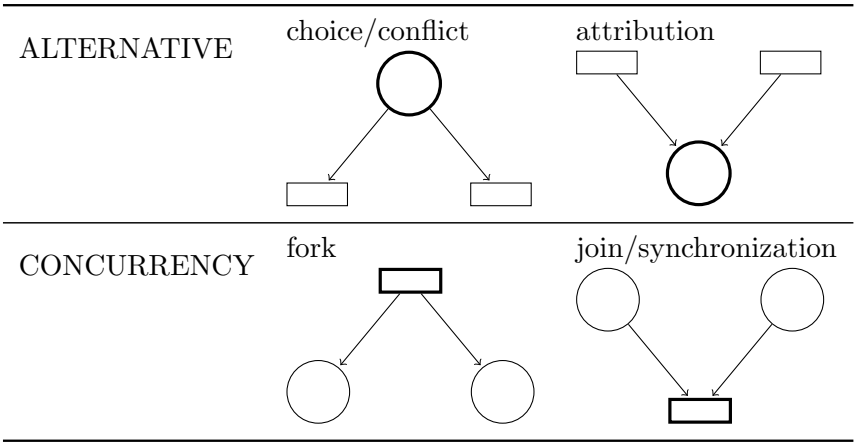

Table 2.1: Elementary conjunctions in Petri nets [Abe90, p. 28].

We assume that each transition has got at least one input place. The possible elementary conjunctions are stated and named in Table 2.1. In the case of choices, we say that transitions are in *conflict relation* if they share at least one common input place. Depending on the conjunctions and the arc weights, a net is

- *join-free* or *choice-free* if is does not have any joins or choices, respectively,
- *fork-attribution* if it is both join-free and choice-free,
- *ordinary* if $W(u, v) = 1$ for all arcs $(u, v) \in F$,
- *pure* if there exist no p and t such that $(p, t) \in F$ and $(t, p) \in F$,
- a *state machine* if $|{}^\bullet t| = |t^\bullet| = 1$ for all $t \in \mathcal{T}$,
- *equal conflict* if for any transitions $t, t' \in \mathcal{T}$ with ${}^\bullet t \cap {}^\bullet t' \neq \emptyset$, it holds that ${}^\bullet t = {}^\bullet t'$ and $W(p, t) = W(p, t')$ for all $p \in {}^\bullet t$.

These and more such classes of Petri nets can be found in, e.g., [Mur89, SJMV11].

To each place $p \in \mathcal{P}$ a number of tokens is assigned, the *marking*. The global state of the net is then given by the marking vector $m = (m_{p_1}, \ldots, m_{p_{|\mathcal{P}|}})^T \in \mathbb{N}_0^{|\mathcal{P}|}$. This state may change due to firing of a transition which is a local action in the net. First, the transition needs to be enabled. For this, the marking of each input place has to be at least as big as the weight of the respective connecting arc. An enabled transition may then fire, changing the values of its adjacent state variables. Tokens are removed from input places while the number of tokens in the output places is increased according to the arc weight. Alternatively, firing can be interpreted by

the *token flow paradigm* where "tokens flow with infinite speed from place to place, sometimes they mutate, join or split in transitions" [DJ01].

In order to describe the change of the state mathematically, we introduce matrices $Pre, Post \in \mathbb{N}^{|\mathcal{P}|\times|\mathcal{T}|}$ where — assuming a fixed ordering of the nodes — $Pre_{p,t} = W(p,t)$ and $Post_{p,t} = W(t,p)$, respectively.[4] If $(p,t) \notin F$ ($(t,p) \notin F$), then $Pre_{p,t} = 0$ ($Post_{p,t} = 0$). As it is possible to reconstruct F and W completely from these matrices, a place/transition net can alternatively be given by the tuple $\langle \mathcal{P}, \mathcal{T}, Pre, Post \rangle$. We define the *token flow matrix*

$$C := Post - Pre.$$

A transition $t \in \mathcal{T}$ is *enabled* in a marking m if $m_p \geq Pre_{p,t}$ for all $p \in \mathcal{P}$. If t *fires*, then $W(p,t)$ tokens are removed from all input places $p \in {}^\bullet t$ and $W(t,p)$ tokens are added at all output places $p \in t^\bullet$. The resulting state is

$$m' = m + Ce_t$$

where $e_t \in \mathbb{R}^{|\mathcal{T}|}$ is a unit vector. We say that m' is *reachable* from m and write $m[t > m'$. When several transitions fire sequentially, we obtain an *occurrence sequence*.

A Petri net $\mathcal{N}$ and an initial marking m_0 form a *Petri net system* $\langle \mathcal{N}, m_0 \rangle$. The set of all markings reachable from m_0 through occurrence sequences is the *reachability set* $RS(\mathcal{N}, m_0)$. Let $v \in \mathbb{N}_0^{|\mathcal{T}|}$ be a vector that denotes for each transition how often it fires during the occurrence sequence starting in m_0, then the sequence results in the marking

$$m = m_0 + Cv. \tag{2.2}$$

This is known as the *fundamental equation*. The vector v is called the *firing count vector* of the corresponding occurrence sequence. This behavior of place/transition nets does not include any notion of time. Neither is the behavior deterministic in the sense that every marking has got a unique subsequent marking. If several transitions are enabled with respect to one marking, any one of them may fire.

[4] In order to keep the notation simple, the form $Pre_{p,t}$ is used to denote $Pre_{i,j}$ with $p_i = p$ and $t_j = t$ and analogously for $Post$. This is possible because of the fixed ordering of the nodes. Likewise, we denote by e_t the $|\mathcal{T}|$-dimensional j-th unit vector if $t_j = t$. In this thesis, this notational principle applies to all matrices or vectors with nodes as indices.

Moreover, an enabled transition may fire but does not have to. Thus, one wants to know which occurrence sequences are "accepted" by the Petri net. The sequence of markings resulting from subsequent firings is traditionally represented by graphs. The best known examples of such graphs are *reachability graphs* which are made up by all markings reachable from m_0 and arcs labeled with the transition whose firing cause the change of the marking. If the set of reachable markings is not finite, *coverability graphs* provide an over-approximation of the reachability set by using macro-markings representing sets of possible markings.

From the fundamental equation, invariants can be computed that allow to derive some structural properties. Let $y \in \mathbb{Z}^{|\mathcal{P}|}$ such that $y^T C = 0$ and let v be the firing count vector of an arbitrary occurrence sequence firable from the initial marking m_0, then

$$y^T m = y^T m_0 + y^T C v = y^T m_0. \tag{2.3}$$

This means that the weighted number of tokens remains constant throughout any occurrence sequence. We call y a *$\mathcal{P}$-invariant* of $\mathcal{N}$ and a *$\mathcal{P}$-semiflow* if y is nonnegative [Bal07]. We furthermore define the *support* of a $\mathcal{P}$-semiflow y as $\text{supp}(y) = \{p \in \mathcal{P} : y_p > 0\}$. A semiflow is *minimal* if its support is not a proper superset of the support of any other semiflow and the greatest common divisor of its elements is one.

Let us assume that all places of a Petri net are contained in the support of $\mathcal{P}$-semiflows. Then, the maximum number of tokens in all places is finite for any initial marking and occurrence sequence and the net is *structurally bounded*. If there exists a single $\mathcal{P}$-semiflow that covers all places, the net is said to be *conservative*. $\mathcal{P}$-invariants are used in Section 4.2.2 in order to reduce the dimension of the state space of the continuous model.

Similar invariants can be defined for transitions. A *$\mathcal{T}$-invariant* is a vector $x \in \mathbb{Z}^{|\mathcal{T}|}$ such that $Cx = 0$. If $x \geq 0$, it is called *$\mathcal{T}$-semiflow*. It corresponds to the firing count vector of an occurrence sequence that does not change the marking, i.e., $m = m_0 + Cx = m_0$. Attention should be paid to the fact, that the existence of a $\mathcal{T}$-semiflow is just a necessary condition for such a sequence to exist as it depends on the initial marking if the transitions are enabled. A net with a $\mathcal{T}$-semiflow $x > 0$ is called *consistent*.

The identification of invariants is just one example of analysis techniques that have been proposed for Petri nets. Most of them are well supported by computer tools. Following [DJ01], we just state briefly the most prominent types of techniques. A first step after the modeling itself is the *validation* of the model in which the model is checked against the modeled system or against desired properties of the system. Validation is used to discover design problems and errors, e.g., it might be detected that some required event may not occur in the system. If a model is valid, its behavior is assumed to be related to the behavior of the original system in the required way. Validation often uses *simulation*. Here, different occurrence sequences are generated and analyzed. Usually only a part of the systems' behavior can be analyzed by simulations due to the fact that Petri nets often accept an astronomical number of different occurrence sequences (cf. Section 2.1.3). The generated sequences are used for the identification of unwanted behavior or for performance evaluation. Proving by formal methods if the net satisfies a given specification is known as *verification*. The methods are typically based on the reachability graph of the net or reduced versions thereof which still provide all information necessary to decide on the concrete specification.

The analysis of Petri nets is often concerned with the detection of typical structural or behavioral properties. An example is the identification whether the net belongs to one of the net classes defined previously. Other properties of Petri net systems are:

- *Reachability*, i.e., a marking m is reachable from the initial marking m_0.
- *Reversibility*, i.e., m_0 is reachable from every marking $m \in RS(\mathcal{N}, m_0)$.
- *Boundedness*, i.e., the number of markings in each place is bounded. In general, boundedness depends on the initial marking but if a strictly positive $\mathcal{P}$-semiflow exists, it is independent of m_0.
- *Deadlock-freeness*, i.e., there is no marking reachable from m_0 such that no transition is enabled.
- *Liveness*, i.e., for every reachable marking m and every transition $t \in \mathcal{T}$ there exists an occurrence sequence containing t that can be fired from m.

Many analysis techniques use semi-decision methods. For instance, reachability of a marking m can be negated if m does not satisfy Equation (2.3).

2.1.2 Timed and Stochastic Petri Nets

In order to evaluate the performance and reliability of complex systems, timing specifications have been added to Petri nets. Petri nets were originally proposed explicitly without time and, in fact, the introduction of time leads to several difficulties in the definition of a coherent model [Chi98]. Surveys on this topic are [ABC+95, Chi98, Bal07]. The introduction of time has led to a great variety of different formalisms motivated by a number of applications in, e.g., hardware and computer architecture design and manufacturing systems. To state just one well-known example, Merlin and Faber [MF76] developed a notion of timing including maximal time delays in order to model timeouts in communication protocols. We introduce the concept of stochastic Petri nets which are a powerful formalism for the performance analysis of discrete event systems while permitting to apply various analysis techniques. Under some assumptions, performance values of Petri nets of this type can be approximated by continuous nets.

Petri nets with time add temporal specifications to the basic net model defined in the previous section. Time may be associated with places or transitions and a change of the marking may be triggered by external events or after a deterministically or stochastically determined period of time. In a stochastic Petri net (SPN), to each transition t a random firing delay is assigned, whose probability density function is exponentially distributed. The structure and the firing rule do not differ from place/transition nets. If a transition t is enabled under some marking, the time that elapses until t fires is exponentially distributed with a rate λ_t. So the average time for t to fire is $\frac{1}{\lambda_t}$.

The introduction of timing through timed transitions has been influenced greatly by concepts from Queueing Networks [Chi98]. In the terminology of this discipline, transitions are interpreted as servers and tokens in the input places represent customers at the stations. SPN formalisms differ in the queueing policies (race policy, preselection policy), server semantics (single server, k server, infinite server), and memory policies (age memory, enabling memory, reset memory). A frequently used timed formalism is that of generalized stochastic Petri nets (GSPN). They extend SPNs by the introduction of immediate transitions which fire without delay as soon as they become enabled. They are used to model the logics of the system rather

than the time-consuming activities. However, many GSPNs can be transformed into equivalent SPNs [ADFN99].

Due to the memoryless property of the exponential distribution of firing delays, an SPN is isomorphic to a continuous time Markov chain (CTMC) whose state space corresponds to the reachability set $RS(\mathcal{N}, m_0)$ and whose transition rates can be computed from the firing rates of the SPN.[5] For this reason, SPNs with exponentially distributed time delays and race policy are also known as Markovian Petri nets (cf. [VRS08, VS09]). If the net is reversible and its reachability set is finite, we can compute the steady-state probability distribution vector of the system which allows us to define a number of *performance measures* [ACB84]. Typical performance measures are the expected value for the number of tokens in a given place or the *throughput* of a transition given by its mean number of firings per unit time (cf. [BK02, pp. 133–134]). In [ABC+95, pp. 117–120], reward functions are used to define more general performance measures.

Example 2.1. The following model of a production line was published in [ZZ94]. The line consists of a buffer of raw materials, machines M_1 and M_2, robots R_1 and R_2, and two conveyors. One of the machines is subject to failure. The corresponding Petri net is shown in Figure 2.1(a) together with an interpretation of its nodes.

We are interested in the utilization of machine M_1 and the system's average production rate which in this net is the throughput of transition t_3. In order to compute these values, we construct the reachability graph and the corresponding Markov chain (see Figures 2.1(b)-(c)). From the Markov chain we can compute the steady state probability vector which is $\begin{pmatrix} 0.05 & 0.4 & 0.5 & 0.05 \end{pmatrix}^T$. Machine M_1 is working if place p_2 is marked. This corresponds to the marking vector m_1. The system is in this state with probability 0.4. The expected utilization of the machine is therefore 40%. Similarly, we may compute how many final products leave the line per time unit. Transition t_3 fires every time a product is completed. This transition is enabled in marking m_2 which has a probability of 0.5. Together with the firing rate of t_3 we obtain a production average of $0.5 \cdot 4 = 2$ workpieces per time unit. ♢

[5] A definition of the corresponding isomorphism can be found in [Mol82]. For the case of single servers, the computation of transition rates is described in detail in [ABC+95, BK02]. For infinite server semantics, the discrete enabling degrees (that is how often a single transition may fire simultaneously at a given marking) have to be taken into account.

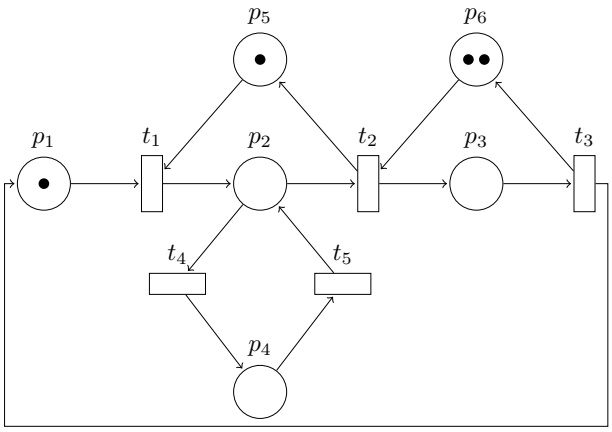

Node	Interpretation (and firing rate)
p_1	Workpieces and pallets available
p_2	Machine M_1 processing a workpiece
p_3	Workpiece ready for processing at M_2
p_4	M_1 in repair
p_5	M_1 available
p_6	Conveyor slots available
t_1	Loading involving M_1 and R_1 ($\lambda_{t_1} = 40$)
t_2	Processing and unloading involving M_1 and R_1 ($\lambda_{t_2} = 50$)
t_3	Loading, processing, and unloading involving M_2 and R_2 ($\lambda_{t_3} = 4$)
t_4	M_1 breaks down ($\lambda_{t_4} = 0.5$)
t_5	M_1 is repaired ($\lambda_{t_5} = 4$)

(a) The stochastic Petri net system

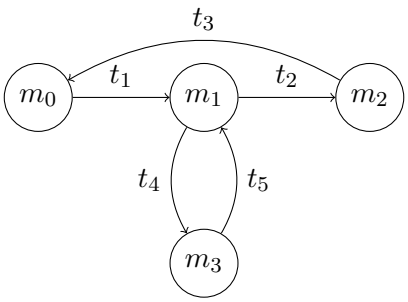

(b) The reachability graph

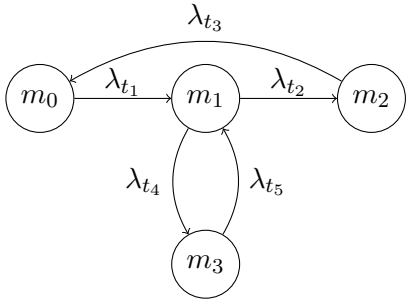

(c) The Markov Chain

Figure 2.1: A production line modeled and analyzed with an SPN. The reachable markings are $m_0 = \begin{pmatrix}1 & 0 & 0 & 0 & 1 & 2\end{pmatrix}^T$, $m_1 = \begin{pmatrix}0 & 1 & 0 & 0 & 0 & 2\end{pmatrix}^T$, $m_2 = \begin{pmatrix}0 & 0 & 1 & 0 & 1 & 1\end{pmatrix}^T$, and $m_3 = \begin{pmatrix}0 & 0 & 0 & 1 & 0 & 2\end{pmatrix}^T$.

2.1.3 The State Explosion Problem

In [DJ01], it is argued that Petri nets can manage the complexity of large systems and are suited to model complex distributed systems. The number of discrete states in traditional automata often grows exponentially with the size of the system. In contrast, the global states of Petri nets are combinations of local states and the number of places and consequently the number of local states grows linearly with the size of the modeled system. Complex systems can therefore be described in a compact manner using Petri nets. However, even if the Petri net itself is relatively small, there often exist so many different runs in a simulation that it is impossible to execute them all. Similarly, analysis techniques such as reachability graphs that are based on an exploration of the state space suffer from the fact that the number of reachable states becomes extremely high very quickly, even exponentially. This is known as the *state explosion problem*. It appears in particular for heavily loaded systems, i.e., if the total number of tokens in the system is high. The computation of performance indicators using continuous time Markov chains with state space $RS(\mathcal{N}, m_0)$ might therefore be computationally expensive or even impossible.

A famous example of this effect is Dijkstra's n dining philosophers problem which is a small mutual exclusion protocol for n agents arranged as a ring (see [Sch00a, Val98]). It has got $4n$ places with a binary marking, i.e., it grows linearly with the number of philosophers. The number of reachable markings, on the other hand, is $3^n - 1$. A similar problem is that the number of reachable markings may grow quickly with the initial load of the system. An example is given in [SR07]. There, a production system with two machines and a shared buffer is studied. As many as 250 markings are reachable from m_0. If this initial marking is doubled, there exist 6 300 reachable markings. If it is multiplied by 5, even 2 159 136 states can be reached.

One approach to deal with this phenomenon is to relax integrality constraints. The basic idea is that a sufficiently large number of tokens in a place may be approximated by a nonnegative real number. Instead of the different discrete states, the evolution of the continuous marking $m \in \mathbb{R}_{\geq 0}^{|\mathcal{P}|}$ is studied. The dimension of the system is $|\mathcal{P}|$ and therefore independent of the initial marking. This has first been suggested in [DA87]. Hybrid Petri nets combining discrete and continuous markings have also been suggested in the literature [DA87, DA05, DFGS08a, DFGS08b].

2.2 Continuous Petri Nets

2.2.1 Relaxing Integrality Constraints

The first step to obtain a continuous model is to relax integrality constraints both on the marking and the amount in which a transition can be fired. To start with, we consider untimed (or autonomous) continuous Petri nets, a generalization of classic discrete place/transition nets where no time is modeled (see [RTS99]). Here, a transition t is enabled if all its input places are marked. Its *continuous enabling degree* under a marking m is

$$\text{enab}(t, m) = \min_{p \in {}^\bullet t} \frac{m_p}{Pre_{p,t}}$$

in contrast to the discrete enabling degree $\lfloor \text{enab}(t, m) \rfloor$. If t is enabled under m, it may fire in any amount $0 \leq \alpha \leq \text{enab}(t, m)$ resulting in the new marking $m + \alpha C e_t$.

Boundedness of the continuous net implies boundedness of its discrete counterpart. Furthermore, a marking is reachable in the discrete Petri net system only if it is reachable in the continuous one where the continuous reachability space is a convex set. A detailed discussion of properties of autonomous continuous Petri nets can be found in [RTS99, SR02, JRS03, RHS10, SJMV11]. The advantage over discrete nets is that they allow "the use of convex geometry and linear programming instead of integer programming, making possible the verification of some properties in polynomial time" [JRS03]. And as stated by [DFGS08a], "the design parameters in fluid models are continuous; hence, it is possible to use gradient information to speed up optimization and to perform sensitivity analysis." The approach is limited by the fact that many properties of the discrete and continuous nets are only weakly linked. For example, liveness of the continuous Petri net is neither sufficient nor necessary for liveness of its discrete counterpart.

2.2.2 Timed Continuous Petri Nets with Infinite Server Semantics

We now add a timing to continuous Petri nets and write $\langle \mathcal{N}, \lambda \rangle$ for the timed net where $\lambda = (\lambda_{t_1}, \ldots, \lambda_{t_{|\mathcal{T}|}})^T$ denotes the firing rates associated with the transitions.[6]

[6] As in the case of arc weights, if no firing rate is given in the graphical representation of a TCPN, the rate is equal to 1.

Starting point is the fundamental equation $m = m_0 + Cv$ of the underlying discrete net. Now, the marking changes continuously due to a continuous firing flow that depends on the current marking. The evolution of the *continuous marking* $m = (m_{p_1}, \ldots, m_{p_{|\mathcal{P}|}})^T \in \mathbb{R}_{\geq 0}^{|\mathcal{P}|}$ is of the form

$$\dot{m} = Cf(m) \tag{2.4}$$

where $f(m) \in \mathbb{R}_{\geq 0}^{|\mathcal{T}|}$ is the *flow* of the transitions for a marking m (cf. [DA05]). The flow through the fluidified transitions has been defined in several ways in the literature. For a detailed discussion on this question see [DA93, SR04, GG04, MRS06, MRS09, LL11, SJMV11]. We now consider the continuous evolution of the marking of *timed continuous Petri nets under infinite server semantics*[7] (TCPN). The term "infinite servers semantics", which stems from queueing theory, means that the flow of a transition is not upper bounded and only restricted by the actual marking of its input places. TCPN systems can serve as an approximation of the expected value of the marking of the corresponding Markovian Petri net [VRS08, SJMV11].

Under infinite server semantics, the flow of each transition $t \in \mathcal{T}$ is the product of the firing rate and the current continuous enabling degree. It is given by

$$f_t(m) = \lambda_t \operatorname{enab}(t, m) = \lambda_t \min_{p \in {}^\bullet t} \frac{m_p}{Pre_{p,t}}. \tag{2.5}$$

If a Petri net is join-free, then $f_t(m)$ depends on the marking of its unique input place only. Thus, (2.5) can be reduced to $f_t(m) = \lambda_t \frac{m_p}{Pre_{p,t}}$ where ${}^\bullet t = \{p\}$. Hence, (2.4) is purely linear. If there are joins, the system shows a linear behavior until the input place of a transition that constrains the flow changes. The dynamics is piecewise linear.

Timed continuous Petri nets with infinite server semantics are used to approximate performance indicators of stochastic Petri nets such as the asymptotic mean marking or the throughput of a transition. In TCPNs, this corresponds to the equilibrium marking m^* — if it exists — and the flow $f_t(m^*)$ of transition t at this equilibrium (cf. [SJMV11]). In this case, we call $f^* = f(m^*)$ the *throughput vector* of the system.

[7] These server semantics are also known as *variable speed* (cf. [SJMV11]).

Let us consider again the production line from Example 2.1. From the initial marking $m_0 = \begin{pmatrix}1 & 0 & 0 & 0 & 1 & 2\end{pmatrix}^T$, the system converges to a steady state $m^* = \begin{pmatrix}0.05 & 0.4 & 0.5 & 0.05 & 0.55 & 1.5\end{pmatrix}^T$ with flow $f^* = (2\ 2\ 2\ 0.2\ 0.2)^T$. In fact, the resulting performance measures are the same as for the discrete net. The utilization of 40% of machine M_1 follows from the average marking of 0.4 of place p_2. The flow of transition t_3 in steady state is 2, exactly as the throughput in the discrete case.

It is important to note that the continuous net is not affected by the state explosion problem. Independent of the initial marking and the size of the corresponding discrete reachability set, the continuous approximation always requires to solve a system of differential equations of dimension $|\mathcal{P}|$. Timed continuous Petri nets can be conveniently simulated with the Matlab toolbox *SimHPN* which, besides the simulation, computes invariants and throughput bounds (cf. [JMV12]).

Continuous Petri nets have been reported to result in good approximations of discrete Markovian Petri nets in many applications. Formally, it has been shown in [VRS08] that the expected marking of an SPN is approximated by the corresponding continuous net if two conditions hold. First, the places constraining the dynamics (i.e., those that lead to the minimum value in (2.5)) do not change over time and second, all transitions of the discrete net are enabled under the markings reached with probability close to 1. Even though these conditions are by far not necessary, there exist examples where the approximation via continuous Petri nets is not satisfactory, not even for large initial markings. In [SJMV11], it is argued that in the case of ordinary join-free Petri nets the approximation by TCPNs is perfect but since this is a very small net class, this does not provide a satisfactory answer to the question which Petri net systems can be suitably approximated. This remains an active field of research. In the case of Petri nets being poorly approximated by timed continuous Petri nets with infinite server semantics, new semantics, i.e., new definitions of the flow f, are being developed [SJMV11, LL11].

For discrete Petri nets a number of subclasses have been defined in Section 2.1.1. These definitions are also valid for continuous Petri nets. In addition, there are subclasses which are of special importance in a continuous setting. The class of equal conflict nets can be extended. A net is of type *continuous equal conflict* (CEQ) if for any transitions $t, t' \in \mathcal{T}$ with ${}^\bullet t \cap {}^\bullet t' \neq \emptyset$, there exists $k > 0$ with

$Pre_{p,t} = k\, Pre_{p,t'}$ for all $p \in {}^\bullet t$. The relaxed enabling condition guarantees that all transitions in a conflict relation are still simultaneously enabled.

A Petri net is *mono-T-semiflow* if it is conservative and has a unique minimal $\mathcal{T}$-semiflow whose support contains all transitions (cf. [CCS91]). A generalization of these nets are *mono-T-semiflow reducible* nets which have been motivated by the concept of visit ratios which is classic in queueing theory (see [JRS05] for details). A net $\langle \mathcal{N}, \lambda \rangle$ belongs to this class if it is consistent, conservative, and the following system has a unique solution $v \in \mathbb{R}^{|\mathcal{T}|}$

$$\begin{cases} Cv = 0 \\ \frac{v_t}{Pre_{p,t}\lambda_t} = \frac{v_{t'}}{Pre_{p,t'}\lambda_{t'}} \text{ for all } t, t' \text{ in CEQ relation} \\ v_{t_1} = 1. \end{cases}$$

In contrast to mono-T-semiflow nets, the visit ratio v may depend on the timing. However, it is independent of the initial marking. Mono-T-semiflow reducible nets can be transformed into mono-T-semiflow nets with identical behavior through a transformation of equal conflicts.

2.3 Continuous Petri Nets as Piecewise Linear Systems

2.3.1 Definition of Piecewise Linear Systems

We have seen that timed continuous Petri nets with infinite server semantics have piecewise linear dynamics. Therefore, it seems natural to study these systems in the classic framework of piecewise linear systems which describe the mutual interaction between continuous dynamics given by ordinary differential equations and discrete modes. They are characterized by a partition of the state space into cells in which the dynamics is linear. We start with some basic definitions.[8]

[8] The definitions of polyhedral partitions to be found in the literature differ slightly from each other with respect to the borders of the regions and their dimension (cf. [GTM08, AMP95, Joh03]). Here, closed full-dimensional polyhedra are used. The reason is, on the one hand, that closed sets appear naturally when dealing with TCPNs and, on the other hand, the dimension is specified for technical reasons in order to exclude redundant degenerate cases when considering symmetries in general piecewise linear systems.

Definition 2.2. *A family of closed n-dimensional polyhedra $(X_i)_{i\in I}$, where I is a finite index set, is called a* polyhedral partition *of $X \subset \mathbb{R}^n$ if*

(i) $\bigcup_{i\in I} X_i = X$,

(ii) $\operatorname{int}(X_i) \cap \operatorname{int}(X_j) = \emptyset$ *if* $i \neq j$.

Definition 2.3. *A* piecewise linear system *(PWL) is a pair $((X_i)_{i\in I}, (A_i, a_i)_{i\in I})$ where I is a finite index set, $(X_i)_{i\in I}$ a polyhedral partition, and $(A_i, a_i)_{i\in I}$ denotes a family of maps $\mathbb{R}^n \to \mathbb{R}^n$, $x \mapsto A_i x + a_i$ ($A_i \in \mathbb{R}^{n\times n}$, $a_i \in \mathbb{R}^n$).*

The dynamics of the system is of the form

$$\dot{x} = A_i x + a_i \text{ for } x \in X_i.$$

If $a_i \neq 0$ for some index i, such systems are also known as *piecewise affine systems*. According to [CFPT04], "piecewise linear systems seem to present almost the same dynamical behavior of general nonlinear systems (limit cycles, homoclinic and heteroclinic orbits, strange attractors, ...)." The dynamics of these systems is well understood only for special low dimensional cases. However, it is possible to identify characteristics of higher dimensional piecewise linear systems stemming from continuous Petri nets due to their special structure.

We focus on continuous systems, i.e., systems where $A_i x + a_i = A_j x + a_j$ if $x \in X_i \cap X_j$. Even though the resulting vector field is nonsmooth on the boundaries, it satisfies a local Lipschitz condition. Thus, existence and uniqueness of solutions are guaranteed. For discontinuous systems this is not always the case. See [Joh03, pp. 14–20] and [IS00] for solution concepts.

2.3.2 Configurations and System Matrices

Having identified the piecewise linear structure of the system, we aim at finding a representation of the form $((X_i)_{i\in I}, (A_i, a_i)_{i\in I})$; thus, we want to find a description of the polyhedral partition and the system matrices. In [MRRS08], the notion of configuration is introduced in order to deal with the different discrete modes or cells.[9]

[9] Several definitions of configurations can be found in the literature. On the one hand, they can be defined as sets of arcs [MRRS08, MRS09] or as maps $\mathcal{T} \to \mathcal{P}$ [SR07]. In this thesis, the latter

Definition 2.4. *For a Petri net $\mathcal{N}$, a map $K : \mathcal{T} \to \mathcal{P}$ is called* configuration *if $K(t) \in {}^\bullet t$ for all $t \in \mathcal{T}$. $\mathcal{K}_\mathcal{N} = \{K_1, K_2, \ldots, K_\gamma\}$ is the set of all possible configurations of $\mathcal{N}$ where $\gamma = \prod_{t\in\mathcal{T}} |{}^\bullet t|$. A configuration K is* active *under a given marking $m \in \mathbb{R}^{|\mathcal{P}|}_{\geq 0}$ if*

$$\forall t \in \mathcal{T} : \ \frac{m_{K(t)}}{Pre_{K(t),t}} = \min_{p\in{}^\bullet t} \frac{m_p}{Pre_{p,t}} \tag{2.6}$$

and we denote by $M_K \subset \mathbb{R}^{|\mathcal{P}|}_{\geq 0}$ the set of all markings under which K is active.

These sets $M_{K_1}, \ldots, M_{K_\gamma}$ partition the state space $\mathbb{R}^{|\mathcal{P}|}_{\geq 0}$. They are closed polyhedra as for each configuration K there exists a matrix G_K such that

$$M_K = \left\{ m \in \mathbb{R}^{|\mathcal{P}|}_{\geq 0} : G_K m \leq 0 \right\} \tag{2.7}$$

where $\leq$ denotes an element-wise comparison of two vectors. We consider two ways to construct such a matrix. The first one is to construct a $\left(\left(\sum_{t\in\mathcal{T}}(|{}^\bullet t| - 1)\right) \times |\mathcal{P}|\right)$-matrix row by row. For each join t and all $p \in {}^\bullet t$ with $p \neq K(t)$, the matrix G_K contains a row $g_{K,t,p}$ of the form

$$g_{K,t,p} = (0, \ldots, 0, \frac{1}{Pre_{K(t),t}}, 0, \ldots, 0, \frac{-1}{Pre_{p,t}}, 0, \ldots, 0) \tag{2.8}$$

where the positive and the negative entry are in the columns associated with $K(t)$ and p, respectively. The rows are normal vectors of the hyperplanes separating two neighboring regions. The order of the rows is not unique, but the polyhedron given by $\{m \in \mathbb{R}^{|\mathcal{P}|}_{\geq 0} : G_K m \leq 0\}$ is independent of the order of the rows.

In [LL11], different matrices are used to describe the regions. They contain many

is used for notational convenience. On the other hand, configurations may be defined either for net systems and depend on the initial marking or independent of m_0 (cf. [MRS09, SR07]). This difference usually comes along with different definitions of the phase space. Incorporating the initial marking leads to a restriction to the set of markings $\{m \in \mathbb{R}^{|\mathcal{P}|}_{\geq 0} : \exists 0 \leq \sigma \in \mathbb{R}^{|\mathcal{T}|}$ such that $m = m_0 + C\sigma\}$. Otherwise, the entire positive orthant $\mathbb{R}^{|\mathcal{P}|}_{\geq 0}$ is used. Even though the first interpretation may be more convenient if we want to define controllability, the latter is used in this thesis. A definition independent of m_0 does not just seem more natural from a dynamical systems point of view as it distinguishes between the dynamical system itself and individual trajectories. The incorporation of the initial marking also imposes an unnecessary restriction that obstructs one's view on the global dynamics and may lead to undefined dynamics in the numerical treatment.

additional redundant rows but can be written in a compact way by

$$G_K^L = \begin{pmatrix} \Pi_K - \Pi_{K_1} \\ \Pi_K - \Pi_{K_2} \\ \vdots \\ \Pi_K - \Pi_{K_\gamma} \end{pmatrix}. \tag{2.9}$$

The superscript L is used to distinguish this matrix from the one described previously. Both G_K and G_K^L are suitable to describe the region M_K.

We check if $(M_K)_{K\in\mathcal{K}_\mathcal{N}}$ is the correct choice for the polyhedral partition of the phase space. Obviously, there is always a configuration active under an arbitrary marking $m \in \mathbb{R}_{\geq 0}^{|\mathcal{P}|}$. In order to see that condition (ii) of Definition 2.2 holds as well, let us consider two different configurations K_1, K_2 of a Petri net $\mathcal{N}$. Let $m \in M_{K_1} \cap M_{K_2}$. As $K_1 \neq K_2$, there exists $t \in \mathcal{T}$ with $K_1(t) =: p \neq p' := K_2(t)$. The marking has to satisfy the inequalities

$$\frac{m_p}{Pre_{p,t}} - \frac{m_{p'}}{Pre_{p',t}} \leq 0 \text{ and } -\frac{m_p}{Pre_{p,t}} + \frac{m_{p'}}{Pre_{p',t}} \leq 0.$$

Therefore, $\frac{m_p}{Pre_{p,t}} = \frac{m_{p'}}{Pre_{p',t}}$, which implies that m lies on the boundary of both regions. In other words, $M_{K_1} \cap M_{K_2} = \partial M_{K_1} \cap \partial M_{K_2}$.

We have verified that $(M_K)_{K\in\mathcal{K}_\mathcal{N}}$ satisfies all conditions of Definition 2.2 but the dimension of the polyhedra. In fact, if the net contains choices, lower dimensional polyhedra may exist. This issue is discussed in detail in Section 2.3.3 where a subset $\mathcal{K}_\mathcal{N}^o \subset \mathcal{K}_\mathcal{N}$ is identified such that $(M_K)_{K\in\mathcal{K}_\mathcal{N}^o}$ is a polyhedral partition.

As a next step, we want to find the system matrices of the timed continuous Petri net. According to [MRRS08], a configuration $K \in \mathcal{K}_\mathcal{N}$ can be associated with a matrix $\Pi_K \in \mathbb{R}^{|\mathcal{T}|\times|\mathcal{P}|}$ with

$$(\Pi_K)_{t,p} = \begin{cases} \frac{1}{Pre_{p,t}} & \text{if } K(t) = p, \\ 0 & \text{otherwise} \end{cases}$$

for $(t, p) \in \mathcal{T} \times \mathcal{P}$. Let furthermore $\Lambda = \text{diag}(\lambda_{t_1}, \ldots, \lambda_{t_{|\mathcal{T}|}})$.

With this notation, the evolution of the marking as defined by Equations (2.4)

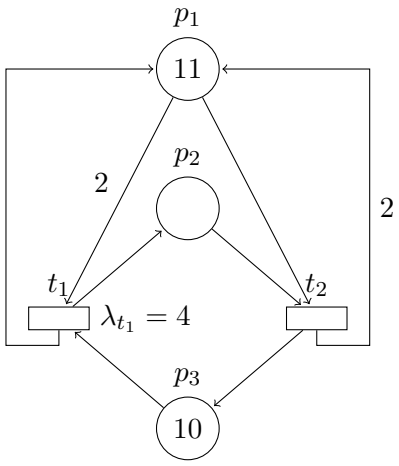

Figure 2.2: A TCPN system with three places and two transitions.

and (2.5) can be written as

$$\dot{m} = Cf(m) = C\Lambda\Pi_K m \tag{2.10}$$

where K is any configuration active under m. If several configurations are active under m, all of them result in the same vector $\Pi_K m$ of continuous enabling degrees. The resulting vector field is continuous and may therefore be defined as

$$F : \mathbb{R}^{|\mathcal{P}|}_{\geq 0} \to \mathbb{R}^{|\mathcal{P}|},\ m \mapsto C\Lambda\Pi_K m \text{ for } m \in M_K. \tag{2.11}$$

The system matrix of each configuration $K \in \mathcal{K}$ is given by

$$A_K = C\Lambda\Pi_K. \tag{2.12}$$

The piecewise linear vector field can therefore be written as

$$F : \mathbb{R}^{|\mathcal{P}|}_{\geq 0} \to \mathbb{R}^{|\mathcal{P}|},\ m \mapsto A_K m \text{ for } m \in M_K. \tag{2.13}$$

Example 2.5. We show how to set up the PWL system for the TCPN in Figure 2.2 which is taken from [JRS05]. The net system is reconsidered later in this thesis with respect to reductions and parameter-dependent TCPNs.

The net structure is described by the matrices

$$Pre = \begin{pmatrix} 2 & 1 \\ 0 & 1 \\ 1 & 0 \end{pmatrix}, \quad Post = \begin{pmatrix} 1 & 2 \\ 1 & 0 \\ 0 & 1 \end{pmatrix} \quad C = Post - Pre = \begin{pmatrix} -1 & 1 \\ 1 & -1 \\ -1 & 1 \end{pmatrix}.$$

This net has four different configurations as the two transitions have two input places each. We denote them by their value pairs and compute the matrices G_{K_i} and Π_{K_i} $(i = 1, \ldots, 4)$:

$$\begin{aligned}
K_1 &= \{(t_1, p_1), (t_2, p_2)\}: \quad G_{K_1} = \begin{pmatrix} \frac{1}{2} & 0 & -1 \\ -1 & 1 & 0 \end{pmatrix}, \quad \Pi_{K_1} = \begin{pmatrix} \frac{1}{2} & 0 & 0 \\ 0 & 1 & 0 \end{pmatrix}, \\
K_2 &= \{(t_1, p_1), (t_2, p_1)\}: \quad G_{K_2} = \begin{pmatrix} \frac{1}{2} & 0 & -1 \\ 1 & -1 & 0 \end{pmatrix}, \quad \Pi_{K_2} = \begin{pmatrix} \frac{1}{2} & 0 & 0 \\ 1 & 0 & 0 \end{pmatrix}, \\
K_3 &= \{(t_1, p_3), (t_2, p_1)\}: \quad G_{K_3} = \begin{pmatrix} -\frac{1}{2} & 0 & 1 \\ 1 & -1 & 0 \end{pmatrix}, \quad \Pi_{K_3} = \begin{pmatrix} 0 & 0 & 1 \\ 1 & 0 & 0 \end{pmatrix}, \\
K_4 &= \{(t_1, p_3), (t_2, p_2)\}: \quad G_{K_4} = \begin{pmatrix} -\frac{1}{2} & 0 & 1 \\ -1 & 1 & 0 \end{pmatrix}, \quad \Pi_{K_4} = \begin{pmatrix} 0 & 0 & 1 \\ 0 & 1 & 0 \end{pmatrix}.
\end{aligned}$$

Together with $\Lambda = \mathrm{diag}(4, 1)$, the associated dynamical system is given by

$$\dot{m} = C\Lambda\Pi_K m \text{ for } m \in M_K = \{m \in \mathbb{R}^3_{\geq 0} : G_K m \leq 0\}$$

with $m_0 = \begin{pmatrix} 11 & 0 & 10 \end{pmatrix}^T$. ♢

2.3.3 Redundant Configurations and Choices

Structurally, a net has $\prod_{t \in \mathcal{T}} |{}^\bullet t|$ different configurations. However, in [MRS08] it is shown that some of these configurations do not contribute to the dynamics of the system. We show that these redundant configurations only appear in the presence of certain net structures and that there always exists a cover of $\mathbb{R}^{|\mathcal{P}|}_{\geq 0}$ by regions of nonredundant configurations. The contents of this section can also be found in

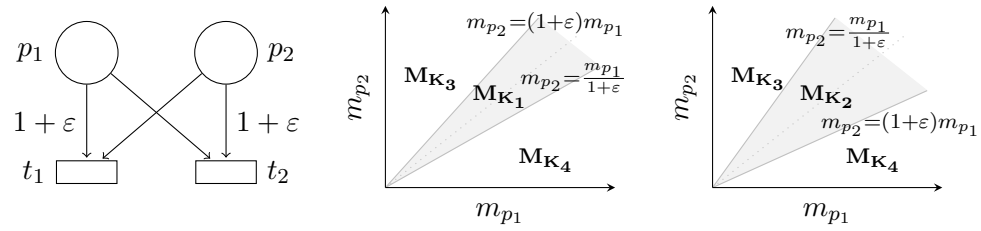

(a) A Petri net with choices (b) Regions for $\varepsilon > 0$ (c) Regions for $-1 < \varepsilon < 0$

Figure 2.3: Redundant configurations.

[MD09].

Definition 2.6. *[MRS08] Let $K \in \mathcal{K}_\mathcal{N}$ be a configuration. K is* redundant *if*

$$M_K \subset \bigcup_{K' \in \mathcal{K}_\mathcal{N} \setminus \{K\}} M_{K'}.$$

We denote by $\mathcal{K}^r_\mathcal{N}$ the set of redundant configurations and by $\mathcal{K}^o_\mathcal{N} = \mathcal{K}_\mathcal{N} \setminus \mathcal{K}^r_\mathcal{N}$ the set of configurations which are not redundant.

Example 2.7. Figure 2.3(a) shows a Petri net with choices. There are four possible configurations which we represent by their value pairs: $K_1 = \{(t_1, p_1), (t_2, p_2)\}$, $K_2 = \{(t_1, p_2), (t_2, p_1)\}$, $K_3 = \{(t_1, p_1), (t_2, p_1)\}$, and $K_4 = \{(t_1, p_2), (t_2, p_2)\}$. Figures 2.3(b)–(c) show the partition of the phase space into the corresponding regions for $\varepsilon > 0$ and $-1 < \varepsilon < 0$, respectively. For $\varepsilon > 0$, the set M_{K_2} consists only of the origin and is thus redundant. For negative ε, region M_{K_1} vanishes and is redundant. If $\varepsilon = 0$, both regions coincide, i.e., $M_{K_1} = M_{K_2} = \{m \in \mathbb{R}^{|\mathcal{P}|}_{\geq 0} : m_{p_1} = m_{p_2}\}$. Then, both configurations are redundant since they lie within the boundaries of M_{K_3} and M_{K_4}. ♢

We now study some characteristics of redundant configurations, first for general net structures and then for particular ones (Propositions 2.11 and 2.12). For the sake of completeness, we include properties (in particular Corollary 2.10) which have already been studied in [MRS08]. We complement these results by a formal proof that there always exists a cover of $\mathbb{R}^{|\mathcal{P}|}_{\geq 0}$ by the corresponding regions of nonredundant configurations.

Lemma 2.8. *Let* $K \in \mathcal{K}_{\mathcal{N}}^{r}$. *Then* $\operatorname{int}(M_K) = \emptyset$.

Proof. Let $m \in M_K$. As K is redundant, there exists $K' \in \mathcal{K}_{\mathcal{N}}$, $K' \neq K$, with $m \in M_{K'}$. As $m \in M_{K_1} \cap M_{K_2} = \partial M_{K_1} \cap \partial M_{K_2}$, m cannot be an interior point of M_K. □

Redundant regions therefore lie within the hyperplanes separating regions from each other. As the nonredundant regions are closed sets, they cover the marking space.

Proposition 2.9. *The marking space is covered by the set of regions with nonempty interior, i.e.,*

$$\bigcup_{\substack{K \in \mathcal{K}_{\mathcal{N}} \\ \operatorname{int}(M_K) \neq \emptyset}} M_K = \mathbb{R}_{\geq 0}^{|\mathcal{P}|}.$$

Proof. All regions are closed (usually unbounded) convex polyhedra. They are a cover of $\mathbb{R}_{\geq 0}^{|\mathcal{P}|}$. Let $m \in \mathbb{R}_{\geq 0}^{|\mathcal{P}|}$. We show that there exists a configuration $K \in \mathcal{K}_{\mathcal{N}}$ with $\operatorname{int}(M_K) \neq \emptyset$ and $m \in M_K$.

Let $B_r(m)$ denote the ball with center m and radius $r > 0$ with respect to an arbitrary vector norm on $\mathbb{R}^{|\mathcal{P}|}$. Since the set of regions is finite, there exists a configuration $K \in \mathcal{K}_{\mathcal{N}}$ with $\operatorname{int}(M_K) \cap B_r(m) \neq \emptyset$. Furthermore, the regions are convex. Thus, $\operatorname{int}(M_K) \cap B_r(m) \neq \emptyset$ for all $r > 0$. Since M_K is closed, it contains m. □

Corollary 2.10. *A configuration* K *is redundant if and only if* $\operatorname{int}(M_K) = \emptyset$.

Proof. By the previous proposition, all configurations whose associated regions have an empty interior are redundant. The equivalence now follows immediately with Lemma 2.8. □

In Section 2.3.2, it is shown that $(M_K)_{K \in \mathcal{K}_{\mathcal{N}}}$ satisfies all conditions of a polyhedral partition according to Definition 2.2 except that polyhedra may not be full-dimensional. The previous proposition tells us that we may restrict the index set to the nonredundant configurations and still have a cover of the entire marking space $\mathbb{R}_{\geq 0}^{|\mathcal{P}|}$. As nonredundant configurations have full-dimensional regions, $(M_K)_{K \in \mathcal{K}_{\mathcal{N}}^{o}}$

satisfies Definition 2.2. Therefore, $((M_K)_{K\in\mathcal{K}^o_\mathcal{N}}, (C\Lambda\Pi_K, 0)_{K\in\mathcal{K}^o_\mathcal{N}})$ is a piecewise linear system in the sense of Definition 2.3. The induced dynamical system is governed by the vector field F.

The following two propositions show that redundant configurations can only exist if the net has choices. They establish a relation between the structure of a Petri net and the dimension of its regions.

Proposition 2.11. *If a Petri net $\mathcal{N}$ is ordinary or CEQ, then $M_K \neq \{0\}$ for all $K \in \mathcal{K}_\mathcal{N}$.*

Proof. In an ordinary Petri net, all configurations are active under $m \neq 0$ with $m_{p_1} = m_{p_2} = \ldots = m_{p_{|\mathcal{P}|}}$.

Let now $\mathcal{N}$ be CEQ and $K \in \mathcal{K}_\mathcal{N}$. We construct a marking $m \in M_K \setminus \{0\}$. To start with, an arbitrary positive marking is assigned to all places without output arcs. For all transitions $t \in \mathcal{T}$ which do not have choices as input places we set $m_{K(t)}$ to an arbitrary positive value. For the input places $p \in {}^\bullet t \setminus \{K(t)\}$, a marking

$$m_p \geq \frac{Pre_{p,t}}{Pre_{K(t),t}} m_{K(t)} \tag{2.14}$$

is chosen.

Let now ${}^\bullet t$ contain a choice. As the net is CEQ, all transitions t' with ${}^\bullet t \cap {}^\bullet t' \neq \emptyset$ share the same input places. We fix their markings simultaneously. We choose a place $p \in {}^\bullet t$ and fix m_p to some positive constant. After that, we set $m_{p'} = \frac{Pre_{p',t}}{Pre_{p,t}} m_p$ for all $p' \in {}^\bullet t \setminus \{p\}$. We proceed with the next transition until all components of m are set. Because of the special structure of the net, this is always possible without fixing a component twice.

We need to verify that K is active under m, i.e., that Equation (2.6) holds for all $t \in \mathcal{T}$. This is obvious by construction if none of the input places of t is a choice. Otherwise, let p and p' be input places of t and let $K(t) = p$. There exist $t^* \in p^\bullet$ and $p^* \in {}^\bullet t^*$ with

$$m_p = \frac{Pre_{p,t^*}}{Pre_{p^*,t^*}} m_{p^*} \text{ and } m_{p'} = \frac{Pre_{p',t^*}}{Pre_{p^*,t^*}} m_{p^*}.$$

As $\mathcal{N}$ is CEQ, there exists for t and t^* a constant $k > 0$ with $Pre_{p,t} = k\, Pre_{p,t^*}$ and $Pre_{p',t} = k\, Pre_{p',t^*}$. Hence,

$$\frac{m_p}{Pre_{p,t}} = \frac{m_p}{kPre_{p,t^*}} = \frac{m_{p^*}}{kPre_{p^*,t^*}},$$
$$\frac{m_{p'}}{Pre_{p',t}} = \frac{m_{p'}}{kPre_{p',t^*}} = \frac{m_{p^*}}{kPre_{p^*,t^*}},$$

and $\frac{m_p}{Pre_{p,t}} \leq \frac{m_{p'}}{Pre_{p't}}$ holds. It follows that $m \in M_K$. □

Proposition 2.12. *If $\mathcal{N}$ is choice-free, then no redundant configurations exist.*

Proof. Let $K \in \mathcal{K}_\mathcal{N}$. We have to show that M_K has an interior point. Then, by Lemma 2.8, K cannot be redundant. As choice-free nets are in particular CEQ, we use the construction described in Proposition 2.11 but with inequality (2.14) being strict. The resulting marking is in $\mathrm{int}(M_K)$. □

2.4 Dynamics of Timed Continuous Petri Nets

In this section, central results on the dynamics of TCPNs are summarized.

Positivity and Flow-Invariant Sets. Petri nets are positive systems.

Theorem 2.13. *[MP05, Corollary 1] For any choice of the firing rates $\lambda > 0$, the continuous marking of a timed continuous Petri net with infinite server semantics remains nonnegative, i.e., for any $m_0 \geq 0$ the marking at time $\tau \geq 0$ satisfies $m(\tau) \geq 0$.*

This is easy to see in the join-free case where the dynamics is purely linear. In this case, $Pre\, \Lambda\Pi_K$ is a diagonal matrix where K is the unique configuration. To see this, consider

$$(Pre\, \Lambda\Pi_K)_{p,p'} = \sum_{t \in \mathcal{T}} Pre_{p,t} \lambda_t (\Pi_K)_{t,p'}.$$

$Pre_{p,t}$ and $(\Pi_K)_{p',t}$ are nonzero only if $p, p' \in {}^\bullet t$. In join-free nets, this implies that all nondiagonal elements have to be zero. As $Post\, \Lambda\Pi_K$ has only nonnegative entries, all nondiagonal elements of the system matrix are nonnegative [MP05, JJS05].

Thus, $C\Lambda\Pi_K$ is a Metzler matrix [FR00, p. 14]. One important consequence is that its dominant eigenvalue is real and unique. Furthermore, a positive eigenvector corresponds to this eigenvalue and no other eigenvector can be strictly positive (cf. [Mit08] and [FR00, p. 36]). Thus, in a bounded net the dominant eigenvector cannot be positive.

In nets with joins, there exists more than one configuration and $C\Lambda\Pi_K$ is generally not Metzler [JJRS04]. Positivity is proved in [MP05] by showing that the positive orthant is a flow-invariant set. Furthermore, necessary and sufficient conditions for the existence of flow-invariant sets of different types are known for join-free nets (cf. [MP05]). In [KMB+08], it is shown how — given a set of initial states — it is possible to construct by means of formal verification a set of unreachable states, i.e., a set such that all trajectories starting from the set of initial states never reach the latter set.

A well-known flow-invariant set that appears in all TCPNs just like in any discrete or continuous Petri net is due to $\mathcal{P}$-invariants. Equality (2.3) also holds for continuous systems (see, e.g., Proposition 2 in [MRRS08]). Thus, a trajectory starting in m_0 cannot leave the affine subspace $m_0 + \mathrm{im}(C)$.

Equilibria. In most simulations, the continuous marking converges quickly to a steady state. However, the dynamics of TCPNs are richer including periodic orbits both within a single region and with repetitive switches between regions as well as convergence to a steady state with infinitely many switches (see [RHS07] for examples). For conservative and consistent join-free nets, convergence to an equilibrium is guaranteed [JJS05]. However, for most net classes it is still unknown when an equilibrium exists and how this is related to the net structure. This issue has been identified as one of the major open problems concerning the "fluidization" of Petri nets in [SR05]. Unfortunately, an answer still does not seem to be near.

Monotonicity. Under this header the question is discussed whether performance measures always increase with respect to an increase in the initial marking or a firing rate. The flow $f(m^*)$ in steady state m^*, which is known as the throughput vector of the system (in case such a unique equilibrium exists), is the most common performance indicator in this case. In general, if the firing rates of all transitions

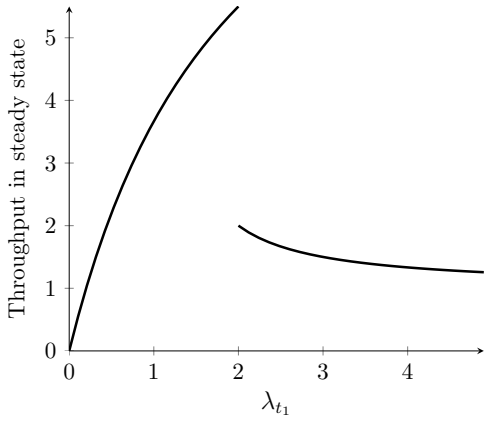

Figure 2.4: Throughput under variation of the firing rate λ_{t_1}.

are multiplied by a factor $\alpha > 0$, then, by linearity, the throughput of the system is also multiplied by α [SJMV11, p. 32]. However, if only some of the firing rates are altered, the throughput may be nonmonotonic or even discontinuous.

Example 2.14. Let us reconsider the TCPN from Example 2.5. In [JRS05], this net illustrates that an increase of the firing rate does not always result in an increase of the throughput. Figure 2.4 shows the throughput of the system for different firing rates of transition t_1. At $\lambda_{t_1} = 2$ the throughput drops abruptly. ♢

In Chapter 5, this example is analyzed in detail. It is shown that such a discontinuity in the throughput is due to a discontinuity-induced bifurcation. Such undesirable jumps in the throughput are also observed if the throughput is monotonic (see Section 5.3.3).

For the same net structure as in the previous example, it is shown in [JRS05] that a reduction of the initial marking may also lead to the counterintuitive effect that the throughput may increase. Both with respect to firing rates and with respect to the initial marking, sufficient conditions for monotonicity of the throughput in mono-T-semiflow reducible nets are proven in [MRS09]. It is shown that systems are monotonic if in any steady state a configuration K such that $K(\mathcal{T})$ contains the support of a $\mathcal{P}$-semiflow is active. Under this condition, the throughput bounds computed in [JRS05] coincide with the actual throughput in steady state.

In general, it is computationally expensive to check if $K(\mathcal{T})$ contains the support of

a $\mathcal{P}$-semiflow. For some subclasses of nets such as equal conflict nets this condition is satisfied by all configurations under some conditions which are easy to check [MRS09, p. 199].

Comparison of server semantics. A well-known alternative to infinite server semantics are finite server semantics where the flow of each transition is limited by a maximal firing speed. We do not consider them in this thesis as infinite server semantics have shown a better approximation of performance indicators of the underlying discrete SPN in many applications. Technically, the following result has been obtained:

Theorem 2.15. *[MRS09, Theorem 1] Let $\langle \mathcal{N}, \lambda, m_0 \rangle$ be a live mono-T-semiflow reducible Petri net system where for every $K \in \mathcal{K}_{\mathcal{N}}$, $K(\mathcal{T})$ contains the support of a $\mathcal{P}$-semiflow. For any probability distribution function for the firing of the transitions, the steady state throughput of the discrete model is better approximated by the continuous relaxation with infinite server semantics than with finite server semantics.*

In nets satisfying the conditions of the theorem, the throughput of the continuous net under infinite server semantics is an upper bound of the throughput in the discrete counterpart (see [JRS05, Proposition 5]). The addition of white noise to the transitions flow may improve the approximation of the mean marking of the corresponding Markovian Petri net (see [SJMV11] where even more modifications of the semantics are discussed).

Control. Control questions for discrete Petri nets typically deal with the question which transitions to limit at certain markings in order to meet some safety criteria such as the avoidance of critical states. For TCPNs, typically, controls of the form $u : \mathbb{R} \to \mathbb{R}^{|\mathcal{T}|}$ such that

$$\dot{m}(\tau) = C(\Lambda \Pi_K m(\tau) - u(\tau))$$

where $0 \leq u(\tau) \leq \Lambda \Pi_K m(\tau)$ are studied. The control is associated with the transitions whose flow may be reduced. A transition's activity may even be stopped

completely. It might happen that only some of the transitions are controllable. In that case, the components of u may differ from zero for controllable components only. A typical question is now if there exists a control function u that drives the system from m_0 to some desired marking m' in finite time. It is immediate to see that only markings $m' \in m_0 + \mathrm{im}(C)$ can be reached. A detailed survey on definitions of controllability, theoretic results on TCPN control problems, and associated algorithms is given by [SJMV11].

3

Symmetries in TCPNs and Generalizations to Other PWL Systems

In Section 2.4, we have seen which types of dynamical behavior timed continuous Petri nets with infinite server semantics (TCPNs) may exhibit and how they are related to the net structure. In this chapter, the structure under consideration is induced by symmetries of the net. We study the interplay of symmetries of the net structure and the corresponding dynamical system. We prove that the symmetries of the net structure are reflected by symmetries of the dynamical system in the classic sense of equivariant dynamics. For this reason, this chapter starts with a short summary of fundamental definitions and results from equivariant dynamical systems theory before symmetries of the net structure are formally defined and discussed in Section 3.2, followed by novel results concerning their effect on the corresponding piecewise linear system (PWL) in Sections 3.3 and 3.4 which are then generalized to general PWL systems in Section 3.5. Those results specific to TCPNs and the generalizations of Section 3.5 have already been published in [MD09, MDH11].

3.1 Equivariant Dynamical Systems

Symmetries appear in various dynamical systems and have been subject of intensive research. In the modeling of real-world phenomena, they appear, for example, due to the system geometry or simplifying modeling assumptions. Petri nets exhibit symmetries, for instance, if the system modeled contains identical components, agents or subprocesses that are symmetrically coupled. Symmetries may simplify the generation of analytic solutions to ordinary differential equations (ODEs). They may be used to increase the efficiency of computational methods or to generate new solutions from known solutions. Symmetries should also be taken into account as the dynamical behavior of generic nonsymmetric systems usually differs significantly from that of systems with symmetries. An example are heteroclinic cycles. It might therefore be necessary to identify the system's symmetries in order to fully understand its dynamics (cf. [GS03, HD11] and [Hyd00, p. 187]).

We consider systems of ordinary differential equations

$$\dot{x} = g(x) \tag{3.1}$$

where $g : \mathbb{R}^n \to \mathbb{R}^n$ is sufficiently smooth.[1] For such systems, we introduce a notion of symmetry for the system as a whole and also for its solutions. In this section, we follow the work of Golubitsky, Stewart, Schaeffer, and Field [GSS88, GS03, Fie96]. As we do not want to over-complicate matters unnecessarily, the presentation is restricted to vector spaces and linear Lie groups, i.e., subgroups of the general linear group $GL(n)$ consisting of all invertible, real $(n \times n)$-matrices[2] with matrix multiplication defining the group operation. When dealing with symmetries in the net structure, we consider permutation of nodes and therefore deal with the *symmetric group* $\mathrm{Sym}(\mathcal{P} \cup \mathcal{T})$.

Symmetries in systems of ODEs and their solutions are expressed by transformations of the variables via group actions.

Definition 3.1. *Let Σ be a linear Lie group and V a vector space. An* action *of Σ*

[1] Actually, we only require that for any $x_0 \in \mathbb{R}^n$ the corresponding initial value problem has got a unique solution which is guaranteed in our case of continuous PWL systems as F satisfies a local Lipschitz condition.

[2] In this thesis, we use matrices also to denote the associated linear map.

on V is a continuous mapping $\Sigma \times V \to V$, $(\sigma, v) \mapsto \sigma v$ that satisfies

(i) $ev = v$ where e is the identity element of Σ and

(ii) $\sigma_1(\sigma_2 v) = (\sigma_1\sigma_2)v$

for all $v \in V$ and $\sigma_1, \sigma_2 \in \Sigma$. If there exists an action of Σ on V, we call V a Σ-set. *The* group orbit *through $v \in V$ is the set $\Sigma v = \{\sigma v : \sigma \in \Sigma\}$.*

We may now define symmetries of systems of ODEs and their solutions.

Definition 3.2. *The group element $\sigma \in GL(n)$ is a* symmetry *of* (3.1) *if*

$$g(\sigma x) = \sigma g(x) \tag{3.2}$$

for all $x \in \mathbb{R}^n$. The set $\Sigma \subset GL(n)$ of all such symmetries is the symmetry group *of the system.*

We call (3.2) an *equivariance condition* and say that g is Σ-*equivariant*. It is equivalent to saying that for every solution $x(t)$ also $\sigma x(t)$ is a solution, i.e., to saying that σ maps solutions onto solutions. To see this, let $y(t) = \sigma x(t)$. Then, $\dot{y}(t) = g(y(t)) = g(\sigma x(t))$ and at the same time $\dot{y}(t) = \sigma \dot{x}(t) = \sigma g(x(t))$. Thus, $g(\sigma x(t)) = \sigma g(x(t))$ holds for solutions for arbitrary initial values.

Example 3.3. A very simple example of symmetries in systems of ODEs can be found in every timed continuous Petri net with infinite server semantics, namely the fact that F is homogeneous. All cells of the polyhedral partition of the marking space are cones, meaning that $m \in M_K$ implies $\kappa m \in M_K$ for any $\kappa \geq 0$. For any $\kappa > 0$, $\sigma = \kappa I_{|\mathcal{P}|} \in GL(|\mathcal{P}|)$ where $I_{|\mathcal{P}|}$ is the identity matrix of dimension $|\mathcal{P}|$. Within each cone, the dynamics are linear and therefore $\sigma F(m) = F(\sigma m)$ for all $m \in \mathbb{R}^{|\mathcal{P}|}_{\geq 0}$.

Let $\Sigma' = \{\kappa I_{|\mathcal{P}|} : \kappa > 0\}$ denote the corresponding infinite subgroup of the symmetry group. The equivariance immediately implies that if m is a marking trajectory for the initial marking m_0, then κm solves the initial value problem for the initial marking κm_0. In particular, if m is a steady state, so is every element of its group orbit $\Sigma' m$. For this reason, steady states or periodic orbits are never isolated in TCPNs. ♢

An important property of equivariant dynamical systems is that they give rise to flow-invariant sets, the so-called fixed-point subspaces, which are used in the next chapter for reductions.

Definition 3.4. *Let $\Sigma' \subset \Sigma$ be a subgroup. The* fixed-point subspace *of Σ' is given by*

$$\mathrm{Fix}(\Sigma') = \{v \in V : \ \sigma v = v \text{ for all } \sigma \in \Sigma'\}.$$

$\mathrm{Fix}(\Sigma')$ is in fact a subspace of V as the name indicates since

$$\mathrm{Fix}(\Sigma') = \bigcap_{\sigma \in \Sigma'} \ker(\sigma - I_n).$$

The important property of these sets is their flow-invariance which is expressed in the following theorem.

Theorem 3.5. *[GS03, Theorem 1.17] Let $g : V \to V$ be Σ-equivariant and $\Sigma' \subset \Sigma$ a subgroup. Then,*

$$g(\mathrm{Fix}(\Sigma')) \subset \mathrm{Fix}(\Sigma').$$

Proof. This follows immediately from the fact that for a $\sigma \in \Sigma'$ and $x \in \mathrm{Fix}(\Sigma')$ the equality $g(x) = g(\sigma x) = \sigma g(x)$ holds, i.e., $g(x) \in \mathrm{Fix}(\Sigma')$. □

An immediate consequence is that the "degree of symmetry" cannot increase or decrease along trajectories. In order to describe this formally we need to define the symmetry of a state.

Definition 3.6. *For a Σ-set V we define the* isotropy subgroup *(or* Σ-stabilizer*) of Σ at $v \in V$ by*

$$\Sigma_v = \{\sigma \in \Sigma : \ \sigma v = v\}.$$

Theorem 3.7. *[GS03, Proposition 1.18] Let $x(t)$ be a solution trajectory of an equivariant ODE. Then,*

$$\Sigma_{x(t)} = \Sigma_{x(0)}$$

for all $t \in \mathbb{R}$. This means that isotropy subgroups remain constant along trajectories.

Proof. We apply Theorem 3.5. As $\mathrm{Fix}(\Sigma_{x(0)})$ is flow-invariant, we have $x(t) \in \mathrm{Fix}(\Sigma_{x(0)})$. Therefore, $\Sigma_{x(t)} \subset \Sigma_{x(0)}$. For the other direction consider that $x(0)$ lies on a trajectory through $x(t)$. □

3.2 Symmetries in the Net Structure

3.2.1 Definition and Examples of Symmetries of Petri Nets

Intuitively, the Petri nets in Figure 3.1 seem to be somehow symmetric. Below, this intuition is formalized, and it is shown how this additional knowledge of the topology of the net helps to understand the dynamics of the continuous marking. For this purpose, the effects of symmetry on the polyhedral partition and the system matrices are studied. Combining these results, we obtain a deeper understanding of the dynamical behavior and show how this can be used for analysis and reduction purposes.

Symmetries appear naturally in many applications, in particular if the system contains several identical units which interact in some systematically structured network. The study of symmetries in Petri nets goes back to [HJJJ85] and has been applied to place/transition nets in [Sta90, Sta91, Sch00a, Sch00b, Jun03]. They are expressed as permutations of places and transitions.

Definition 3.8. *Let $\langle \mathcal{N}, \lambda \rangle$ be a timed Petri net and $\sigma : (\mathcal{P} \cup \mathcal{T}) \to (\mathcal{P} \cup \mathcal{T})$ be a permutation of its nodes such that $\sigma(\mathcal{P}) = \mathcal{P}$ and $\sigma(\mathcal{T}) = \mathcal{T}$. We say that σ*

- weakly preserves the structure *if $Pre_{p,t} = Pre_{\sigma(p),\sigma(t)}$ for all $p \in \mathcal{P}, t \in \mathcal{T}$,*
- strongly preserves the structure *if it weakly preserves the structure and, in addition, $Post_{p,t} = Post_{\sigma(p),\sigma(t)}$ for all $p \in \mathcal{P}, t \in \mathcal{T}$,*
- preserves the timing *if $\lambda_t = \lambda_{\sigma(t)}$ for all $t \in \mathcal{T}$.*

We denote by $\Sigma^w_{\mathcal{N}}$ and $\Sigma^s_{\mathcal{N}}$ all permutations of the Petri net that weakly and strongly, respectively, preserve the structure. The set of permutations that strongly preserve the structure and the timing is denoted by $\Sigma^t_{\langle \mathcal{N}, \lambda \rangle}$.

Example 3.9. For the nets $\mathcal{N}_a$ and $\mathcal{N}_b$ in Figure 3.1 all three sets coincide. In cycle

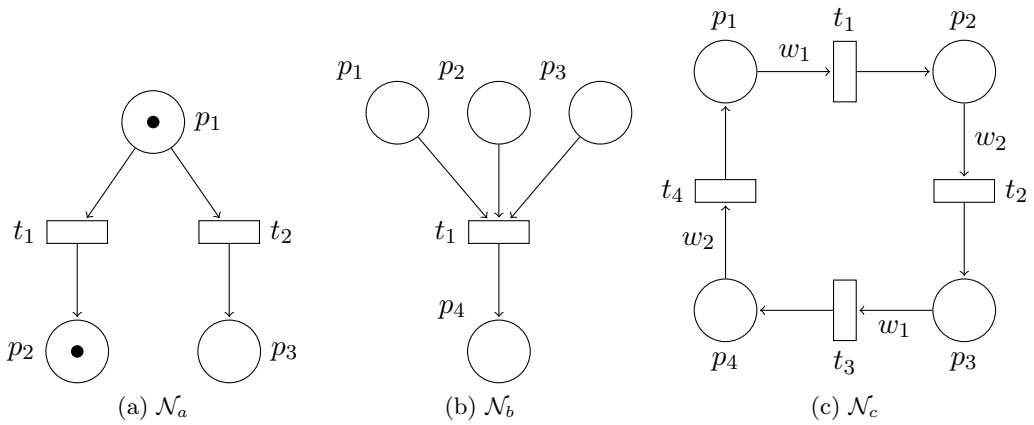

Figure 3.1: Petri nets with symmetries.

notation the symmetry groups are

$$\Sigma^w_{\mathcal{N}_a} = \Sigma^s_{\mathcal{N}_a} = \Sigma^t_{\langle \mathcal{N}_a, \lambda_a \rangle} = \{id, (t_1\, t_2)(p_2\, p_3)\}$$

and

$$\Sigma^w_{\mathcal{N}_b} = \Sigma^s_{\mathcal{N}_b} = \Sigma^t_{\langle \mathcal{N}_b, \lambda_b \rangle} = \{id, (p_1\, p_2), (p_1\, p_3), (p_2\, p_3), (p_1\, p_2\, p_3), (p_1\, p_3\, p_2)\}.$$

The net $\mathcal{N}_c$ can be "rotated by 180°" without changing the structure. This corresponds to

$$\Sigma^s_{\mathcal{N}_c} = \{id, (p_1\, p_3)(t_1\, t_3)(p_2\, p_4)(t_2\, t_4)\}.$$

In addition, there exist permutations that only weakly preserve the structure and

$$\Sigma^w_{\mathcal{N}_c} = \Sigma^s_{\mathcal{N}_c} \cup \{(p_1\, p_3)(t_1\, t_3), (p_2\, p_4)(t_2\, t_4)\}.$$

$\diamondsuit$

$\Sigma^s_{\mathcal{N}}$ and $\Sigma^t_{\langle \mathcal{N}, \lambda \rangle}$ consist of *graph automorphisms* of the directed, bipartite graph $\mathcal{N}$. Permutations in $\Sigma^w_{\mathcal{N}}$ are not necessarily graph automorphisms since only the input structure of the transitions is preserved. However, it is this structure that defines the configurations and makes these permutations worth studying. $\Sigma^t_{\langle \mathcal{N}, \lambda \rangle}$ is the

natural choice for defining symmetries of directed, vertex- and edge-labeled graphs (cf. [Jun03, p. 21]). It is easy to see that $\Sigma^w_{\mathcal{N}}$, $\Sigma^s_{\mathcal{N}}$ and $\Sigma^t_{\langle\mathcal{N},\lambda\rangle}$ form groups under the composition operation.

Symmetries of the net structure induce equivalence relations on the nodes and states.

Definition 3.10. *Let Σ be a subgroup of $\Sigma^w_{\mathcal{N}}$, $\Sigma^s_{\mathcal{N}}$, or $\Sigma^t_{\langle\mathcal{N},\lambda\rangle}$. Two nodes $v, v' \in (\mathcal{P} \cup \mathcal{T})$ are* equivalent *with respect to Σ ($v \sim_\Sigma v'$) if there exists $\sigma \in \Sigma$ such that $\sigma(v) = v'$.*

For a state m and a symmetry $\sigma \in \Sigma$ we denote by $\sigma(m)$ the state with $(\sigma(m))_{\sigma(p)} = m_p$ for all $p \in \mathcal{P}$. Two markings m and m' are equivalent *with respect to Σ ($m \sim_\Sigma m'$) if there exists a permutation $\sigma \in \Sigma$ with $\sigma(m) = m'$.*

By $\Sigma \times \mathbb{R}^{|\mathcal{P}|}_{\geq 0} \to \mathbb{R}^{|\mathcal{P}|}_{\geq 0}$, $(\sigma, m) \mapsto \sigma(m)$ a group action of Σ on the markings as defined in Section 3.1 is given. Therefore, the terms fixed-point subspace ($\mathrm{Fix}(\Sigma)$), isotropy subgroup (Σ_m), and group orbit (Σm) carry over naturally.

For the upcoming calculations, we use permutation matrices to describe the group action. We denote by $S_\sigma \in \{0,1\}^{|\mathcal{P}|\times|\mathcal{P}|}$ the permutation matrix of $\sigma_{|\mathcal{P}}$ and by $T_\sigma \in \{0,1\}^{|\mathcal{T}|\times|\mathcal{T}|}$ the permutation matrix of $\sigma_{|\mathcal{T}}$. These two matrices can be conveniently represented by making use of the Kronecker delta $\delta_{i,j}$. They are $(S_\sigma)_{p,p'} = \delta_{\sigma^{-1}(p),p'}$ and $(T_\sigma)_{t,t'} = \delta_{\sigma^{-1}(t),t'}$. An action on a marking is then given by $\sigma(m) = S_\sigma m$.

With permutation matrices the definition of symmetries of a timed continuous Petri net may be stated using matrix equalities.

Lemma 3.11. *Let $\langle\mathcal{N},\lambda\rangle$ be a timed Petri net and σ a permutation of its nodes that preserves the type of nodes.*

$$\sigma \in \Sigma^w_{\mathcal{N}} \Leftrightarrow S_\sigma Pre = Pre\, T_\sigma \tag{3.3}$$

$$\sigma \in \Sigma^s_{\mathcal{N}} \Leftrightarrow \sigma \in \Sigma^w_{\mathcal{N}} \text{ and } S_\sigma Post = Post\, T_\sigma. \tag{3.4}$$

$$\sigma \in \Sigma^t_{\langle\mathcal{N},\lambda\rangle} \Leftrightarrow \sigma \in \Sigma^s_{\mathcal{N}} \text{ and } T_\sigma \Lambda = \Lambda T_\sigma. \tag{3.5}$$

Proof. All equivalences can be proved by matrix multiplication. The matrix equality

$S_\sigma Pre = Pre\, T_\sigma$ is equivalent to $Pre_{p,t} = Pre_{\sigma(p),\sigma(t)}$ for all $(p,t) \in \mathcal{P} \times \mathcal{T}$ as

$$\begin{aligned}(S_{\sigma^{-1}} Pre\, T_\sigma)_{p,t} &= \sum_{p' \in \mathcal{P}} \delta_{\sigma(p),p'} (Pre\, T_\sigma)_{p',t} = (Pre\, T_\sigma)_{\sigma(p),t} \\ &= \sum_{t' \in \mathcal{T}} Pre_{\sigma(p),t'} \delta_{\sigma^{-1}(t'),t} = Pre_{\sigma(p),\sigma(t)}.\end{aligned}$$

Likewise, $(S_{\sigma^{-1}} Post\, T_\sigma)_{p,t} = Post_{\sigma(p),\sigma(t)}$. For the timing we obtain

$$T_\sigma^{-1} \Lambda T_\sigma = \mathrm{diag}(\lambda_{\sigma(t_1)}, \ldots, \lambda_{\sigma(t_{|\mathcal{T}|})})$$

which equals Λ if and only if $\lambda_t = \lambda_{\sigma(t)}$ for all $t \in \mathcal{T}$. □

Remark 3.12. As invariants are defined with respect to the token flow matrix C, which has just been shown to be symmetric, invariants also have symmetric properties. Let y be a $\mathcal{P}$-invariant, i.e., $y^T C = 0$, and x a $\mathcal{T}$-invariant of a Petri net $\mathcal{N}$, i.e., $Cx = 0$. The lemma states that for every $\sigma \in \Sigma^s_{\mathcal{N}}$ the equality $S_\sigma C = C T_\sigma$ holds. Therefore, also $S_\sigma y$ and $T_\sigma x$ are $\mathcal{P}$- and $\mathcal{T}$-invariants, respectively.

3.2.2 Symmetries in Place/Transition Nets and Their Properties

In the literature devoted to place/transition nets (i.e., untimed discrete nets with weighted arcs and no restrictions on the net topology), typically the class $\Sigma^s_{\mathcal{N}}$ is studied. Here, symmetries are used to compute a reduced reachability graph. The idea is that equivalent markings have the same enabling properties as stated in the following theorem.

Theorem 3.13. *Let $\mathcal{N}$ be a place/transition net and $\sigma \in \Sigma^s_{\mathcal{N}}$. A transition $t \in \mathcal{T}$ may fire in a state $m \in \mathbb{R}^{|\mathcal{P}|}_{\geq 0}$ leading to a marking m' if and only if $\sigma(t)$ is enabled in $\sigma(m)$ and firing leads to the marking $\sigma(m')$. As a formula,*

$$m[t > m' \Leftrightarrow \sigma(m)[\sigma(t) > \sigma(m'). \tag{3.6}$$

Proof. See Lemma 1 in [Sta91] or Proposition 1 in [Sch00a]. □

A reduction in the size of the reachability graph is achieved by considering equivalence classes of markings with respect to the symmetries instead of the markings

themselves. Many analysis tasks can be performed on the reduced graph, e.g., a marking is not reachable if the reduced reachability graph does not contain the corresponding equivalence class. Weakened forms of deadlock freeness or liveness can also be checked on the reduced graph [Sta90, Sta91, Sch00a]. Furthermore, symmetry reductions can be combined with other methods in model checking if the property to be checked is invariant under the applied symmetry group.[3]

The analysis of the reduced reachability graph is notedly significant if the isotropy subgroup of the initial marking is big. In particular, if the reduction is performed with respect to Σ_{m_0}, then a marking m is reachable if and only if the reduced reachability graph contains a node which is equivalent to m [Sta90, p. 66].

The following example shows that reachable markings of a discrete Petri net system may have different isotropy subgroups. It turns out that in this respect discrete nets differ significantly from TCPNs.

Example 3.14. The net $\mathcal{N}_a$ in Figure 3.1(a) is symmetric with

$$\Sigma^s_{\mathcal{N}_a} = \{id, (t_1\, t_2)(p_2\, p_3)\}.$$

Both transitions are enabled for the initial marking $m_0 = \begin{pmatrix}1 & 1 & 0\end{pmatrix}^T$ whose isotropy subgroup is trivial. Firing t_1 leads to the marking $\begin{pmatrix}0 & 2 & 0\end{pmatrix}^T$ which is not symmetric either. On the other hand, the marking $\begin{pmatrix}0 & 1 & 1\end{pmatrix}^T$ resulting from firing t_2 has a nontrivial isotropy subgroup. Let us now consider the same net for the initial marking $\begin{pmatrix}1 & 1 & 1\end{pmatrix}^T$ with isotropy subgroup $\Sigma^s_{\mathcal{N}}$. The subsequent markings $\begin{pmatrix}0 & 2 & 1\end{pmatrix}^T$ and $\begin{pmatrix}0 & 1 & 2\end{pmatrix}^T$ have trivial isotropy subgroup but are equivalent. ♢

It follows from the equivalence (3.6) that it is a general property of place/transition nets that firing equivalent transitions from a symmetric marking m results in equivalent markings. If the reduction is performed with respect to some subgroup $\Sigma \subset \Sigma_m$ and t is enabled in $m = \sigma(m)$ with $m[t > m'$, then $m[\sigma(t) > \sigma(m')$.

The example furthermore shows that firing can create or destroy symmetries of markings. In continuous Petri nets, the individual firings become somewhat "blurred"

[3] See [Jun03, pp. 6–8] for an overview of symmetry methods in model checking of Petri nets.

such that the flow through the two transitions is identical. Thus, the isotropy subgroup of the marking cannot change over time. This fact is discussed in detail in the course of this chapter and can be used for a reduction.

For the upcoming considerations, we also use the following property.[4]

Lemma 3.15. *Let $\mathcal{N}$ be a Petri net and $\sigma \in \Sigma^w_{\mathcal{N}}$. Then $\sigma(^\bullet t) = {}^\bullet(\sigma(t))$ for all $t \in \mathcal{T}$.*

Proof. Let $t \in \mathcal{T}$. We have $p \in {}^\bullet(\sigma(t))$ if and only if $Pre_{p,\sigma(t)} \neq 0$. As $\sigma \in \Sigma^w_{\mathcal{N}}$, this is equivalent to $Pre_{\sigma^{-1}(p),t} \neq 0$, i.e., $\sigma^{-1}(p) \in {}^\bullet t$ and therefore $p \in \sigma(^\bullet t)$. □

3.2.3 Computation of Symmetries

Symmetry reduction is a powerful technique in the analysis and model checking of highly structured Petri nets. In order to compute the symmetries we may use standard tools for the graph automorphism problem that support directed and labeled graphs. However, these are usually not optimized for sparse and directed graphs [Jun03, p. 28]. Against this background, efficient algorithms have been developed for computing such symmetries and have been implemented, for instance, in the software LoLA[5] which is integrated in several Petri net tools.

The algorithm in [Sch00a] is designed for very general classes of Petri nets with arbitrary inscriptions assigned to arcs and nodes. If we interpret arc weights and firing rates as inscriptions in this sense, the algorithm can be used in order to compute $\Sigma^s_{\mathcal{N}}$ and $\Sigma^t_{\langle \mathcal{N},\lambda\rangle}$. The principle also works for $\Sigma^w_{\mathcal{N}}$.

The computation of symmetries is performed by a backtracking algorithm (see, e.g., [Sed88]) which we sketch here. The idea is to systematically generate partial candidate solutions which can then be completed to symmetries of the Petri net. It uses *constraints* of the form $A \mapsto B$ for $A, B \subset (\mathcal{P} \cup \mathcal{T})$ where a permutation of nodes σ is *consistent* with $A \mapsto B$ if $\sigma(A) = B$. A set of constraints forms a *symmetry specification* and σ is consistent with a symmetry specification if it is consistent with all constraints contained in it.

[4] A similar result has been shown in [Sta90, p. 63].
[5] http://wwwteo.informatik.uni-rostock.de/ls_tpp/lola/index.htm

The condition that permutations have to respect the node type can by expressed by the two constraints $\mathcal{P} \mapsto \mathcal{P}$ and $\mathcal{T} \mapsto \mathcal{T}$. The preservation of firing rates can be assured by constraints of this form with $A = B = \{t \in \mathcal{T} : \ \lambda_t = \alpha\}$ for every possible firing rate $\alpha > 0$. Any symmetry of the net can be defined by such a symmetry specification. The easiest representation is by singletons, i.e., for nodes $v, v' \in \mathcal{P} \cup \mathcal{T}$ the equality $\sigma(v) = v'$ is assured by $\{v\} \mapsto \{v'\}$. In the backtracking algorithm, symmetries are gradually constructed by adding constraints to the symmetry specification.

The computation of symmetries is performed by the exploration of a tree. An operation called DEFINE corresponds to branching nodes in the tree by adding constraints. A REFINE-operation is then used to narrow a specification and to prune the search tree by checking if candidate solutions can be completed to symmetries. Afterwards, the DEFINE-operation is applied again and so on. This is most easily understood considering the following example from [Sch00a, Example 2] which shows the stepwise refinement of constraints until the symmetry specification represents a single automorphism. For a full definition of the operations, the reader is referred to the original paper.

Example 3.16. We want to compute the symmetries of the net graph in Figure 3.2(a). The search tree generated in the backtracking search is shown in Figure 3.2(b). Initially, it is only required that a solution respects the node type. With every application of the DEFINE-operation new constraints are added and hence new branches in the tree are generated. The REFINE-operation then adds constraints which necessarily have to be satisfied by the candidate solution. Pruning with the REFINE-operation avoids an exhaustive search. Finally, two graph automorphism including the trivial symmetry are given by constraints on every single node. ♢

The reductions of Chapter 4 sometimes require to compute not the entire symmetry group of a TCPN but the isotropy subgroup of the initial marking. This can be achieved by including the constraints $A \mapsto B$ with $A = B = \{p \in \mathcal{P} : \ (m_0)_p = a\}$ for all possible markings $a \in \{(m_0)_p : \ p \in \mathcal{P}\}$.

In [Sch00a, Sch00b, Jun03] it is explained how this algorithm can be used in the generation of a reduced reachability graph that — for some subgroup of $\Sigma^s_{\mathcal{N}}$ —

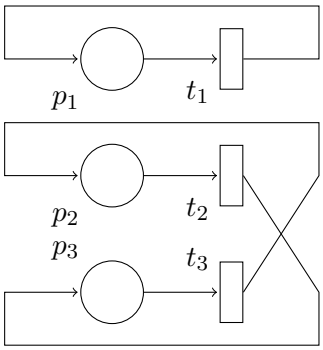

(a) The Petri net

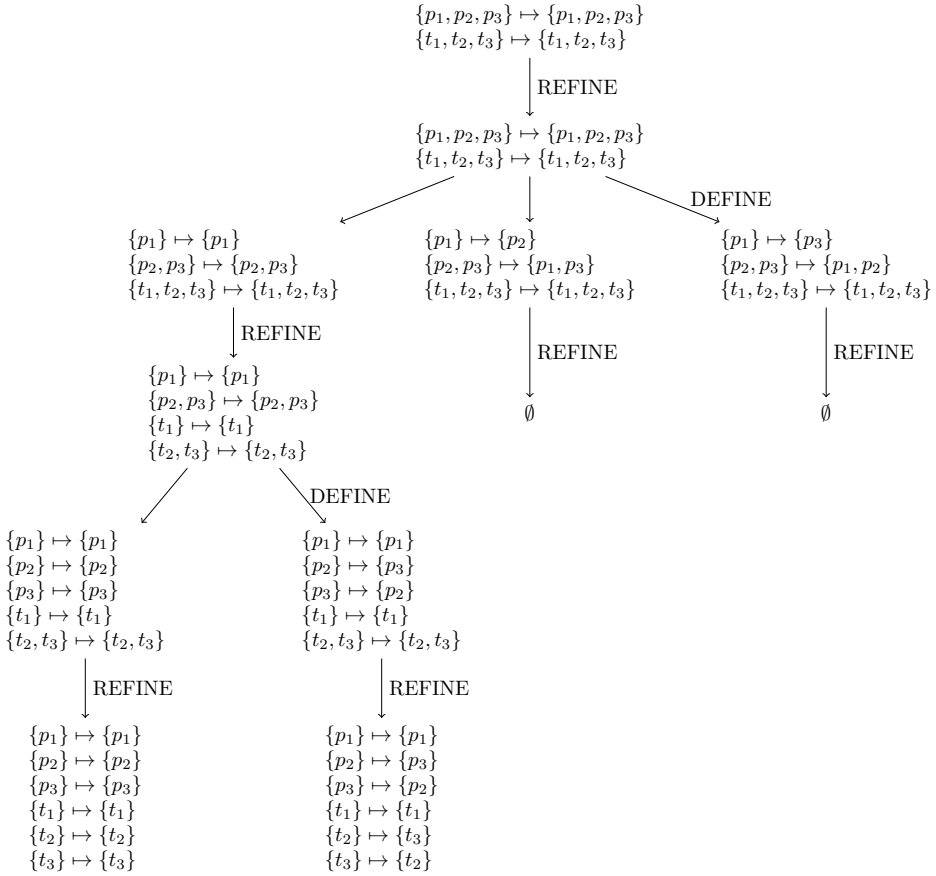

(b) The search tree

Figure 3.2: Computation of symmetries with a backtracking algorithm (adapted from [Sch00a, Example 2]).

contains the markings reachable from m_0 only up to symmetry. The complexity of this and related problems is discussed in detail in the latter publication where also variations of the algorithm are explained.

In [Sta91] a place/transition net with k transition, $2k$ places, and $k \cdot 2^k$ symmetries is shown. Therefore, it is not possible to find an algorithm that computes all symmetries and is polynomial in the size of the net. However, algorithms to compute generating sets for the symmetries which are polynomial in the size of the net are known [Sch00a]. For the algorithm sketched above, polynomial implementations of the split- and refine operations exist. And even though no polynomial-time algorithm is known for computing the symmetries of a net, in practice, even large problems can be solved efficiently [Sch00a, JK09].

3.3 Permutation of Configurations

Let $m \in \mathbb{R}_{\geq 0}^{|\mathcal{P}|}$ be a marking such that configuration $K \in \mathcal{K}_{\mathcal{N}}$ is active. We apply a permutation $\sigma \in \Sigma_{\mathcal{N}}^{w}$. Which configuration K' is active under the new marking $\sigma(m)$? We show that σ actually transfers the entire polyhedron M_K into $M_{K'}$.

Theorem 3.17. *For a Petri net $\mathcal{N}$ let $\sigma \in \Sigma_{\mathcal{N}}^{w}$ and $K \in \mathcal{K}_{\mathcal{N}}$. The map*

$$K' : \mathcal{T} \to \mathcal{P},\ t \mapsto \sigma(K(\sigma^{-1}(t)))$$

is a configuration of $\mathcal{N}$. If $m \in M_K$, then $\sigma(m) \in M_{K'}$.

Proof. Let $t \in \mathcal{T}$. Since K is a configuration, $K(\sigma^{-1}(t)) \in {}^\bullet(\sigma^{-1}(t))$ holds for every $t \in \mathcal{T}$. Application of Lemma 3.15 yields $K'(t) = \sigma(K(\sigma^{-1}(t))) \in \sigma(\sigma^{-1}({}^\bullet t)) = {}^\bullet t$. Therefore, K' is a configuration.

Let $m \in M_K$. For $M_{K'}$ to be active under $S_\sigma m$ we have to show that for all $t \in \mathcal{T}$ and all $p \in {}^\bullet t$

$$\frac{(\sigma(m))_{K'(t)}}{Pre_{K'(t),t}} \leq \frac{(\sigma(m))_p}{Pre_{p,t}}.$$

We fix a $t \in \mathcal{T}$. As $m \in M_K$, we know that

$$\frac{m_{K(t)}}{Pre_{K(t),t}} \leq \frac{m_p}{Pre_{p,t}} \text{ for all } p \in {}^\bullet t$$

and

$$\frac{m_{K(\sigma^{-1}(t))}}{Pre_{K(\sigma^{-1}(t)),\sigma^{-1}(t)}} \leq \frac{m_p}{Pre_{p,\sigma^{-1}(t)}} \text{ for all } p \in {}^\bullet(\sigma^{-1}(t)).$$

As ${}^\bullet(\sigma^{-1}(t)) = \sigma^{-1}({}^\bullet t)$, the second inequality can be written as

$$\frac{m_{K(\sigma^{-1}(t))}}{Pre_{K(\sigma^{-1}(t)),\sigma^{-1}(t)}} \leq \frac{m_{\sigma^{-1}(p)}}{Pre_{\sigma^{-1}(p),\sigma^{-1}(t)}} \text{ for all } p \in {}^\bullet t.$$

Therefore, for all $p \in {}^\bullet t$

$$\frac{(\sigma(m))_{K'(t)}}{Pre_{K'(t),t}} = \frac{m_{K(\sigma^{-1}(t))}}{Pre_{K(\sigma^{-1}(t)),\sigma^{-1}(t)}} \leq \frac{m_{\sigma^{-1}(p)}}{Pre_{\sigma^{-1}(p),\sigma^{-1}(t)}} = \frac{(\sigma(m))_p}{Pre_{p,t}}.$$

□

This means that the map

$$\pi_\sigma : \mathcal{K}_\mathcal{N} \to \mathcal{K}_\mathcal{N}, K \mapsto \sigma \circ K \circ \sigma^{-1} \tag{3.7}$$

is a permutation of configurations. Its inverse map is $\pi_{\sigma^{-1}}$ as for all $K \in \mathcal{K}_\mathcal{N}$

$$\pi_\sigma(\pi_{\sigma^{-1}}(K)) = \sigma \circ (\sigma^{-1} \circ K \circ \sigma) \circ \sigma^{-1} = K$$

since the composition of functions is always associative. It tells us to which region a marking is mapped by S_σ. A symmetry as a permutation of the nodes therefore induces a permutation of the polyhedral cells underlying the piecewise linear vector field F.

Remark 3.18. An alternative way to state Theorem 3.17 is via the matrices G_K as introduced in Section 2.3.2. The basic idea is that $m \in M_K$ requires $G_K m \leq 0$. For $S_\sigma m$ we then search for the configuration K' with $G_{K'} S_\sigma m \leq 0$. When we study the matrix product $G_{K'} S_\sigma$, we observe that $G_{K'} S_\sigma \cong G_K$ where $\cong$ denotes equality

up to the order of the rows which is irrelevant for the description of the regions. The map π_σ is then defined such that a configuration K is mapped on that configuration K' with $G_{K'}S_\sigma \cong G_K$. These results are stated in detail in [MD09].

Using the alternative description of M_K via matrices G_K^L as in Equation 2.9, the corresponding equality $G_K^L \cong G_{\pi_\sigma(K)}^L S_\sigma$ is easy to prove using the upcoming matrix equality (3.8).

In this thesis, however, π_σ is defined according to (3.7) as it is an immediate application of the definition of symmetries without the intermediate step via the regions. Furthermore, the consideration via regions requires a restriction to nonredundant configurations introducing unnecessary technical details wherever π_σ is used.

3.4 Equivariant Dynamics in TCPNs

In the previous section, the effects of symmetries in the net structure on the polyhedral partition have been discussed. Now, we address the effects on the dynamics. Recall that the system matrices are of the form $A_K = C\Lambda\Pi_K$ ($K \in \mathcal{K}_\mathcal{N}$). Lemma 3.11 established a link between the matrices C and Λ and the permutation of the nodes by saying that $S_\sigma C = CT_\sigma$ and $T_\sigma\Lambda = \Lambda T_\sigma$ if $\sigma \in \Sigma^t_{\langle\mathcal{N},\lambda\rangle}$. The following lemma claims a similar connection for Π_K.

Lemma 3.19. *Let $\langle\mathcal{N},\lambda\rangle$ be a timed Petri net and σ a permutation of its nodes. If $\sigma \in \Sigma^w_\mathcal{N}$, then for all $K \in \mathcal{K}_\mathcal{N}$*

$$T_\sigma\Pi_K = \Pi_{\pi_\sigma(K)}S_\sigma. \tag{3.8}$$

Proof. Let $\sigma \in \Sigma^w_\mathcal{N}$. For $(t,p) \in \mathcal{T}\times\mathcal{P}$

$$\begin{aligned}(T_\sigma\Pi_K)_{t,p} &= \sum_{t'\in\mathcal{T}} \delta_{\sigma^{-1}(t),t'}(\Pi_K)_{t',p} = (\Pi_K)_{\sigma^{-1}(t),p}\\ &= \begin{cases}\frac{1}{Pre_{p,\sigma^{-1}(t)}} & \text{if } K(\sigma^{-1}(t)) = p,\\ 0 & \text{otherwise,}\end{cases}\end{aligned}$$

$$(\Pi_{\pi_\sigma(K)} S_\sigma)_{t,p} = \sum_{p' \in \mathcal{P}} (\Pi_{\pi_\sigma(K)})_{t,p'} \delta_{\sigma^{-1}(p'),p} = (\Pi_{\pi_\sigma(K)})_{t,\sigma(p)}$$
$$= \begin{cases} \frac{1}{Pre_{\sigma(p),t}} & \text{if } \pi_\sigma(K)(t) = \sigma(p), \\ 0 & \text{otherwise.} \end{cases}$$

The equality of the two matrices follows immediately from $Pre_{p,\sigma^{-1}(t)} = Pre_{\sigma(p),t}$ and $K(\sigma^{-1}(t)) = p \Leftrightarrow \pi_\sigma(K)(t) = \sigma(K(\sigma^{-1}(t))) = \sigma(p)$. □

Having studied the effects of symmetries in the net structure on both the polyhedral partition and the system matrices, we now consider the entire vector field F as defined in Equation (2.11).

Theorem 3.20. *Let $\langle \mathcal{N}, \lambda \rangle$ be a timed Petri net and $\sigma \in \Sigma^t_{\langle \mathcal{N},\lambda \rangle}$. Then,*

$$S_\sigma \circ F = F \circ S_\sigma. \tag{3.9}$$

Proof.

$$\begin{aligned} S_\sigma F(m) &= S_\sigma C \Lambda \Pi_K m \overset{(3.3),(3.4)}{=} C T_\sigma \Lambda \Pi_K m \\ &\overset{(3.5)}{=} C \Lambda T_\sigma \Pi_K m \overset{(3.8)}{=} C \Lambda \Pi_{\pi_\sigma(K)} S_\sigma m \\ &= F(S_\sigma m) \end{aligned}$$ □

This is an equivariance condition as in Definition 3.2. That is, F is equivariant with respect to the group action of $\Sigma^t_{\langle \mathcal{N},\lambda \rangle}$. Let us note that $\Sigma^t_{\langle \mathcal{N},\lambda \rangle}$ is a proper subgroup of the symmetry group of the system. As seen in Example 3.3, any dilation κI ($\kappa > 0$) is also a symmetry. In contrast to the group of dilations, $\Sigma^t_{\langle \mathcal{N},\lambda \rangle}$ is finite as the number of permutations of the finite set of nodes is bounded by $|\mathcal{P}|! \cdot |\mathcal{T}|!$ (cf. [Jun03]).

Due to this theorem, we may apply the results for general equivariant systems that are stated in Section 3.1 to continuous Petri nets with symmetries. In particular, we know that isotropy subgroups remain constant along trajectories and that fixed-point sets

$$\mathrm{Fix}(\Sigma) = \{m \in \mathbb{R}^{|\mathcal{P}|}_{\geq 0} : S_\sigma m = m \text{ for all } \sigma \in \Sigma\},$$

where $\Sigma \subset \Sigma^t_{\langle \mathcal{N},\lambda \rangle}$ is a subgroup, are invariant under the flow of the vector field F.

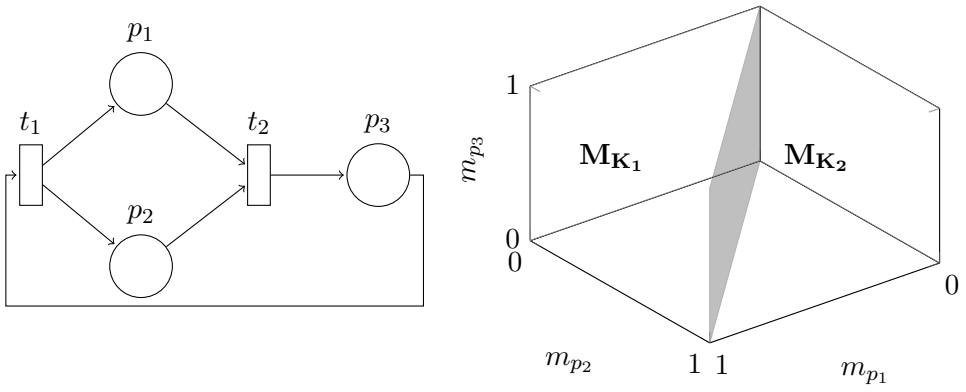

(a) (b)

Figure 3.3: A symmetric Petri net and the corresponding partition of the phase space. The gray surface represents $\mathrm{Fix}(\Sigma^t_{\langle\mathcal{N},\lambda\rangle})$.

We now apply this result to a Petri net in order to illustrate how symmetries can assist us in the analysis of continuous nets.

Example 3.21. Let us consider the Petri net in Figure 3.3. It has two configurations, K_1 with $K_1(t_2) = p_1$ and K_2 with $K_2(t_2) = p_2$. It is symmetric with $\Sigma^t_{\langle\mathcal{N},\lambda\rangle} = \{id, (p_1\, p_2)\}$. The corresponding fixed-point set is $\mathrm{Fix}(\Sigma^t_{\langle\mathcal{N},\lambda\rangle}) = \{m \in \mathbb{R}^3_{\geq 0} : m_{p_1} = m_{p_2}\}$. This set coincides with the hyperplane separating M_{K_1} and M_{K_2}. As the fixed-point set is flow-invariant, a trajectory starting in M_{K_1} cannot cross it and continue in M_{K_2} and vice versa. Thus, the sets M_{K_1} and M_{K_2} are flow-invariant, too. Note that this result is independent of the explicit system of differential equations. ♢

The equivariance condition tells us that if m is a solution with respect to the initial marking m_0, then $S_\sigma m$ solves the system for the initial marking $S_\sigma m_0$. In particular, S_σ maps steady states onto steady states. If a system with initial marking m_0 approaches a steady state with associated flow vector f^*, then the system also converges to a steady state for the initial marking $S_\sigma m_0$ and the resulting flow vector is $T_\sigma f^*$. More generally, we may deduce from the equivariance condition that the dynamics in two regions that permute are effectively the same. It is therefore sufficient to study one region M_K to understand the behavior in all regions $\{M_{\pi_\sigma(K)} : \sigma \in \Sigma^t_{\langle\mathcal{N},\lambda\rangle}\}$. In this sense, symmetric systems carry some redundancy. In the

next chapter we explain how to remove this redundancy in symmetric Petri nets by reducing either the corresponding vector field or the net itself.

3.5 Symmetries in Polyhedral Piecewise Linear Systems

For continuous Petri nets, we have seen that a symmetry in the net structure induces a permutation of the configurations in a way that configurations are mapped onto configurations with similar system matrices ($A_{\pi_\sigma(K)} = S_\sigma A_K S_\sigma^{-1}$). The vector field F commutes with the permutation of places. We now consider the situation from the reverse angle. Suppose that F satisfies an equivariance condition of the form (3.9). Does this equivariance come along with a permutation of the configurations? The answer is yes, and what is more, this is true for general piecewise linear systems and any linear transformation of variables as the following theorem shows.

Lemma 3.22. *Let $((X_i)_{i\in I}, (A_i, a_i)_{i\in I})$ be a continuous polyhedral piecewise linear system in which two neighboring polyhedra have different dynamics, i.e., $(A_i, a_i) \neq (A_j, a_j)$ if X_i and X_j have a common facet. Let G denote the corresponding piecewise linear vector field defined on $X = \bigcup_{i\in I} X_i \subset \mathbb{R}^n$ given by $G : X \to \mathbb{R}^n$, $x \mapsto A_i x + a_i$ for $x \in X_i$.*

Let $\phi \in GL(n)$ be such that $\phi(X) = X$. If ϕ is a symmetry of $\dot{x} = G(x)$, i.e., $G \circ \phi = \phi \circ G$, it maps regions on regions.

Proof. Let $i \in I$. We have to show that there exists an index $j \in I$ such that $\phi(X_i) = X_j$. We start with a proof by contradiction that boundary points of X_i are mapped onto boundary points. Let $x \in \partial X_i$. Then, there exists an index $j \in I$ where possibly $i = j$ such that $\phi(x) \in X_j$. We assume that $\phi(x) \in \mathrm{int}(X_j)$.

Let $U \subset X_j$ be a neighborhood of $\phi(x)$. Since ϕ is a homeomorphism, $V := \phi^{-1}(U)$ is a neighborhood of x. This means that x is an interior point of X. As it is also on the boundary of X_i, there has to exist $k \in I$ such that X_i and X_k share a facet and $x \in X_i \cap X_k$. Thus, $V \cap X_k$ has a nonempty interior. It follows from the equivariance

condition $\phi \circ G = G \circ \phi$ that for all $x' \in \operatorname{int}(V \cap X_k)$

$$\begin{aligned} \phi(A_k x' + a_k) = \phi G(x') = G(\phi x') = A_j \phi x' + a_j \\ \Leftrightarrow (A_j \phi - \phi A_k) x' = \phi a_k - a_j. \end{aligned}$$

This linear system of equations can only be satisfied by all $x' \in \operatorname{int}(V \cap X_k)$ if $A_j \phi - \phi A_k = 0$ and $\phi a_k - a_j = 0$. With the same argument for $x' \in \operatorname{int}(V \cap X_i)$ it follows that $A_i = A_k$ and $a_i = a_k$ which contradicts the assumption that $(A_i, a_i) \neq (A_k, a_k)$ if X_i and X_j share a facet. Therefore, $\phi(x)$ has to be on the boundary of X_j. Since ϕ^{-1} is also a symmetry, it follows immediately that ϕ maps interior points of the polyhedra onto interior points.

We have shown that $\phi(\operatorname{int}(X_i)) \subset \bigcup_{j \in I} \operatorname{int}(X_j)$. Furthermore, $\phi(\operatorname{int}(X_i))$ is the image of a simply connected set under a continuous function and is thus connected itself. Thus, $\phi(X_i) \in \{X_j : j \in I\}$. □

Theorem 3.23. *Let $((X_i)_{i \in I}, (A_i, a_i)_{i \in I})$ and $\phi \in GL(n)$ be the piecewise linear system and the symmetry from Lemma 3.22, respectively. The map*

$$\pi_\phi : I \to I,\ i \mapsto j \text{ such that } \phi(X_i) = X_j$$

is bijective and $\pi_\phi^{-1} = \pi_{\phi^{-1}}$. That is, π_ϕ is a permutation of the polyhedral cells induced by ϕ.

Proof. Because of the previous lemma π_ϕ is well-defined. Bijectivity follows immediately from the fact that ϕ is bijective and I is finite. □

The theorem also holds for discontinuous systems if $\phi \circ G = G \circ \phi$ is interpreted as an equality of sets where $G(x) = \{A_i x + a_i : x \in X_i\}$ and the differential inclusion $\dot{x} \in G(x)$ is considered. Continuity of G has only been used in the proof of the lemma which can easily be extended for discontinuous systems. For $x \in X$ either $|G(x)| = 1$ and the above reasoning can be used or $|G(\phi(x))| = |\phi(G(x))| > 1$ and both x and $\phi(x)$ have to be boundary points. However, results about equivariant dynamics such as invariant fixed-point subspaces cannot be applied in a straightforward manner.

4

Reduction Techniques

Fluidification has been introduced as a technique to deal with the state explosion problem. Then again, it is claimed in [JTMZ01] that net reduction is one of the most important techniques to deal with the problem. In this chapter, both approaches are combined where the reductions are based on the result about symmetry stated in the previous chapter. We follow two different approaches. First, the piecewise linear system associated with a TCPN is reduced with respect to flow-invariant affine subspaces without modifying the net itself. Second, a reduced net is set up by exploiting symmetries. Each node of the reduced net represents an equivalence class of nodes of the original one. The derivation of the reduction procedure and the proof of its correctness is based on the first reduction method.

4.1 Classic Transformations and Reductions

A great variety of transformations of Petri nets are known to simplify verification and analysis tasks. They range from the fusion of nodes to the removal of entire subnets. A traditional approach in verification is to apply transformations that preserve a specific relevant property of the net such as boundedness, safety, or liveness (see [Ber86, Ber87] and references therein for the case of ordinary Petri nets) or the support of $\mathcal{P}$-invariants (see [JD93]). The resulting net is expected to be easier to analyze with respect to that property. With some reduction rules, as in the case of [HJC05], the original and the reduced systems are not equivalent with respect to liveness or boundedness but these properties are easy to verify after the reduction. The overall behavior of the net may change significantly.

In [LFB87] and [KD91], reduction techniques for general place/transition nets, i.e., allowing arc weights different from 1, are formulated. The idea behind these techniques is to condense the net by representing simple subnets by single nodes in a way that liveness, boundedness, and proper termination are preserved. In contrast to ordinary nets, arc weights of incoming and outgoing arcs of the subnet might have to be adapted. A popular technique is the removal of (structural) implicit places which are redundant places that do not affect the enabling degree of transitions (cf. [STC98, ES91]). This technique is known for various types of Petri nets (cf. [SJMV11, RMS06, ADFN99]). Their counterparts in the set of transitions are structural bypasses (see [ES91]).

Reduction techniques developed for untimed nets are usually not valid for timed systems. In [JTMZ01], it is illustrated that in time Petri nets, where timing is associated with places and firing occurs in fixed time intervals, deadlock freeness is not even preserved in very simple nets. Reduction rules for the class of delay time Petri nets are suggested guaranteeing schedule and deadlock equivalence. Similarly, in [SB96], the reduction techniques for ordinary untimed nets described in [Ber86] are extended to time Petri nets and extended by rules to reduce redundant places. The reduced net is considered to be equivalent to the original net if occurrence sequences and safety are preserved.

In stochastic Petri nets, the focus is typically on performance analysis. This task is directly affected by the state explosion problem as the size of the corresponding

continuous time Markov chain (CTMC) depends directly on the number of reachable markings. Reduction rules for such nets are not designed to preserve a specific property such as liveness. Instead, the reduced net should represent the behavior of the original one, meaning that its corresponding CTMC aggregates the performance prediction of the original net without altering the values (see [ADFN99]). This is sometimes called *exhibited behavior equivalence* [SA92]. Some of the reduction rules defined in the two last mentioned articles remove immediate transitions from generalized stochastic Petri nets (GSPNs). If all such transitions can be removed the resulting net is a stochastic Petri net (SPN) with exponentially distributed firing delays which could then be interpreted as a continuous net.

An example of a reduction technique for (G)SPNs is the deletion of timed transitions that do not modify the marking (see reduction rule RR_2 in [ADFN99]). If the firing of a transition does not change the marking of the net, it may be deleted together with all its input and output arcs. Other rules, like the deletion of implicit places, are in general not purely structural as they depend on the initial marking and can therefore be applied to net systems only.

Let us consider reduction rule RR_{11} "Folding of identical subnets" in the same publication as it provides an example of symmetry reduction. We assume that the net contains identical subnets which are ordinary state machines. We further assume that input arcs to each subnet go to a single place and that arcs out of each subnet enter a place common to all subnets. Under these conditions all but one subnet can be removed. This rule eliminates "symmetries from the underlying stochastic process, corresponding to a lumping of the CTMC underlying the GSPN" [ADFN99]. The reduction method proposed in Section 4.3 can be understood as an extension to this rule that can be applied to far more general types of subnets and provides a structured procedure based on the definitions and results of the previous chapter.

In TCPNs, we use transformations such that the original marking trajectory can be obtained from that of the reduced system by a linear transformation. Always assuming infinite server semantics, the easiest such transformations are the $\mathcal{T}$*-rule* and the $\mathcal{P}$*-rule* that change the weights of the input and output arc of a transition or place, respectively.[1] Take the net in Figure 4.1(a). Multiplying both w_1 and w_2 by

[1] This rule was illustrated by M. Silva in a personal communication in May 2010.

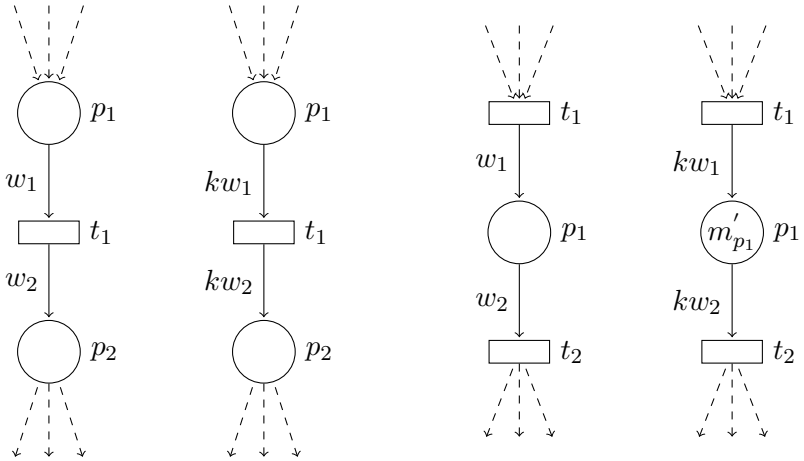

(a) $\mathcal{T}$-rule

(b) $\mathcal{P}$-rule

Figure 4.1: Transformation rules for TCPNs.

some constant $k > 0$ does not change the dynamical system associated with the net. To see this, consider, on the one hand, the marking flow that leaves p_1. It is given by $Pre_{p_1,t} \cdot \lambda_{t_1} \frac{m_{p_1}}{Pre_{p_1,t}} = \lambda_{t_1} m_{p_1}$, i.e., it is independent of the arc weight.[2] The marking flow entering place p_2 is not affected either as it is given by $Post_{p_2,t} \lambda_{t_1} \frac{m_{p_1}}{Pre_{p_1,t}} = kw_2 \lambda_{t_1} \frac{m_{p_1}}{kw_1} = w_2 \lambda_{t_1} \frac{m_{p_1}}{w_1}$ as in the original net. Similarly, we can multiply the arc weights in the subnet in Figure 4.1(b) by a factor $k > 0$. The computations are analogous to the previous case. However, also the initial marking of p_1 has to multiplied by k and the original continuous marking of that place is obtained if the resulting marking m'_{p_1} is divided by k. At any time $\tau > 0$, the marking of the original system can be obtained from the transformed one by multiplication of its marking by k at that point in time. These rules may not be applied to discrete nets where the enabling degree is always given by a nonnegative integer.

The transformations considered so far use the following principle: first, a specific local structure is identified in the net, e.g., implicit places. Then, certain nodes and arcs are being removed. Finally, arc weights or firing rates might have to be adapted.

[2] This is a distinctive property of continuous Petri nets where transitions are enabled if all their input places are marked independent of the particular amount of fluidified tokens. Furthermore, the enabling degree is a rational number. It is this property that makes some discrete nets being not well approximated by continuous ones if the enabling degree is generally low.

In the upcoming sections, two different approaches are presented that take advantage of the global structure of the net. To start with, reductions are performed on a purely mathematical level, meaning that the dimension of the system of the associated piecewise linear system is lowered while the net remains unchanged. The results are then used to transform the net itself. The advantage over the purely mathematical reduction is that the net becomes more manageable for the human modeler and further reduction techniques that use local structures may be performed.

4.2 Reductions of the PWL System Associated with a TCPN System

4.2.1 Reduction to Flow-Invariant Affine Subspaces

This section is dedicated to a reduction approach that can be applied to the piecewise linear system associated with a TCPN system. The result is a piecewise linear system of smaller dimension. The net itself is not changed and, in general, there exists no direct interpretation of the reduced dynamical system in terms of the Petri net. However, trajectories of the reduced system provide exact solutions to the original system after an (affine) linear transformation. The approach has already been published in an alternative formulation in [MDH11]. It can be applied whenever there exist flow-invariant (affine) subspaces, i.e., sets such that marking trajectories with an initial marking in that set remain there for all time. Two such subspaces we already know of. Since C appears as the first factor in the system matrices of all regions (cf. Equation (2.12)), only markings in $m_0 + \mathrm{im}(C)$ can be reached. This is equivalent to saying that reachable markings satisfy the conservation laws imposed by $\mathcal{P}$-invariants. Similarly, symmetries in the net structure and initial marking give rise to a flow-invariant set, namely the fixed-point set $\mathrm{Fix}(\Sigma_{m_0})$.

The reduction results in a PWL system whose dimension is the same as the dimension of the flow-invariant (affine) subspace. However, the benefits are not restricted to the fact that the new system is of smaller dimension. The reduction with respect to $\mathrm{Fix}(\Sigma_{m_0})$ serves as a basis for a symmetry reduction on the net level later in this chapter and the reduction with respect to $m_0 + \mathrm{im}(C)$ allows the analysis of parameter-dependent systems carried out in Chapter 5.

The idea is the following. Let a flow-invariant, affine, linear subspace containing m_0 be given by $m' + U$ for some d-dimensional linear subspace U. Let $D \in \mathbb{R}^{|\mathcal{P}| \times d}$ be a matrix whose columns are a basis of U. Then, for any reachable marking m, there exists a unique $\widetilde{m} \in \mathbb{R}^d$ with $m = m' + D\widetilde{m}$. We therefore rewrite the PWL system associated with the TCPN system in terms of this new variable $\widetilde{m}$.

The reduction uses properties of the Moore-Penrose pseudoinverse which we recall here briefly. Alternative definitions and numerous properties are stated, e.g., in [CM79, Cli79, BG74].

Definition 4.1. *(Penrose definition of the generalized inverse) If $A \in \mathbb{C}^{m \times n}$, then the* Moore-Penrose pseudoinverse *$A^+ \in \mathbb{C}^{n \times m}$ is the unique matrix such that*

1. *$AA^+A = A$,*
2. *$A^+AA^+ = A^+$,*
3. *AA^+ and A^+A are hermitian.*

The following properties of the generalized inverse are used in this chapter.

Lemma 4.2. *Let $A \in \mathbb{C}^{m \times n}$ and A^+ its Moore-Penrose pseudoinverse.*

1. *$A^+x = 0$ if $x \in \mathrm{im}(A)^\perp$.*
2. *AA^+ is the orthogonal projector of $\mathbb{C}^m$ onto $\mathrm{im}(A)$, i.e., $AA^+x = x$ if $x \in \mathrm{im}(A)$ and $AA^+x = 0$ if $x \in (\mathrm{im}(A))^\perp$.*
3. *If A has full row rank, then $A^+ = A^*(AA^*)^{-1}$ and $AA^+ = I_m$. If A has full column rank, then $A^+ = (A^*A)^{-1}A^*$ and $A^+A = I_n$.*

Proof. See [CM79, p. 9] for the first two properties and [Cli79, p. 13] for the last one. □

We now use these properties for the study of the dynamical system associated with a TCPN system

$$\dot{m} = F(m), \quad m(0) = m_0 \tag{4.1}$$

with $F : \mathbb{R}_{\geq 0}^{|\mathcal{P}|} \to \mathbb{R}^{|\mathcal{P}|}$, $m \mapsto A_K m = C\Lambda\Pi_K m$ for $m \in M_K$. If there exists a flow-invariant (affine) subspace of dimension $d < |\mathcal{P}|$, then an equivalent initial value problem can be posed on a d-dimensional space.

Theorem 4.3. *Let $U \subset \mathbb{R}^{|\mathcal{P}|}_{\geq 0}$ be a linear subspace of dimension d and let $m' \in \mathbb{R}^{|\mathcal{P}|}_{\geq 0}$ be such that $m_0 \in m' + U$. Let $D \in \mathbb{R}^{|\mathcal{P}| \times d}$ be a matrix whose columns are a basis of U.*

If $(m' + U) \cap \mathbb{R}^{|\mathcal{P}|}_{\geq 0}$ is flow-invariant with respect to F, then the reduced system

$$\begin{cases} \dot{\widetilde{m}} = D^+ F(D\widetilde{m} + m') = (D^+ A_K D)\widetilde{m} + (D^+ A_K m') \text{ if } m' + D\widetilde{m} \in M_K \\ \widetilde{m}(0) = D^+(m_0 - m') \end{cases} \tag{4.2}$$

is equivalent to the original system in the sense that $\widetilde{m} : [0, \infty) \to \mathbb{R}^d$ is a solution to the reduced system (4.2) if and only if $m = m' + D\widetilde{m}$ solves system (4.1).

Proof. The reduced PWL system is also continuous as it results from the composition of the original continuous system with smooth functions. Thus, the existence and uniqueness of a solution is guaranteed.

Let $\widetilde{m}$ solve the reduced system and $m = m' + D\widetilde{m}$. The initial value condition is satisfied since $m(0) = m' + D\widetilde{m}(0) = m' + DD^+(m_0 - m') = m' + m_0 - m' = m_0$. The second last equality holds since $m_0 - m' \in U$.

In addition, m satisfies the differential equation

$$\begin{aligned} \frac{d}{d\tau} m(\tau) &= \frac{d}{d\tau}(m' + D\widetilde{m}(\tau)) = D\dot{\widetilde{m}}(\tau) \\ &= DD^+ \underbrace{F(D\widetilde{m}(\tau) + m')}_{\in U} = F(D\widetilde{m}(\tau) + m') = F(m(\tau)) \end{aligned}$$

Let now m solve the original system and let $\widetilde{m}$ be such that $m = m' + D\widetilde{m}$. The initial value condition is obviously satisfied since

$$\widetilde{m}(0) = D^+ D\widetilde{m}(0) = D^+(m(0) - m') = D^+(m_0 - m').$$

For the differential equation, we obtain

$$\begin{aligned} \frac{d}{d\tau}\widetilde{m}(\tau) &= \frac{d}{d\tau} \underbrace{D^+ D}_{=I_d} \widetilde{m}(\tau) = \frac{d}{d\tau} D^+(D\widetilde{m}(\tau) + m') \\ &= \frac{d}{d\tau} D^+ m(\tau) = D^+ F(m(\tau)) = D^+ F(m' + D\widetilde{m}(\tau)). \end{aligned}$$

□

In the same way, we say that $m : [0, \infty) \to \mathbb{R}^{|\mathcal{P}|}_{\geq 0}$ solves the original system if and only if $D^+(m - m')$ solves the reduced one. This follows immediately from the above theorem as $D^+(m-m')$ solves the reduced system if and only if $m' + D(D^+(m-m'))$ solves the original one. As m is a solution, we have $m(\tau) \in m' + U$ for all $\tau \geq 0$ and therefore $m' + DD^+(m - m') = m$.

In general, the reduced system that we obtain is piecewise affine. The canonical choice of m' would then be m_0. However, if $m_0 \in U$, we can choose $m' = 0$ and the affine part $D^+ A_K m'$ vanishes.

Simulations of the reduced system can be conveniently run using the Matlab tool PWLTool (cf. [HJ99b, HJ99a]). The tool needs the system matrices and the matrices describing the reduced polyhedral regions as an input. The reduced system matrices are obtained from the original system matrices by simple matrix multiplications. The new regions $\widetilde{M}_K$ ($K \in \mathcal{K}_\mathcal{N}$) are again polytopes which can be described by a system of linear inequalities, namely

$$\begin{aligned}
\widetilde{M}_K &= \{\widetilde{m} \in \mathbb{R}^d : \ m' + D\widetilde{m} \in M_K\} \\
&= \{\widetilde{m} \in \mathbb{R}^d : \ m' + D\widetilde{m} \geq 0 \text{ and } G_K(m' + D\widetilde{m}) \leq 0\} \\
&= \left\{\widetilde{m} \in \mathbb{R}^d : \ \begin{bmatrix} -D \\ G_K D \end{bmatrix} \widetilde{m} \leq \begin{bmatrix} m' \\ -G_K m' \end{bmatrix}\right\}.
\end{aligned}$$

with G_K as in (2.7). For some K it might hold that $\dim(\widetilde{M}_K) < d$ and even $\widetilde{M}_K = \emptyset$. This is because some regions do not intersect with the affine subspace.

4.2.2 Reduction to $m_0 + \mathrm{im}(C)$

In practically all Petri nets, $\mathcal{P}$-invariants appear. These are vectors $y \in \mathbb{R}^{|\mathcal{P}|}$ with $y^T C = 0$. They serve as conservation laws on the markings in the sense that $y^T m(\tau) = y^T m_0$ for all $\tau \geq 0$. In discrete place/transition nets they are — among other purposes — used to represent markings by fewer components. For example, if a net with three places has a $\mathcal{P}$-invariant $y = \begin{pmatrix} 1 & 0 & 1 \end{pmatrix}^T$, then the marking of place p_3 is given by $m_{p_3}(\tau) = y^T m_0 - m_{p_1}(\tau)$ for all $\tau \geq 0$. Therefore, only the first two components of the marking vector have to be stored.

Experiments conducted in [Sch03] suggest that the number of components of the reduced marking vector typically ranges between 50% and 70% of the original dimension $|\mathcal{P}|$. In [KMB+08, VMM+08, Lef11], the same idea is used for continuous Petri nets leading to a piecewise affine system. The piecewise affine system studied in [KALD09] can also be interpreted as a reduction in that sense if all $\mathcal{P}$-invariants are due to single servers made explicit.

A marking m is consistent with the $\mathcal{P}$-invariants if and only if $m \in m_0 + \mathrm{im}(C)$. So this affine subspace is flow-invariant and the reduction procedure described above can be applied. As in the discrete case, we can expect that the dimension of the reduced system typically ranges between $0.5 \cdot |\mathcal{P}|$ and $0.7 \cdot |\mathcal{P}|$.

Let $C_r \in \mathbb{R}^{|\mathcal{P}| \times r}$ be a matrix whose columns are a basis of $\mathrm{im}(C)$. We apply the reduction procedure with $D = C_r$ and $m' = m_0$ and obtain the r-dimensional system

$$\begin{cases} \dot{\widetilde{m}} = C_r^+ F(m_0 + C_r \widetilde{m}) \text{ if } m_0 + C_r \widetilde{m} \in M_K \\ \widetilde{m}(0) = 0. \end{cases}$$

Introducing the matrices and vectors

$$\widetilde{A}_K = C_r^+ A_K C_r \text{ and } \widetilde{a}_K = C_r^+ A_K m_0 \tag{4.3}$$

with A_K as in Equation (2.12) as well as the sets

$$\widetilde{M}_K = \{\widetilde{m} \in \mathbb{R}^r : \ m_0 + C_r \widetilde{m} \in M_K\},$$

the reduced system is expressed by

$$\begin{cases} \dot{\widetilde{m}} = \widetilde{A}_K \widetilde{m} + \widetilde{a}_K \text{ if } \widetilde{m} \in \widetilde{M}_K \\ \widetilde{m}(0) = 0. \end{cases} \tag{4.4}$$

The reduced regions can again be stated in matrix-vector notation by

$$\begin{aligned} \widetilde{M}_K &= \{\widetilde{m} \in \mathbb{R}^r : \ m_0 + C_r \widetilde{m} \geq 0 \text{ and } G_K(m_0 + C_r \widetilde{m}) \leq 0\} \\ &= \left\{ \widetilde{m} \in \mathbb{R}^r : \ \begin{bmatrix} -C_r \\ G_K C_r \end{bmatrix} \widetilde{m} \leq \begin{bmatrix} m_0 \\ -G_K m_0 \end{bmatrix} \right\}. \end{aligned} \tag{4.5}$$

Example 4.4. Let us perform the reduction for the TCPN studied in Example 2.5. With three places, the original system is three-dimensional. As $\operatorname{rank}(C) = 1$, the reduced system is only one-dimensional. We use

$$C_r = \begin{pmatrix} -1 \\ 1 \\ -1 \end{pmatrix} \text{ with } C_r^+ = \frac{1}{3}\begin{pmatrix} -1 & 1 & -1 \end{pmatrix}.$$

The net is bounded as the support of the $\mathcal{P}$-semiflow $\begin{pmatrix} 1 & 2 & 1 \end{pmatrix}^T$ contains all places. For the initial marking $m_0 = \begin{pmatrix} 11 & 0 & 10 \end{pmatrix}^T$, the reduced phase space consists of three intervals

$$\widetilde{M}_{K_1} = \left[0, \frac{11}{2}\right], \qquad \widetilde{M}_{K_2} = \left[\frac{11}{2}, 9\right], \qquad \widetilde{M}_{K_3} = [9, 10].$$

Region M_{K_4} cannot be reached from this initial marking due to the conservation law imposed by the $\mathcal{P}$-invariants. Therefore, $\widetilde{M}_{K_4} = \emptyset$.

The system matrices are computed according to Equation (4.3). The resulting dynamics is given by

$$\dot{\widetilde{m}} = \begin{cases} -3\widetilde{m} + 22 & \text{if } \widetilde{m} \in \widetilde{M}_{K_1}, \\ -\widetilde{m} + 11 & \text{if } \widetilde{m} \in \widetilde{M}_{K_2}, \\ -3\widetilde{m} + 29 & \text{if } \widetilde{m} \in \widetilde{M}_{K_3}. \end{cases}$$

We see that only region $\widetilde{M}_{K_3}$ contains a steady state to which the system converges from $\widetilde{m}(0) = 0$. ♢

The reduction is performed with respect to a specific initial marking. However, as F is homogeneous, the qualitative behavior is equivalent to that of the system with initial marking κm_0 ($\kappa > 0$). Furthermore, the reduced dynamical system incorporates all markings contained in the affine subspace $m_0 + \operatorname{im}(C)$.

In Chapter 5, this reduction is used as a basis to analyze bifurcations in parameter-dependent Petri nets as the reduction does not only affect the dimension of the system but also removes zero eigenvalues which hamper the analysis. Roughly speaking, the spectrum of A_K is preserved by the reduction and so are the algebraic and ge-

ometric multiplicities of the eigenvalues. The only exception are zero eigenvalues. We look at the eigenvalues first.

Proposition 4.5. *Let χ_{A_K} and $\chi_{\widetilde{A}_K}$ denote the characteristic polynomials of A_K and $\widetilde{A}_K$, respectively. Then,*

$$\chi_{A_K}(\mu) = \mu^{|\mathcal{P}|-r} \cdot \chi_{\widetilde{A}_K}(\mu).$$

The proof uses a similarity transformation based on the following partition of $\mathbb{R}^{|\mathcal{P}|}$ where Y is a matrix whose columns are a basis of the set of all $\mathcal{P}$-invariants.

$$\begin{aligned}\mathbb{R}^{|\mathcal{P}|} &= \operatorname{im}(C_r) \oplus \operatorname{im}(C_r)^{\perp} \\ &= \operatorname{im}(C_r) \oplus \operatorname{im}(C)^{\perp} \\ &= \operatorname{im}(C_r) \oplus \ker(C^T) \\ &= \operatorname{im}(C_r) \oplus \operatorname{im}(Y)\end{aligned}$$

Lemma 4.6. *The matrix $\begin{pmatrix} C_r & Y \end{pmatrix}$ is invertible with $\begin{pmatrix} C_r & Y \end{pmatrix}^{-1} = \begin{pmatrix} C_r^+ \\ Y^+ \end{pmatrix}$.*

Proof. Invertibility follows immediately from the above partition of $\mathbb{R}^{|\mathcal{P}|}$.

$$\begin{pmatrix} C_r^+ \\ Y^+ \end{pmatrix} \begin{pmatrix} C_r & Y \end{pmatrix} = \begin{pmatrix} C_r^+ C_r & C_r^+ Y \\ Y^+ C_r & Y^+ Y \end{pmatrix}.$$

As the columns of C_r and Y, respectively, are linearly independent by definition, we get $C_r^+ C_r = I_r$ and $Y^+ Y = I_{|\mathcal{P}|-r}$.

Combining the above partition with Property 1 of the Moore-Penrose pseudoinverse in Lemma 4.2, the equalities $C_r^+ Y = 0$ and $Y^+ C_r = 0$ follow immediately. We obtain

$$\begin{pmatrix} C_r^+ \\ Y^+ \end{pmatrix} \begin{pmatrix} C_r & Y \end{pmatrix} = \begin{pmatrix} I_r & 0_{r,|\mathcal{P}|-r} \\ 0_{|\mathcal{P}|-r,r} & I_{|\mathcal{P}|-r} \end{pmatrix} = I_{|\mathcal{P}|}. \qquad \square$$

Proof of Proposition 4.5. Due to the previous lemma

$$\begin{pmatrix} C_r^+ \\ Y^+ \end{pmatrix} A_K \begin{pmatrix} C_r & Y \end{pmatrix} = \begin{pmatrix} C_r^+ A_K C_r & C_r^+ A_K Y \\ Y^+ A_K C_r & Y^+ A_K Y \end{pmatrix} = \begin{pmatrix} \widetilde{A}_K & C_r^+ A_K Y \\ 0_{|\mathcal{P}|-r,r} & 0_{|\mathcal{P}|-r,|\mathcal{P}|-r} \end{pmatrix} =: A'$$

is a similarity transformation. Thus, A_K and A' have the same characteristic polynomial. Making use of the block structure of A' we compute

$$\begin{aligned}\chi_{A_K}(\mu) &= \chi_{A'}(\mu) = \det(\mu I_{|\mathcal{P}|} - A') \\ &= \det(\mu I_r - \widetilde{A}_K) \cdot \det(\mu I_{|\mathcal{P}|-r} - 0_{|\mathcal{P}|-r,|\mathcal{P}|-r}) \\ &= \chi_{\widetilde{A}_K}(\mu) \cdot \mu^{|\mathcal{P}|-r}.\end{aligned}$$ □

We see that the spectrum of A_K is composed of the spectrum of $\widetilde{A}_K$ and zero eigenvalues. Algebraic multiplicity is preserved by the reduction for all nonzero eigenvalues. The following lemma considers the corresponding eigenvectors and geometric multiplicities which are in fact also preserved — again for nonzero eigenvalues only.

Proposition 4.7. *1. Let $\tilde{v}_1, \ldots, \tilde{v}_k$ be linearly independent eigenvectors of $\widetilde{A}_K$ to the eigenvalue μ. Then, $C_r\tilde{v}_1, \ldots, C_r\tilde{v}_k$ are linearly independent eigenvectors of A_K to the same eigenvalue.*

2. Let now $v_1, \ldots, v_k$ be linearly independent eigenvectors of A_K to the eigenvalue $\mu \neq 0$. Then, $C_r^+v_1, \ldots, C_r^+v_k$ are linearly independent eigenvectors of $\widetilde{A}_K$ to the eigenvalue μ.

Proof. 1. Let $i \in \{1, \ldots, k\}$ and $\widetilde{A}_K\tilde{v}_i = \mu\tilde{v}_i$. Multiplication with C_r yields $C_rC_r^+A_KC_r\tilde{v}_i = \mu C_r\tilde{v}_i$. As $A_KC_r\tilde{v}_i \in \mathrm{im}(C)$, we obtain with Lemma 4.2 that $C_rC_r^+A_KC_r\tilde{v}_i = A_KC_r\tilde{v}_i$. It follows that $A_KC_r\tilde{v}_i = \mu C_r\tilde{v}_i$. Linear independence is preserved since C_r has full column rank.

2. Let now $i \in \{1, \ldots, k\}$ and $A_Kv_i = \mu v_i$. We first show that $\widetilde{A}_KC_r^+v_i = \mu C_r^+v_i$.

$$A_Kv_i = C\Lambda\Pi_Kv_i \in \mathrm{im}(C_r) \Rightarrow \mu v_i \in \mathrm{im}(C_r) \overset{\mu\neq 0}{\Rightarrow} v_i \in \mathrm{im}(C_r).$$

By Property 2 of Lemma 4.2, this implies $C_rC_r^+v_i = v_i$ and we can write

$$\widetilde{A}_KC_r^+v_i = C_r^+A_KC_rC_r^+v_i = C_r^+A_Kv_i = \mu C_r^+v_i.$$

We need to show linear independence of $C_r^+v_1, \ldots, C_r^+v_k$. Again, this property is not influenced by multiplication with C_r and thus follows from $C_rC_r^+v_i = v_i$ which holds by Property 2 as $v_i \in \mathrm{im}(C_r)$. □

The condition $\mu \neq 0$ of the second part of this proposition is vital. The reduction singles out the dynamics of the original piecewise linear system which take place in the affine subspace $m_0 + \mathrm{im}(C)$. Its flow-invariance results in zero eigenvalues in A_K which do not appear in $\widetilde{A}_K$ any more. We take advantage of this fact in Chapter 5.

4.2.3 Reduction to Fixed-Point Sets

In the previous chapter, we have seen that isotropy subgroups remain constant along trajectories, i.e.,

$$\Sigma_{m_0} = \Sigma_{m(\tau)}$$

for all $\tau \geq 0$ where $\Sigma_{m(\tau)} \subset \Sigma^t_{\langle \mathcal{N}, \lambda \rangle}$. This can be understood as a conservation law for a system with given initial marking and can be used to reduce the associated PWL system analogously to the reduction in Section 4.2.1. Let m_0 be the initial marking and Σ_{m_0} its isotropy subgroup. We reduce the dynamics to the flow-invariant fixed-point set $\mathrm{Fix}(\Sigma_{m_0})$.

Let $\phi \in \mathbb{R}^{|\mathcal{P}| \times s}$ be a matrix whose columns form a basis of the subspace

$$\{m \in \mathbb{R}^{|\mathcal{P}|} : S_\sigma m = m \text{ for all } \sigma \in \Sigma_{m_0}\}$$

which contains $\mathrm{Fix}(\Sigma_{m_0})$. Flow-invariance of $\mathrm{Fix}(\Sigma_{m_0})$ means that $m(\tau) \in \mathrm{Fix}(\Sigma_{m_0})$ for all $\tau \geq 0$. Therefore, there exist unique $\widetilde{m}(\tau) \in \mathbb{R}^s$ such that $m(\tau) = \phi\, \widetilde{m}(\tau)$. We apply our reduction technique with $D = \phi$ and $m' = 0$ and obtain the reduced system

$$\begin{cases} \dot{\widetilde{m}} = \phi^+ F(\phi \widetilde{m}) = \phi^+ A_K \phi\, \widetilde{m} \text{ if } \widetilde{m} \in \phi^{-1}(M_K) \\ \widetilde{m}(0) = \phi^+ m_0 \end{cases} \tag{4.6}$$

which is equivalent to the original system on $\mathrm{Fix}(\Sigma_{m_0})$. Since the flow-invariant set is not affine, there is no affine part in this PWL system. In the sequel of this chapter, this reduced system is the starting point for the development of a reduction technique modifies the net itself. For a particular choice of ϕ, this s-dimensional system is identical to the PWL system induced by the reduced net. In this case, $\widetilde{m}$ has a direct interpretation on the net level.

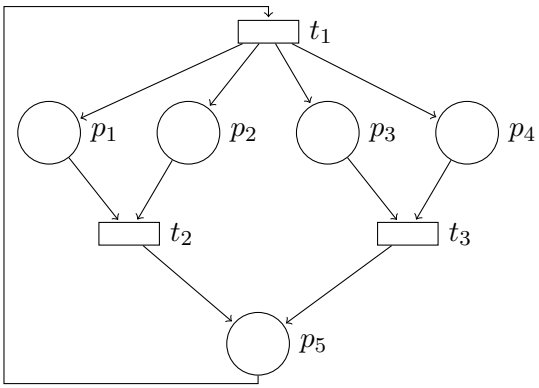

Figure 4.2: A Petri net with $|\Sigma^t_{\langle \mathcal{N},\lambda\rangle}| = 8$.

4.2.4 A Joint Reduction

We have performed reductions to the flow-invariant sets $m_0 + \mathrm{im}(C)$ and $\mathrm{Fix}(\Sigma_{m_0})$. Of course, also their intersection is a flow-invariant affine subspace to which we can reduce. As $\phi\phi^+$ is the orthogonal projector onto $\mathrm{Fix}(\Sigma_{m_0})$, this set is given by

$$\begin{aligned}\mathrm{Fix}(\Sigma_{m_0}) \cap (m_0 + \mathrm{im}(C)) &= (m_0 + \mathrm{im}(\phi)) \cap (m_0 + \mathrm{im}(C)) \cap \mathbb{R}^{|\mathcal{P}|}_{\geq 0} \\ &= \{m_0 + m' : \ m' \in \mathrm{im}(\phi) \cap \mathrm{im}(C)\} \cap \mathbb{R}^{|\mathcal{P}|}_{\geq 0} \\ &= (m_0 + \mathrm{im}(\phi\phi^+ C)) \cap \mathbb{R}^{|\mathcal{P}|}_{\geq 0}.\end{aligned}$$

The reduction technique can therefore be applied with $U = \mathrm{im}(\phi\phi^+ C)$ and $m' = m_0$.

The size of the reduced system with respect to $\mathrm{Fix}(\Sigma_{m_0})$ depends on the size of the isotropy subgroup of m_0 while the dimension of system (4.4) is independent of m_0. It is not surprising that the joint reduction to $m_0 + \mathrm{im}(\phi\phi^+ C)$ leads in general to a system whose dimension is smaller than r or s. This can be seen in the following example. However, due to the fact that the token flow matrix C is symmetric itself ($S_\sigma C = C T_\sigma$), the reduction to the flow-invariant set $m_0 + \mathrm{im}(C)$ already removes redundancies stemming from symmetries such that the gain of the joint reduction may be small.

Example 4.8. Let us consider the net in Figure 4.2. Its token flow matrix is

$$C = \begin{pmatrix} 1 & -1 & 0 \\ 1 & -1 & 0 \\ 1 & 0 & -1 \\ 1 & 0 & -1 \\ -1 & 1 & 1 \end{pmatrix}.$$

As $\operatorname{rank}(C) = 3$ a reduction with respect to $m_0 + \operatorname{im}(C)$ would yield a three-dimensional system for any choice of m_0. The Petri net is highly symmetric with $|\Sigma^t_{\langle \mathcal{N},\lambda \rangle}| = 8$. For the "most symmetric" initial marking where the first four components are equal, the symmetry reduction would even yield a two-dimensional system.

Let us consider the reduction for the initial marking, $m_0 = \begin{pmatrix} 1 & 2 & 2 & 1 & 1 \end{pmatrix}^T$. The isotropy subgroup is $\Sigma_{m_0} = \{id, (p_1\, p_4)(p_2\, p_3)(t_2\, t_3)\}$ and the corresponding fixed-point subspace is spanned by the columns of

$$\phi = \begin{pmatrix} 1 & 0 & 0 \\ 0 & 1 & 0 \\ 0 & 1 & 0 \\ 1 & 0 & 0 \\ 0 & 0 & 1 \end{pmatrix}$$

inducing a three-dimensional system just as in the case of a reduction with respect to $m_0 + \operatorname{im}(C)$. However, $\operatorname{rank}(\phi\phi^+ C) = 2$ such that the joint reduction results in a two-dimensional system. ♢

4.3 Symmetry Reduction of the Petri Net

4.3.1 Problem Statement and Solution Approach

It has been shown in the previous section that symmetries may be taken advantage of for reducing the dimension of the state space. We now take this idea a step further by reducing not just the equations but also the net itself. The model of a multi-computer programmable logic controller studied in [ŽS10, p. 53] serves as

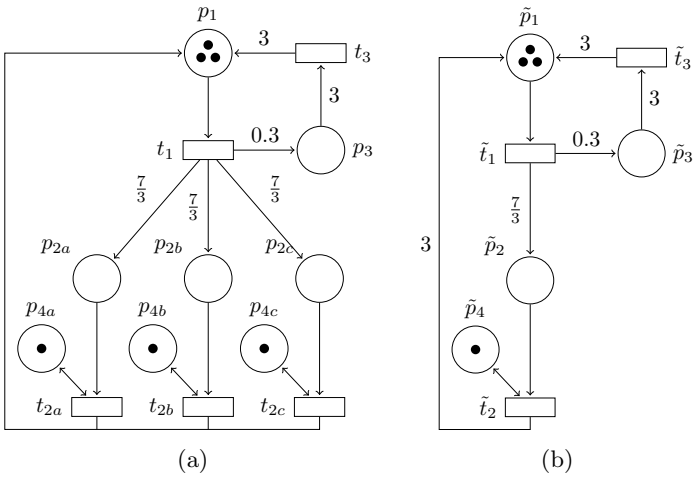

Figure 4.3: Original and reduced model of the MCPLC example.

a motivation. This system has been decolorized using a combination of reduction techniques and unfolding. The resulting net contains symmetries as there are three identical subnets (see Figure 4.3(a)). As a last reduction step these three subnets are substituted by a single subnet and the weight of the new arc $(\tilde{t}_2, \tilde{p}_1)$ is adapted accordingly. Figure 4.3(b) shows the resulting net. This section deals with the question if this last step in the reduction procedure can be performed automatically for any system of this form. The task includes the selection of nodes, the construction of arcs between them, and the choice of arc weights and firing speeds. The method has already been published in [MS12].

The idea to reduce Petri nets if they contain symmetries is not new. In [ACB84], for instance, a multiprocessor system comprising several identical processors, memories, and buses is modeled. The net is then replaced by a smaller one that results from folding subnets representing the common memory accesses without loss of information about the associated stochastic process. However, no systematic approach to the reduction is suggested and the modeler has to check carefully if the folding is really valid. Furthermore, in the above example, a simple folding of the identical subnets cannot be applied as it ignores the necessary change of the arc weight.

In Section 4.1 the rule “Folding of identical subnets“ as suggested in [ADFN99] has been stated as a formalized version of this reduction approach. As the prerequisites

of this rule are very restrictive we may not apply it in the above example. First, that rule is designed for ordinary subnets only and does not incorporate any changes of arc weights. Second, the subnets contain joins and are therefore no state machines. We are seeking for a more general reduction rule.

In the two articles just mentioned, symmetry is understood in terms of identical ordinary subnets which are symmetrically coupled. It seems just natural to extend this view to the more general definition of symmetry in terms of graph automorphisms that is used throughout this work. The resulting Petri nets can then be understood as quotient nets where each node represents an equivalence class of nodes of the original net. The concept of quotient nets can already be found in the literature on ordinary Petri nets where they are considered in terms of net morphisms [Des91]. Unfortunately, it is not straightforward to generalize these results to weighted nets. This is discussed in Section 4.3.9.

A similar method is known from coupled cell systems which are networks of dynamical systems. For such systems it is shown in [GST05] that a symmetry in the network induces a unique canonical coupled cell network whose nodes represent equivalence classes of the original nodes. The authors introduce multiple arrows which to a certain extend corresponds to the change of arc weights we have encountered in the motivating example.

The reduction technique proposed in this section is based on the same idea as the reduction with respect to isotropy subgroups shown in Section 4.2.3. The marking trajectory remains inside the fixed-point set $\mathrm{Fix}(\Sigma_{m_0})$. As the reduction on the net level also affects the transitions, which do not contribute to the dimension of the PWL system, we make similar considerations for the transitions. The basic observation is that a similar conservation law exists for the flow as well.

Let $\sigma \in \Sigma_{m_0} \subset \Sigma^t_{\langle\mathcal{N},\lambda\rangle}$. Then, $m(\tau) \in M_K$ implies $m(\tau) = S_\sigma m(\tau) \in M_{\pi_\sigma(K)}$. Hence, by Lemmas 3.11 and 3.19

$$\begin{aligned} f(m(\tau)) &= \Lambda\Pi_K m(\tau) = \Lambda\Pi_{\pi_\sigma(K)} m(\tau) = \Lambda\Pi_{\pi_\sigma(K)} S_\sigma m(\tau) \\ &= \Lambda T_\sigma \Pi_K m(\tau) = T_\sigma \Lambda\Pi_K m(\tau) = T_\sigma f(m(\tau)) \end{aligned}$$

holds for all $\tau \geq 0$. It therefore makes sense to define — in analogy to $\mathrm{Fix}(\Sigma)$ —

the set

$$\mathrm{Fix}^{\mathcal{T}}(\Sigma) = \left\{ v \in \mathbb{R}_{\geq 0}^{|\mathcal{T}|} : T_\sigma v = v \text{ for all } \sigma \in \Sigma \right\}.$$

Let now θ be a matrix with full column rank whose columns span $\mathrm{Fix}^{\mathcal{T}}(\Sigma_{m_0})$ and θ^+ the corresponding pseudoinverse. System (4.6) can then be written as

$$\begin{cases} \dot{\widetilde{m}} = \phi^+ C\theta\theta^+\Lambda\theta\theta^+\Pi_K\phi\,\widetilde{m} \text{ if } \widetilde{m} \in \phi^{-1}(M_K) \\ \widetilde{m}(0) = \phi^+ m_0. \end{cases} \tag{4.7}$$

We may insert $\theta\theta^+$ in this way since it is the identity map if restricted to $\mathrm{Fix}^{\mathcal{T}}(\Sigma_{m_0})$ and as we have seen before $f(m) \in \mathrm{Fix}^{\mathcal{T}}(\Sigma_{m_0})$ if $m \in \mathrm{Fix}(\Sigma_{m_0})$.

The idea for the reduction is now the following. Let us introduce the matrices

$$\widetilde{Pre} = \phi^+ Pre\,\theta,\ \widetilde{Post} = \phi^+ Post\,\theta \text{ and } \widetilde{\Lambda} = \theta^+\Lambda\,\theta. \tag{4.8}$$

System (4.7) can then be written as $\dot{\widetilde{m}} = (\widetilde{Post} - \widetilde{Pre})\widetilde{\Lambda}\theta^+\Pi_K\phi\,\widetilde{m}$. The new matrices define a net with less places and transitions. In the case of the MCPLC example, these matrices describe exactly the expected Petri net. However, for some net structures containing choices the computation of firing rates is more complicated (or even impossible). This is discussed in detail in Section 4.3.5.

Example 4.9. To illustrate the idea of the reduction procedure, we consider again the Petri net system in Figure 4.3 which models a multi-computer programmable logic controller (cf. [ŽS10]). Assuming that the nodes are ordered as $p_1, p_{2a}, p_{2b}, p_{2c}$, $p_3, p_{4a}, p_{4b}, p_{4c}$ and $t_1, t_{2a}, t_{2b}, t_{2c}, t_3$ its net structure and firing rates are described by the matrices

$$Pre = \begin{pmatrix} 1 & 0 & 0 & 0 & 0 \\ 0 & 1 & 0 & 0 & 0 \\ 0 & 0 & 1 & 0 & 0 \\ 0 & 0 & 0 & 1 & 0 \\ 0 & 0 & 0 & 0 & 3 \\ 0 & 1 & 0 & 0 & 0 \\ 0 & 0 & 1 & 0 & 0 \\ 0 & 0 & 0 & 1 & 0 \end{pmatrix}, \quad Post = \begin{pmatrix} 0 & 1 & 1 & 1 & 3 \\ 7/30 & 0 & 0 & 0 & 0 \\ 7/30 & 0 & 0 & 0 & 0 \\ 7/30 & 0 & 0 & 0 & 0 \\ 3/10 & 0 & 0 & 0 & 0 \\ 0 & 1 & 0 & 0 & 0 \\ 0 & 0 & 1 & 0 & 0 \\ 0 & 0 & 0 & 1 & 0 \end{pmatrix} \text{ and } \Lambda = I_5.$$

The symmetry group of the net contains all possible permutations of the three subnets and is given by

$$\begin{aligned}\Sigma^t_{\langle\mathcal{N},\lambda\rangle} = \{&id,\ (p_{2a}\ p_{2b})(p_{4a}\ p_{4b})(t_{2a}\ t_{2b}),\ (p_{2a}\ p_{2c})(p_{4a}\ p_{4c})(t_{2a}\ t_{2c}),\\ &(p_{2b}\ p_{2c})(p_{4b}\ p_{4c})(t_{2b}\ t_{2c}),\ (p_{2a}\ p_{2b}\ p_{2c})(p_{4a}\ p_{4b}\ p_{4c})(t_{2a}\ t_{2b}\ t_{2c}),\\ &(p_{2a}\ p_{2c}\ p_{2b})(p_{4a}\ p_{4c}\ p_{4b})(t_{2a}\ t_{2c}\ t_{2b})\}.\end{aligned}$$

This is also the isotropy subgroup of the initial marking

$$m_0 = \begin{pmatrix}3 & 0 & 0 & 0 & 0 & 1 & 1 & 1\end{pmatrix}^T.$$

We choose the following matrices ϕ and θ to describe the corresponding subspaces:

$$\phi = \begin{pmatrix}1&0&0&0\\0&1&0&0\\0&1&0&0\\0&1&0&0\\0&0&1&0\\0&0&0&1\\0&0&0&1\\0&0&0&1\end{pmatrix} \text{ and } \theta = \begin{pmatrix}1&0&0\\0&1&0\\0&1&0\\0&1&0\\0&0&1\end{pmatrix}.$$

We now compute the reduced matrices

$$\widetilde{Pre} = \begin{pmatrix}1&0&0\\0&1&0\\0&0&3\\0&1&0\end{pmatrix}, \quad \widetilde{Post} = \begin{pmatrix}0&3&3\\7/30&0&0\\3/10&0&0\\0&1&0\end{pmatrix} \text{ and } \widetilde{\Lambda} = I_3.$$

These matrices $\widetilde{Pre}$, $\widetilde{Post}$ and $\widetilde{\Lambda}$ define a new net up to the labeling of the nodes. It is shown in Figure 4.3(b).

This is exactly the subnet of the original net one would expect. Also the weight of the input arc to place p_1 has changed as expected. We compare the marking in steady state m^* and the corresponding flow $f^* = f(m^*)$ of the original and the

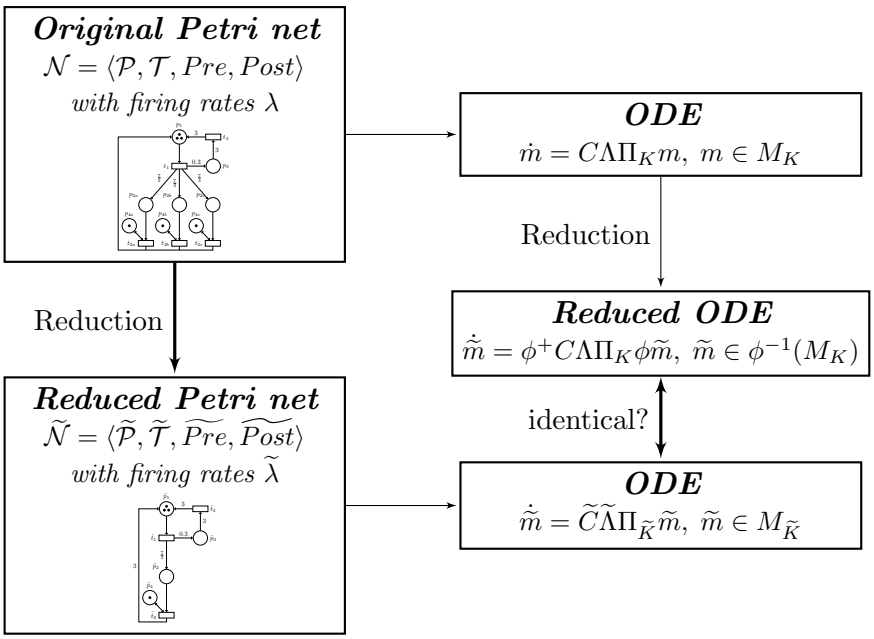

Figure 4.4: Schematic representation of the reduction approach.

reduced net system and obtain for the original net

$$
\begin{aligned}
m_0 &= \begin{pmatrix} 3 & 0 & 0 & 0 & 0 & 1 & 1 & 1 \end{pmatrix}^T \\
m^* &= \begin{pmatrix} 1.5 & 0.35 & 0.35 & 0.35 & 0.45 & 1 & 1 & 1 \end{pmatrix}^T \\
f^* &= \begin{pmatrix} 1.5 & 0.35 & 0.35 & 0.35 & 0.15 \end{pmatrix}^T
\end{aligned}
$$

and for the reduced net

$$
\begin{aligned}
\widetilde{m}_0 &= \phi^+ m_0 = \begin{pmatrix} 3 & 0 & 0 & 1 \end{pmatrix}^T \\
\widetilde{m}^* &= \begin{pmatrix} 1.5 & 0.35 & 0.45 & 1 \end{pmatrix}^T \\
\tilde{f}^* &= \begin{pmatrix} 1.5 & 0.35 & 0.15 \end{pmatrix}^T .
\end{aligned}
$$

We see that $\phi\,\widetilde{m}^* = m^*$ and $\theta\tilde{f}^* = f^*$ as required. Thus, the reduced net is appropriate to analyze the original one. ♢

Figure 4.4 summarizes the general approach. The original Petri net system comes with its associated PWL system. Having identified its symmetries an equivalent PWL system with smaller phase space can be obtained as described in Section 4.2.3. From that reduced PWL system a Petri net system with fewer places and transitions can be deduced as we have just seen. This system again comes with an associated PWL system. If this PWL system and the reduced PWL system of the original net are identical, then the reduction is exact. The reduced TCPN system has the same dynamical properties as the original one and the trajectories of its associated dynamical systems are identical up to a linear transformation. The reduction on the ODE level is used for the development of the reduction method and to prove the correctness of the approach. However, the reduction itself can be performed without the intermediate step of the reduction of the PWL system.

In the following sections, the deduction of the new Petri net from the reduced PWL system is formalized. It is shown that in the presence of choices, it might be necessary to modify the computation of $\widetilde{\Lambda}$ and that some conflicts require a restriction to a subgroup of Σ_{m_0}. Afterwards, the equivalence of the two PWL systems is proven.

4.3.2 The Nodes, Arcs, and Arc Weights of the Reduced Net

It must be observed first of all that the reduction approach is always applied with respect to a group

$$\Sigma \subset \Sigma_{m_0} \subset \Sigma^t_{\langle \mathcal{N},\lambda \rangle}.$$

In Section 4.2.3, an arbitrary basis of $\mathrm{Fix}(\Sigma_{m_0})$ is used to perform a reduction of the PWL system to be solved. The state vector in the reduced space might not have an immediate interpretation on the net level but can be transformed to the original marking vector by a linear transformation. Here, where we search for a smaller Petri net, special attention is to be paid to the choice of the basis. First of all, ϕ and θ have to be chosen in a way that $\widetilde{Pre}$ and $\widetilde{Post}$ actually define a new net, i.e., all entries have to be nonnegative. The same holds for the marking in reduced space which must not be negative. Second, we want to choose the bases in a way that allows to draw conclusions from the reduced system about the original system easily as in the given example, where the marking of nodes in the reduced net is the marking of the corresponding nodes in the original net.

For this purpose we choose ϕ and θ in the same way as in the previous example. We first group the nodes in equivalence classes with respect to Σ. Each equivalence class results in one column of the corresponding matrix as each node in the reduced net shall represent one equivalence class of nodes of the original net. Let s and q denote the order of the quotient sets $\mathcal{P}/\sim_\Sigma = \{[p]_{\sim_\Sigma} : p \in \mathcal{P}\}$ and $\mathcal{T}/\sim_\Sigma = \{[t]_{\sim_\Sigma} : t \in \mathcal{T}\}$, respectively. Let $\widetilde{\mathcal{P}} = \{\tilde{p}_1, \ldots, \tilde{p}_s\}$ and $\widetilde{\mathcal{T}} = \{\tilde{t}_1, \ldots, \tilde{t}_q\}$ be sets of places and transitions. In analogy to the traditional canonical projection map we define

$$\mu : \mathcal{P} \cup \mathcal{T} \to \widetilde{\mathcal{P}} \cup \widetilde{\mathcal{T}}$$

such that $\mu(\mathcal{P}) = \widetilde{\mathcal{P}}$, $\mu(\mathcal{T}) = \widetilde{\mathcal{T}}$ and $\mu(v) = \mu(v')$ if and only if $v \sim_\Sigma v'$. The sets $\mathcal{P}/\sim_\Sigma$ and $\widetilde{\mathcal{P}}$ are isomorphic as are $\mathcal{T}/\sim_\Sigma$ and $\widetilde{\mathcal{T}}$. Let $\langle v \rangle$ denote the cardinality of the equivalence class $[v]_{\sim_\Sigma}$ for a $v \in \mathcal{P} \cup \mathcal{T}$. We use this symbol also to denote $\langle \tilde{v} \rangle = |\mu^{-1}(\tilde{v})|$ for all $\tilde{v} \in \widetilde{\mathcal{P}} \cup \widetilde{\mathcal{T}}$.

The $(|\mathcal{P}| \times s)$-matrix ϕ and the $(|\mathcal{T}| \times q)$-matrix θ are constructed as in Example 4.9 such that each column corresponds to an equivalence class of nodes and thus to one node in the reduced net:

$$\phi_{p,\tilde{p}} = \delta_{\mu(p),\tilde{p}} = \begin{cases} 1 & \text{if } \mu(p) = \tilde{p} \\ 0 & \text{otherwise} \end{cases} \quad \text{and} \quad \theta_{t,\tilde{t}} = \delta_{\mu(t),\tilde{t}} = \begin{cases} 1 & \text{if } \mu(t) = \tilde{t} \\ 0 & \text{otherwise.} \end{cases} \tag{4.9}$$

The corresponding Moore-Penrose pseudoinverses are

$$(\phi^+)_{\tilde{p},p} = \frac{\delta_{\tilde{p},\mu(p)}}{\langle \tilde{p} \rangle} = \begin{cases} \frac{1}{\langle \tilde{p} \rangle} & \text{if } \mu(p) = \tilde{p} \\ 0 & \text{otherwise} \end{cases} \quad \text{and} \quad (\theta^+)_{\tilde{t},t} = \frac{\delta_{\tilde{t},\mu(t)}}{\langle \tilde{t} \rangle} = \begin{cases} \frac{1}{\langle \tilde{t} \rangle} & \text{if } \mu(t) = \tilde{t} \\ 0 & \text{otherwise.} \end{cases}$$

For the arcs and arc weights we compute

$$\begin{aligned} (\phi^+ Pre\, \theta)_{\tilde{p},\tilde{t}} &= \sum_{p \in \mathcal{P}} \frac{1}{\langle \tilde{p} \rangle} \delta_{\tilde{p},\mu(p)} \left(\sum_{t \in \mathcal{T}} Pre_{p,t} \delta_{\mu(t),\tilde{t}} \right) \\ &= \frac{1}{\langle \tilde{p} \rangle} \sum_{p \in \mathcal{P}} \sum_{t \in \mathcal{T}} Pre_{p,t} \delta_{\tilde{p},\mu(p)} \delta_{\mu(t),\tilde{t}} = \frac{1}{\langle \tilde{p} \rangle} \sum_{\substack{(p,t) \\ \in \mu^{-1}(\tilde{p}) \times \mu^{-1}(\tilde{t})}} Pre_{p,t}. \end{aligned}$$

Let $p \in \mu^{-1}(\tilde{p})$ and $\sigma \in \Sigma$, then,

$$\sum_{t \in \mu^{-1}(\tilde{t})} Pre_{p,t} = \sum_{t \in \mu^{-1}(\tilde{t})} Pre_{\sigma(p),\sigma(t)} = \sum_{t \in \mu^{-1}(\tilde{t})} Pre_{\sigma(p),t}.$$

Therefore, for an arbitrary $p \in \mu^{-1}(\tilde{p})$,

$$(\phi^+ Pre\, \theta)_{\tilde{p},\tilde{t}} = \frac{1}{\langle \tilde{p} \rangle} \sum_{\substack{(p,t) \\ \in \mu^{-1}(\tilde{p}) \times \mu^{-1}(\tilde{t})}} Pre_{p,t} = \frac{1}{\langle \tilde{p} \rangle} \langle \tilde{p} \rangle \sum_{t \in \mu^{-1}(\tilde{t})} Pre_{p,t} = \sum_{t \in \mu^{-1}(\tilde{t})} Pre_{p,t} \quad (4.10)$$

and the same for $Post$. That implies that arc weights may increase compared to the original ones if choices (for Pre) or attributions (for $Post$) have less output or input arcs, respectively, after the reduction. Note that the condition that every transition has at least one input arc is preserved by the reduction. As a result, the net $\widetilde{\mathcal{N}} = \langle \widetilde{\mathcal{P}}, \widetilde{\mathcal{T}}, \widetilde{Pre}, \widetilde{Post} \rangle$ is defined.

4.3.3 Configurations

In order to show that the dynamical system associated with $\langle \widetilde{\mathcal{N}}, \widetilde{\lambda} \rangle$ is identical to System (4.6), we need to compare both the polyhedral partitions involved and the constraint matrices Π_K and their counterparts in the reduced net. These tasks require a matching of the configurations of the original Petri net and those of the reduced Petri net.

Considering our initial example given in Figure 4.3(a), we observe that some configurations become redundant in the presence of symmetries. If p_{4a} constrains the flow of transition t_{2a}, then at the same time, p_{4b} constrains the flow of t_{2b}. That means that we may neglect a configuration K with, for instance, $K(t_{2a}) = p_{4a}$ and $K(t_{2b}) = p_{2b}$.

We may in fact restrict to configurations which are symmetric with respect to the symmetry group Σ considered. They are given by

$$\mathcal{K}_{\mathcal{N}}^{\Sigma} = \{K \in \mathcal{K}_{\mathcal{N}} : \mu(K(t)) = \mu(K(\sigma(t))) \text{ for all } t \in \mathcal{T}, \sigma \in \Sigma\}.$$

All others do not contribute to the dynamics.

Lemma 4.10. *Let $K \in \mathcal{K}_{\mathcal{N}} \setminus \mathcal{K}_{\mathcal{N}}^{\Sigma}$. Then,* $\mathrm{int}(\phi^{-1}(M_K)) = \emptyset$.

Proof. For such a configuration, there exist a transition t and a symmetry σ with $\mu(K(t)) \neq \mu(K(\sigma(t)))$. Let $p := K(t)$ and $p' := \sigma^{-1}(K(\sigma(t))) = \pi_{\sigma^{-1}}(K)(t)$. We know that $p' \in {}^{\bullet}t$ as $\pi_{\sigma^{-1}}(K)$ is a configuration. Furthermore, $t \neq \sigma(t)$ and $p \neq p'$.

The reduced marking vector $\widetilde{m} \in \mathbb{R}^{s}_{\geq 0}$ is an element of $\phi^{-1}(M_K)$ if and only if $G_K \phi \, \widetilde{m} \leq 0$. Matrix G_K contains rows (cf. Equation (2.8), specifying only nonzero elements)

$$\begin{array}{rcccccc} g_{K,t,p'} & = (\ldots & \frac{1}{Pre_{p,t}} & \cdots & \frac{-1}{Pre_{p',t}} & \ldots) \\ & & \uparrow & & \uparrow & \\ & & p & & p' & \end{array}$$

and as $\sigma(p') = K(\sigma(t))$ and $K(\sigma(t)) \neq \sigma(p)$, also

$$\begin{array}{rcccccc} g_{K,\sigma(t),\sigma(p)} & = (\ldots & \frac{1}{Pre_{\sigma(p')\sigma(t)}} & \cdots & \frac{-1}{Pre_{\sigma(p),\sigma(t)}} & \ldots) \\ & & \uparrow & & \uparrow & \\ & & \sigma(p') & & \sigma(p) & \\ & = (\ldots & \frac{1}{Pre_{p',t}} & \cdots & \frac{-1}{Pre_{p,t}} & \ldots). \end{array}$$

Taking into consideration that $K \notin \mathcal{K}_{\mathcal{N}}^{\Sigma}$ implies $\mu(p) \neq \mu(p')$, multiplication with ϕ leads to

$$\begin{array}{rcccccc} \begin{pmatrix} g_{K,t,p'} \\ g_{K,\sigma(t),\sigma(p)} \end{pmatrix} \phi & = \begin{pmatrix} \ldots & \frac{1}{Pre_{p,t}} & \cdots & \frac{-1}{Pre_{p',t}} & \ldots \\ & \frac{-1}{Pre_{p,t}} & & \frac{1}{Pre_{p',t}} & \end{pmatrix} . \\ & & \uparrow & & \uparrow & \\ & & \mu(p) & & \mu(p') & \end{array}$$

Then, $g_{K,t,p'}\phi = -g_{K,\sigma(t),\sigma(p)}\phi$. Therefore, $\phi^{-1}(M_K)$ cannot contain an interior point. □

With the same reasoning as in Proposition 2.9, which confirms that redundant configurations can in fact be neglected, we may neglect those configurations studied in the previous lemma.

For a configuration $K \in \mathcal{K}_{\mathcal{N}}^{\Sigma}$, we define the corresponding configuration $\widetilde{K}$ of the reduced net as

$$\widetilde{K} : \widetilde{\mathcal{T}} \to \widetilde{\mathcal{P}},\ \tilde{t} \mapsto \mu(K(t)) \text{ for a } t \in \mu^{-1}(\tilde{t}).$$

This map is well-defined as it is independent of the choice of t by definition of the set $\mathcal{K}_{\mathcal{N}}^{\Sigma}$. Let us confirm that $\widetilde{K}$ is really a configuration of $\widetilde{N}$. As for the chosen $t \in \mu^{-1}(\tilde{t})$ the inequality $\widetilde{Pre}_{\widetilde{K}(\tilde{t}),\tilde{t}} = \sum_{t' \in [t]_{\sim_\Sigma}} Pre_{K(t),t'} \geq Pre_{K(t),t} > 0$ holds, it follows that $\mu(K(t)) \in {}^\bullet\tilde{t}$.

This construction defines a map

$$\mu^{\Sigma} : \mathcal{K}_{\mathcal{N}}^{\Sigma} \to \mathcal{K}_{\widetilde{N}}.$$

Lemma 4.11. *The map μ^{Σ} is surjective.*

Proof. Choose a $\widetilde{K} \in \mathcal{K}_{\widetilde{N}}$. We construct $K \in \mathcal{K}_{\mathcal{N}}^{\Sigma}$ with $\mu(K) = \widetilde{K}$.

Let $t \in \mathcal{T}$. Choose a place $p \in (\mu^{-1}(\widetilde{K}(\mu(t))) \cap {}^\bullet t)$. Let us confirm that this is always possible. Let $p' \in \mu^{-1}(\widetilde{K}(\mu(t)))$. We have to show that there exists $p \in {}^\bullet t$ with $p \sim_\Sigma p'$. From $\widetilde{Pre}_{\mu(p'),\mu(t)} = \sum_{t' \in [t]_{\sim_\Sigma}} Pre_{p',t'} > 0$, it follows that there exists $\sigma \in \Sigma$ with $Pre_{p',\sigma(t)} > 0$. We choose $p = \sigma^{-1}(p')$. This is an input place of t as $Pre_{p,t} = Pre_{p',\sigma(t)} > 0$. It is equivalent to p'.

We put $K(t) = p$. For all $t' \sim_\Sigma t$ choose $\sigma \in \Sigma$ with $t' = \sigma(t)$ and let $K(t') = \sigma(p)$. If the values of K are fixed for all transition in that equivalence class, then choose a transition from another equivalence class and proceed in the same way until K is defined. By construction, $K \in \mathcal{K}_{\mathcal{N}}^{\Sigma}$ and $\mu(K) = \widetilde{K}$. □

4.3.4 Polyhedral Regions

Now, as a matching between the regions of the original and the reduced net is defined, we need to verify that the corresponding regions are related by

$$M_{\mu^{\Sigma}(K)} = \phi^{-1}(M_K).$$

In Example 4.9, this equation is satisfied for both configurations in $\mathcal{K}_{\mathcal{N}}^{\Sigma_{m_0}}$. However, problems may occur when unequal conflicts are present in the net, i.e, when there exist transitions with a common input place whose input structures in terms of nodes or arc weights are not identical. This is illustrated by the following example.

Example 4.12. The Petri net in Figure 4.5 is an example of a net where the

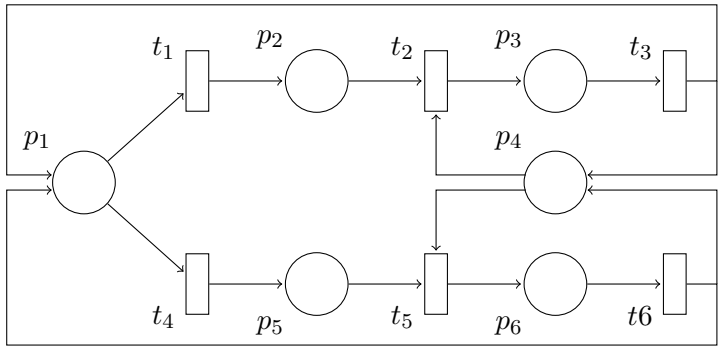

(a) The original net

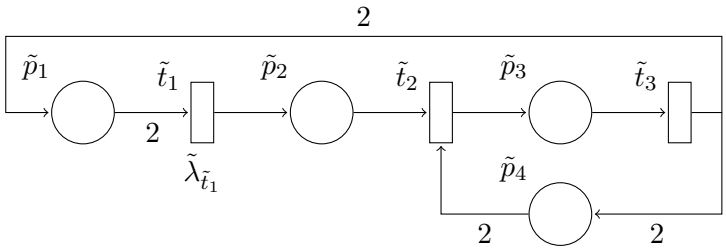

(b) The reduced net

Original Net		**Reduced Net**	
Configuration	Region	Configuration	Region
$K_1(t_2)=p_2, K_1(t_5)=p_5$	$\max(m_{p_2}, m_{p_5}) \leq m_{p_4}$	$\widetilde{K}_1(\tilde{t}_2)=\tilde{p}_2$	$\widetilde{m}_{\tilde{p}_2} \leq \frac{1}{2}\widetilde{m}_{\tilde{p}_4}$
$K_2(t_2)=K_2(t_5)=p_4$	$m_{p_4} \leq \min(m_{p_2}, m_{p_5})$	$\widetilde{K}_2(\tilde{t}_2)=\tilde{p}_4$	$\frac{1}{2}\widetilde{m}_{\tilde{p}_4} \leq \widetilde{m}_{\tilde{p}_2}$
$K_3(t_2)=p_2,\ K_3(t_5)=p_4$	$m_{p_2} \leq m_{p_4} \leq m_{p_5}$		
$K_4(t_2)=p_4,\ K_4(t_5)=p_5$	$m_{p_5} \leq m_{p_4} \leq m_{p_2}$		

(c) Configurations (specifying joins only) and regions

Figure 4.5: The reduction removes the unequal conflict of p_4. The two nets exhibit different behavior.

reduction fails due to the choice p_4. The set of symmetries of the net is given by $\Sigma^t_{\langle\mathcal{N},\lambda\rangle} = \{id, (t_1\ t_4)(p_2\ p_5)(t_2\ t_5)(p_3\ p_6)(t_3\ t_6)\}$. Let us assume an initial marking with isotropy subgroup $\Sigma^t_{\langle\mathcal{N},\lambda\rangle}$.

Figure 4.5(b) shows the resulting reduced net. Both conflicts p_1 and p_4 are "resolved" by the reduction. In the case of p_1, whose output transitions are in CEQ relation (cf. Section 2.2.2), this does not cause any problems. Place p_4, on the other hand, has output transitions t_2 and t_5 which are not in CEQ relation. The solution of a conflict is therefore marking dependent and as such we can expect that a purely structural reduction technique does not lead to the expected result.

The reduction changes the weight of one input arc to transition $\tilde{t}_2$ to the value 2 while the weight of the other arc remains. In the original net the active configuration is determined by comparing m_{p_2} and m_{p_4}. In the reduced net, $\widetilde{m}_{\tilde{p}_2}$ and $\frac{1}{2}\widetilde{m}_{\tilde{p}_4}$ are compared. Thus, the regions of the reduced net are not simply given by the preimages of the original regions under ϕ. Simulations confirm that the net in Figure 4.5(b) cannot be used for the study of the original net. However, the reduced PWL system (4.6) can be used for computations in reduced space. ♢

This problem occurs only if unequal conflicts are "resolved" by the reduction. We therefore define the following property.

Definition 4.13. *A Petri net $\langle\mathcal{N},\lambda\rangle$ is of type* restricted symmetry conflict *(RSC) with respect to a subgroup $\Sigma \subset \Sigma^t_{\langle\mathcal{N},\lambda\rangle}$ if any pair of equivalent transitions with a common input place is in continuous equal conflict relation.*

This property is of special importance for symmetry reductions because if weights of input arcs to a join are changed by the reduction, then all arc weights change in the same manner. This is made precise below. The easiest examples of nets with the RSC property are join-free, choice-free, and CEQ nets.

It is important to note that a restriction to RSC nets does not necessarily imply that unequal conflicts cannot be involved in the reduction. If two or more equivalent but independent unequal conflicts appear, then it might be possible that only one appears in the reduced net. This depends on the existence of an appropriate subgroup.

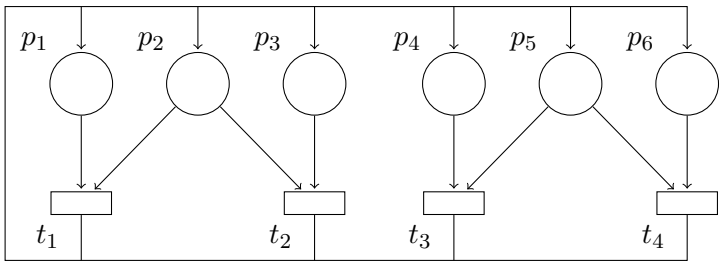

Figure 4.6: A net that is RSC only with respect to a proper subgroup of its symmetry group.

Let us consider the net in Figure 4.6. Its symmetry group is given by

$$\begin{aligned}\Sigma^t_{\langle\mathcal{N},\lambda\rangle} = \{&id,\ (t_1\,t_2)(p_1\,p_3),\ (t_3\,t_4)(p_4\,p_6),\ (t_1\,t_2)(t_3\,t_4)(p_1\,p_3)(p_4\,p_6),\\ &(t_1\,t_3\,t_2\,t_4)(p_1\,p_4\,p_3\,p_6)(p_2\,p_5),\ (t_1\,t_4\,t_2\,t_3)(p_1\,p_6\,p_3\,p_4)(p_2\,p_5),\\ &(t_1\,t_3)(t_2\,t_4)(p_1\,p_4)(p_3\,p_6)(p_2\,p_5),\ (t_1\,t_4)(t_2\,t_3)(p_1\,p_6)(p_3\,p_4)(p_2\,p_5)\}.\end{aligned}$$

In addition to the identity, only the last two elements of this set satisfy the RSC condition. They are of order two and therefore each of them builds a subgroup together with *id*. The net is RSC with respect to either of these two subgroups. They can therefore be used for a reduction that reduces the size of the net by half. The composition of the two permutations does not satisfy the RSC condition. Therefore no bigger subgroup can be found. This procedure is always possible if the relevant subnets are not coupled by an unequal conflict.

Below, the following implications of the RSC property are used.

Lemma 4.14. *Let $\mathcal{N}$ be RSC with respect to $\Sigma \subset \Sigma^t_{\langle\mathcal{N},\lambda\rangle}$.*

1. *If $t \sim_\Sigma t'$ are in conflict relation, then $Pre_{p,t} = Pre_{p,t'}$ for all $p \in \mathcal{P}$.*
2. *For two input places $p \sim_\Sigma p'$ of $t \in \mathcal{T}$, the equality $Pre_{p,t} = Pre_{p',t}$ holds.*
3. *Let $K \in \mathcal{K}^\Sigma_\mathcal{N}$ and $t \sim_\Sigma t'$. Then, $Pre_{K(t),t} = Pre_{K(t'),t'}$.*
4. *Let $p \in {}^\bullet t$. Then,*
$$\frac{\widetilde{Pre}_{\mu(p),\mu(t)}}{Pre_{p,t}} = |p^\bullet \cap [t]_{\sim_\Sigma}|$$
and for $p' \in {}^\bullet t$ the equality $|p'^\bullet \cap [t]_{\sim_\Sigma}| = |p^\bullet \cap [t]_{\sim_\Sigma}|$ holds.

Proof.

1. Let t, t' be two transitions in CEQ relation. Equivalence of the transitions means that there exists $\sigma \in \Sigma$ such that $t' = \sigma(t)$. As t and t' are in CEQ relation, there exists $k > 0$ such that $Pre_{p,t'} = kPre_{p,t}$ for all $p \in \mathcal{P}$. Let $p \in \mathcal{P}$. Then,

$$\begin{aligned} Pre_{p,t} &= Pre_{\sigma(p),\sigma(t)} && (\sigma \text{ is symmetry}) \\ &= k\, Pre_{\sigma(p),t} && (t' = \sigma(t) \text{ and CEQ}) \\ &= k\, Pre_{\sigma^2(p),\sigma(t)} && (\sigma \text{ is symmetry}) \\ &= k^2\, Pre_{\sigma^2(p),t} && (t' = \sigma(t) \text{ and CEQ}) \\ &= \dots \\ &= k^r Pre_{\sigma^r(p),t} \end{aligned}$$

   for $r \in \mathbb{N}$. As Σ is a finite group, there exists r with $\sigma^r(p) = p$ and therefore $Pre_{p,t} = k^r\, Pre_{p,t}$ and as $Pre_{p,t} > 0$ this implies $k = 1$.

2. Let $p, p' \in {}^\bullet t$ and $p' = \sigma(p)$ for a $\sigma \in \Sigma$. As σ is a symmetry, $Pre_{p,t} = Pre_{p',\sigma(t)}$ holds. If $\sigma(t) = t$, there is nothing to show. Otherwise, t and $\sigma(t)$ are two transitions in CEQ relation as p' is a common input place and the net is of type RSC. The equality $Pre_{p',\sigma(t)} = Pre_{p',t}$ follows immediately from Property 1.

3. Let $\sigma \in \Sigma$ be such that $t' = \sigma(t)$. Since $Pre_{\sigma(K(t)),t'} = Pre_{K(t),t} > 0$, both $\sigma(K(t))$ and $K(t')$ are (possibly identical) input places of t'. By definition of $\mathcal{K}_\mathcal{N}$, they have to be equivalent. Application of Property 2 yields $Pre_{K(t'),t'} = Pre_{\sigma(K(t)),t'} = Pre_{K(t),t}$.

4. Let $p \in {}^\bullet t$. If there exists $t' \neq t$ with $t' \in (p^\bullet \cap [t]_{\sim_\Sigma})$, then t and t' are in CEQ relation and, by Property 1, $Pre_{p,t'} = Pre_{p,t}$. Therefore,

$$\begin{aligned} \frac{\widetilde{Pre}_{\mu(p),\mu(t)}}{Pre_{p,t}} &= \frac{\sum_{t' \in [t]_{\sim_\Sigma}} Pre_{p,t'}}{Pre_{p,t}} = \frac{\sum_{t' \in (p^\bullet \cap [t]_{\sim_\Sigma})} Pre_{p,t'}}{Pre_{p,t}} \\ &= \frac{|p^\bullet \cap [t]_{\sim_\Sigma}| \cdot Pre_{p,t}}{Pre_{p,t}} = |p^\bullet \cap [t]_{\sim_\Sigma}|. \end{aligned}$$

   Let now $p' \in {}^\bullet t$. If there exist $t' \neq t$ with $t' \in (p^\bullet \cap [t]_{\sim_\Sigma})$, the transitions

t and t' are in CEQ relation and $0 < Pre_{p',t} = Pre_{p',t'}$ implies that p' is an input place of t'. Thus, $p^\bullet \cap [t]_{\sim_\Sigma} \subset p'^\bullet \cap [t]_{\sim_\Sigma}$. We argue in the same way that $p'^\bullet \cap [t]_{\sim_\Sigma} \subset p^\bullet \cap [t]_{\sim_\Sigma}$. In all other cases obviously $|p'^\bullet \cap [t]_{\sim_\Sigma}| = |p^\bullet \cap [t]_{\sim_\Sigma}| = 1$.

□

The last property states that the arc weights of the reduced net are identical to the original arc weights up to multiplication by an integer factor. The more equal conflicts are resolved by the reduction, the bigger is the factor. If the net is not of type RSC with respect to Σ, the property does not hold. For the net in Figure 4.7 with $\Sigma = \{id, (p_2\, p_3)(t_2\, t_3)\}$, for example, we have $\widetilde{Pre}_{\mu(p_2),\mu(t_2)}/Pre_{p_2,t_2} = \frac{w_1+w_2}{w_1}$ which is in general not a natural number. The net in Figure 4.5 is not of type RSC either and $|p_2^\bullet \cap [t_2]_{\sim_\Sigma}| = 1 \neq 2 = |p_4^\bullet \cap [t_2]_{\sim_\Sigma}|$ if $t_2 \sim_\Sigma t_5$.

The following lemma shows how regions of the original net and the reduced net are related in RSC nets. More precisely, it is shown that the polyhedral partition induced by the reduced net $\widetilde{\mathcal{N}}$ is the same as the one of the reduced PWL system (4.6).

Lemma 4.15. *Let $\mathcal{N}$ be RSC with respect to Σ. Let $K \in \mathcal{K}_{\mathcal{N}}^{\Sigma}$ and $\widetilde{K} = \mu^{\Sigma}(K)$. Then, $\phi^{-1}(M_K) = M_{\widetilde{K}}$.*

Proof. We show that each row $\neq 0$ of $G_K\phi$ appears also in $G_{\widetilde{K}}$ and vice versa using the definition of G_K via Equation (2.8). Let $\tilde{g} \neq 0$ be a row of $G_K\phi$. It stems from a row $g_{K,t,p}$ of G_K. The condition $\tilde{g} \neq 0$ together with Property 2 of Lemma 4.14 implies that $\mu(K(t)) \neq \mu(p)$. Also $\mu(t)$ has to be a join and $\mu(K(t))$ and $\mu(p)$ are among its input places as

$$\widetilde{Pre}_{\mu(K(t)),\mu(t)} = \sum_{t' \in [t]_{\sim_\Sigma}} Pre_{K(t),t'} \geq Pre_{K(t),t} > 0,$$
$$\widetilde{Pre}_{\mu(p),\mu(t)} = \sum_{t' \in [t]_{\sim_\Sigma}} Pre_{p,t'} \geq Pre_{p,t} > 0.$$

By definition, $\widetilde{K}(\mu(t)) = \mu(K(t))$. Therefore, $g_{K,t,p}\,\phi$ and $\tilde{g}_{\widetilde{K},\mu(t),\mu(p)}$ have the positive and negative elements at the same position and are equal if and only if $\widetilde{Pre}_{\mu(K(t)),\mu(t)} = Pre_{K(t),t}$ and $\widetilde{Pre}_{\mu(p),\mu(t)} = Pre_{p,t}$. However, we do not need the rows to be equal in order to define the same set of markings as the description of the polyhedron by a matrix is not unique. In particular, each row may be multiplied by

an arbitrary positive constant without changing the polyhedron it describes. The equality of the elements of Pre and $\widetilde{Pre}$ can therefore be weakened to

$$\frac{\widetilde{Pre}_{\mu(K(t)),\mu(t)}}{Pre_{K(t),t}} = \frac{\widetilde{Pre}_{\mu(p),\mu(t)}}{Pre_{p,t}}. \tag{4.11}$$

This condition is always satisfied in RSC nets according to Property 4 of Lemma 4.14.

Let now $\tilde{g}_{\widetilde{K},\tilde{t},\tilde{p}}$ be a row of $G_{\widetilde{K}}$. We show that there exists a corresponding row in $G_K\phi$. Let $t \in \mu^{-1}(\tilde{t})$. By definition of $\widetilde{K}$, we get $\mu(K(t)) = \widetilde{K}(\tilde{t}) \neq \tilde{p}$. As $\tilde{p} \in {}^\bullet\tilde{t}$, there exist $(p', t') \in (\mu^{-1}(\tilde{p}), \mu^{-1}(\tilde{t}))$ with $p' \in {}^\bullet t'$. Let $\sigma \in \Sigma$ be such that $t' = \sigma(t)$. Then, $0 < Pre_{p',t'} = Pre_{\sigma^{-1}(p'),t}$. Let $p := \sigma^{-1}(p')$. It follows that $p \in {}^\bullet t$ and $\mu(p) = \mu(p')$.

The row $g_{K,t,p}\phi$ has the positive and negative elements at the same position as $\tilde{g}_{\widetilde{K},\tilde{t},\tilde{p}}$. Equality up to multiplication by a positive factor is given again if Equation (4.11) is satisfied which is guaranteed under the RSC condition. □

The following property follows immediately.

Corollary 4.16. *Let $\mathcal{N}$ be RSC with respect to Σ. Let $K, K' \in \mathcal{K}^\Sigma_\mathcal{N}$ be configurations with $\mu^\Sigma(K) = \mu^\Sigma(K')$. Then, $\phi^{-1}(M_{K'}) = \phi^{-1}(M_K)$.*

This means that in order to describe $M_{\widetilde{K}}$, we may choose any configuration $K \in \mathcal{K}^\Sigma_\mathcal{N}$ with $\mu^\Sigma(K) = \widetilde{K}$ to describe the corresponding region via $\phi^{-1}(M_K)$.

The prerequisite that the net is RSC is crucial as the following example shows.

Example 4.17. Let us consider the net in Figure 4.7. Suppose that $w_1 > w_2$. The net is symmetric with $\Sigma^t_{\langle\mathcal{N},\lambda\rangle} = \{id, \sigma\}$ where $\sigma = (p_2\, p_3)(t_2\, t_3)$. The equivalent transitions t_2 and t_3 are in an unequal conflict relation. Thus, the net is not RSC with respect to $\Sigma^t_{\langle\mathcal{N},\lambda\rangle}$. It is $Pre_{p_2,t_2} = w_1 \neq w_2 = Pre_{p_3,t_2}$ even though p_2 and p_3 are equivalent input places of t_2. The previous proof was based on the property of RSC nets that such arcs have always got the same weight.

The net has four configurations. As $\mu(p_2) = \mu(p_3)$, all configurations are elements of $\mathcal{K}^\Sigma_\mathcal{N}$ and μ^Σ maps all these configurations onto the single configuration $\widetilde{K} = \{(\tilde{t}_1, \tilde{p}_1), (\tilde{t}_2, \tilde{p}_2)\}$.

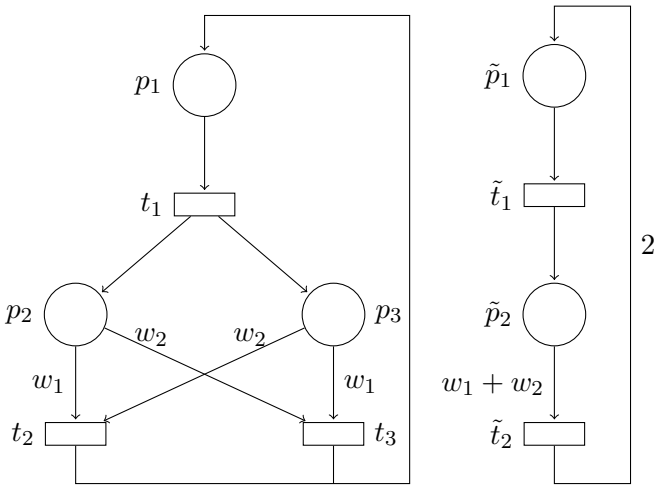

(a) The original net (b) The reduced net

Figure 4.7: A net which is not of type RSC and the corresponding reduction.

We consider the regions that correspond to the configurations

$$K_1 = \{(t_1, p_1), (t_2, p_2), (t_3, p_2)\} \text{ and } K_2 = \{(t_1, p_1), (t_2, p_2), (t_3, p_3)\}.$$

All symmetric markings, i.e., those with $m_{p_1} = m_{p_2}$, are contained in region M_{K_2}. Even though $\mu^\Sigma(K_1) = \mu^\Sigma(K_2)$, the preimages of their regions under ϕ

$$\phi^{-1}(M_{K_1}) = \{\widetilde{m} \in \mathbb{R}^2_{\geq 0} \,|\, \widetilde{m}_{\tilde{p}_2} = 0\} \text{ and } \phi^{-1}(M_{K_2}) = \mathbb{R}^2_{\geq 0}$$

do not coincide. ♢

4.3.5 Firing Rates

In order to fully describe the reduced net we need to define firing rates. It has been suggested in Section 4.3.1 to compute $\widetilde{\Lambda} = \theta^+ \Lambda \, \theta$ and use the diagonal elements as the new firing rates. This is the same as to adopt the firing rates of the original net, i.e., $\lambda_{\mu(t)} = \lambda_t$ for all $t \in \mathcal{T}$. The following example shows that this does not always work and suggests a procedure to adapt the firing rates.

Example 4.18. Figure 4.8 shows a Petri net with Z_2-symmetry and the corre-

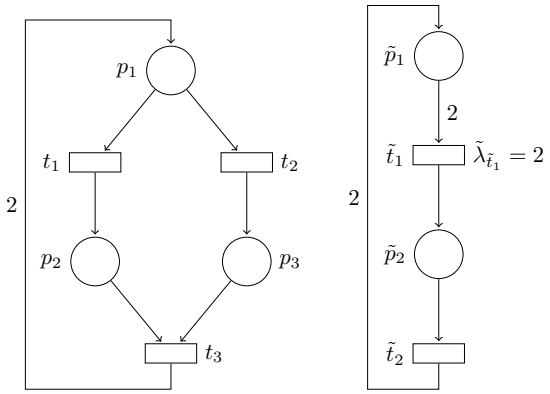

Figure 4.8: A Petri net with symmetry and the corresponding reduced net with adjusted firing rate.

sponding reduced net we obtain from $\widetilde{Pre}$ and $\widetilde{Post}$. Assuming the same firing rates as in the original net ($\widetilde{\Lambda} = \theta^+ \Lambda \, \theta$, i.e., $\lambda_{\tilde{t}_1} = \lambda_{t_1} = \lambda_{t_2} = 1$ and $\lambda_{\tilde{t}_2} = \lambda_{t_3} = 1$), the marking in steady state and the corresponding flow of the original net and the reduced net do not coincide even though the RSC property holds. Traditional reduction techniques for Petri nets like reduction rule RR_5 in [ADFN99], which covers a similar scenario, suggest that the firing rate of transition $\tilde{t}_1$ should be chosen to be 2. For this value, the marking in steady state and the throughput are as required. How can we obtain this change of the firing rate automatically? Our original approach of $\widetilde{\Lambda} = \theta^+ \Lambda \theta$ cannot be used as it just assigns the original firing rates to the corresponding transitions of the reduced net. Instead, we consider Λ and Π_K jointly. In the original net, there are two configurations K_1 and K_2. We take the part of Equation (4.7) that contains both matrices and obtain

$$\theta^+ \Lambda \Pi_{K_1} \phi = \theta^+ \Lambda \Pi_{K_2} \phi = \begin{pmatrix} \lambda_{t_1} & 0 \\ 0 & \lambda_{t_3} \end{pmatrix}.$$

The reduced net does not have any join, consequently there is only one configuration $\widetilde{K}$ with

$$\widetilde{\Lambda} \Pi_{\widetilde{K}} = \begin{pmatrix} \frac{\tilde{\lambda}_{\tilde{t}_1}}{2} & 0 \\ 0 & \tilde{\lambda}_{\tilde{t}_2} \end{pmatrix}.$$

The matrices coincide if $\tilde{\lambda}_{\tilde{t}_1} = 2\lambda_{t_1} = 2$ and $\tilde{\lambda}_{\tilde{t}_2} = \lambda_{t_3} = 1$. For this choice of firing rates the reduction is valid. However, this example immediately raises the question if the firing rates computed with this method change with the configuration. This is an important issue for the analysis of this method since firing rates should be independent of the active configuration. ♢

As in the previous example, we choose $\widetilde{\Lambda} = \mathrm{diag}(\tilde{\lambda}_{\tilde{t}_1}, \ldots, \tilde{\lambda}_{\tilde{t}_q})$ such that for a $K \in \mathcal{K}_{\mathcal{N}}^{\Sigma}$

$$\phi^+ \Lambda \Pi_K \phi = \widetilde{\Lambda} \Pi_{\mu^{\Sigma}(K)}. \tag{4.12}$$

If this equality holds for all configurations, then — by the previous results — equality of the PWL system associated with the reduced net $\widetilde{\mathcal{N}}$ and the reduced PWL system (Equation (4.6)) of the original net is guaranteed.

Let $\widetilde{K} = \mu^{\Sigma}(K)$. In the original and reduced net,

$$(\Lambda \Pi_K)_{t,p} = \begin{cases} \frac{\lambda_t}{Pre_{p,t}} & \text{if } K(t) = p \\ 0 & \text{otherwise} \end{cases} \text{ and } (\widetilde{\Lambda}\Pi_{\widetilde{K}})_{\tilde{t},\tilde{p}} = \begin{cases} \frac{\tilde{\lambda}_{\tilde{t}}}{\widetilde{Pre}_{\tilde{p},\tilde{t}}} & \text{if } \widetilde{K}(\tilde{t}) = \tilde{p} \\ 0 & \text{otherwise.} \end{cases}$$

Furthermore,

$$(\Lambda \Pi_K \phi)_{t,\tilde{p}} = \sum_{p \in \mathcal{P}} \lambda_t (\Pi_K)_{t,p} \delta_{\mu(p),\tilde{p}} = \lambda_t (\Pi_K)_{t,K(t)} \delta_{\mu(K(t)),\tilde{p}} = \frac{\lambda_t}{Pre_{K(t),t}} \delta_{\mu(K(t)),\tilde{p}}$$

and finally

$$(\theta^+ \Lambda \Pi_K \phi)_{\tilde{t},\tilde{p}} = \sum_{t \in \mathcal{T}} \frac{1}{\langle \tilde{t} \rangle} \delta_{\tilde{t},\mu(t)} (\Lambda \Pi_K \phi)_{t,\tilde{p}} = \frac{1}{\langle \tilde{t} \rangle} \sum_{t \in \mu^{-1}(\tilde{t})} \frac{\lambda_t}{Pre_{K(t),t}} \delta_{\mu(K(t)),\tilde{p}}.$$

By definition of $\mathcal{K}_{\mathcal{N}}^{\Sigma}$, $\mu(K(t)) = \tilde{p}$ if and only if $\widetilde{K}(\mu(t)) = \tilde{p}$. Therefore, the nonzero elements of the two matrices are at the same positions. We can furthermore simplify the last term if the net is RSC with respect to Σ. Then, Property 3 of Lemma 4.14 guarantees that the denominators in the sum are all identical. Thus, for $t \in \mu^{-1}(\tilde{t})$,

$$\frac{1}{\langle \tilde{t} \rangle} \sum_{t \in \mu^{-1}(\tilde{t})} \frac{\lambda_t}{Pre_{K(t),t}} = \frac{1}{\langle \tilde{t} \rangle} \langle \tilde{t} \rangle \frac{\lambda_t}{Pre_{K(t),t}} = \frac{\lambda_t}{Pre_{K(t),t}}.$$

We conclude

$$(\theta^+ \Lambda \Pi_K \phi)_{\tilde{t},\tilde{p}} = \begin{cases} \frac{\lambda_t}{Pre_{K(t),t}} & \text{if } \mu^\Sigma(K)(\tilde{t}) = \tilde{p} \\ 0 & \text{otherwise} \end{cases}$$

where $t \in \mu^{-1}(\tilde{t})$.

We assume that the net is RSC with respect to Σ. Equality (4.12) holds if for all $t \in \mathcal{T}$

$$\tilde{\lambda}_{\mu(t)} = \lambda_t \frac{\widetilde{Pre}_{\mu^\Sigma(K)(\mu(t)),\mu(t)}}{Pre_{K(t),t}} = \lambda_t \frac{\sum_{t' \in [t]_{\sim_\Sigma}} Pre_{K(t),t'}}{Pre_{K(t),t}}. \tag{4.13}$$

If the net is RSC with respect to Σ, this formula holds for a transition t if and only if it holds for a transition equivalent to t. Under the RSC condition, the formula is also independent of the configuration. This is a direct consequence of Property 4 in Lemma 4.14. Furthermore, Equation (4.13) shows that firing rates have to be increased only for transitions in conflict relations.

To summarize:

Lemma 4.19. *Let $\mathcal{N}$ be RSC with respect to Σ. The firing rates $\tilde{\lambda}_{\tilde{t}_1}, \ldots, \tilde{\lambda}_{\tilde{t}_q}$ as given by Equation (4.13) are such that with $\widetilde{\Lambda} = \mathrm{diag}(\tilde{\lambda}_{\tilde{t}_1}, \ldots, \tilde{\lambda}_{\tilde{t}_q})$ the equality*

$$\phi^+ \Lambda \Pi_K \phi = \widetilde{\Lambda} \Pi_{\mu^\Sigma(K)}$$

holds for all $K \in \mathcal{K}^\Sigma_\mathcal{N}$.

The restriction to nets which are RSC with respect to Σ is important. In fact, Equation (4.13) can yield different values for different configurations if t is in an unequal conflict relation. An example is given by the net in Figure 4.5 which has been studied in Example 4.12. There exists no firing rate $\tilde{\lambda}_{\tilde{t}_2}$ such that the matrix products studied above are equal. Applying formula (4.13) we obtain

$$\tilde{\lambda}_{\tilde{t}_2} = \lambda_{t_2} \frac{\widetilde{Pre}_{\tilde{p}_2,\tilde{t}_2}}{Pre_{p_2,t_2}} = \lambda_{t_2} \text{ and } \tilde{\lambda}_{\tilde{t}_2} = \lambda_{t_2} \frac{\widetilde{Pre}_{\tilde{p}_4,\tilde{t}_2}}{Pre_{p_4,t_2}} = 2\lambda_{t_2}$$

for K_1 and K_2, respectively. No firing rates independent of the configuration can be found.

4.3.6 Case Study I: A Manufacturing System

We apply the reduction technique to a Petri net that models a manufacturing system. The net, which is shown in Figure 4.9 together with an interpretation of its nodes, is adapted from [RJS02]. It is a marked graph with two shared resources. The system describes how two materials are being preprocessed by two machines before being assembled to the final product by a third machine.

In detail, material of two types A and B is stored in buffers modeled by places p_1 and p_9, respectively. Initially, there are 15 pallets with material of type A and B, respectively, in the two buffers. Both materials are preprocessed by the same machines M_1 and M_2 which are therefore shared resources. However, for material of type A, machine M_1 performs the first preprocessing step and M_2 the second one while material of type B is processed by machine M_2 first and by M_2 afterwards. The resulting intermediate goods are stored in buffers modeled by p_6 and p_{14}, respectively. Machine M_3 assembles the final product from the intermediate goods. This is then stored in buffer p_{18} until its removal from the production line.

The manufacturing system is symmetric due to the fact that both materials A and B are preprocessed in the same way before the final assembly. We may permute nodes referring to A with those referring to B. The table in Figure 4.9 already indicates the symmetry as nodes that appear in one row of the table are equivalent. Therefore, $\Sigma^t_{\langle \mathcal{N},\lambda \rangle} = \{id, \sigma\}$ with

$$\sigma = (p_1\, p_9)(p_2\, p_{10})(p_3\, p_{11})(p_4\, p_{12})(p_5\, p_{13})(p_6\, p_{14})(p_7\, p_8)(t_1\, t_5)(t_2\, t_6)(t_3\, t_7)(t_4\, t_8).$$

The permutation of p_7 and p_8 (i.e., the usage of machines M_1 and M_2) reflects the different order in which the two machines are used for the preprocessing process.

This symmetry satisfies the RSC condition. The only choices in the system are p_7 and p_8 representing the use of machines as shared resources and their output nodes t_1 and t_7 (resp. t_3 and t_5) are not equivalent.

The net that results from the reduction is shown in Figure 4.10. It contains the part for preprocessing material only once while the subnet that models the final assembly remains unchanged. The reduced net has only 11 places and 7 transitions compared to 18 places and 11 transitions in the original net. Only one place, namely

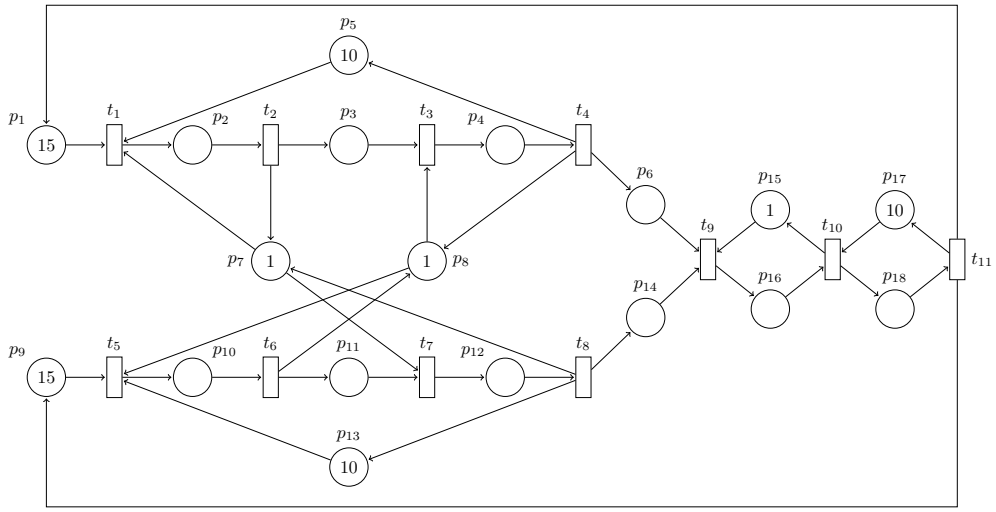

Node	Interpretation (and firing rate)
p_1, p_9	buffers for material A and B, respectively
p_2, p_{10}	material being processed by machines M_1 and M_2, respectively
p_3, p_{11}	intermediate buffers for material having been processed once
p_4, p_{12}	material being processed by machines M_2 and M_1, respectively
p_5, p_{13}	capacity of the production lines for materials A and B, respectively
p_6, p_{14}	buffers for intermediate goods
p_7, p_8	availability of shared machines M_1 and M_2, respectively
p_{15}	availability of machine M_3
p_{16}	finished goods in machine M_3
p_{17}	capacity of buffer p_{18}
p_{18}	buffer for final good
t_1, t_5	first preprocessing step using the shared machines ($\lambda_{t_1} = \lambda_{t_5} = 1$)
t_2, t_6	finish of first preprocessing step ($\lambda_{t_2} = \lambda_{t_6} = 3$)
t_3, t_7	second preprocessing step using the shared machines ($\lambda_{t_3} = \lambda_{t_7} = 1$)
t_4, t_8	finish of preprocessing of materials A and B ($\lambda_{t_4} = \lambda_{t_8} = 4$)
t_9	assembly of final product from preprocessed materials ($\lambda_{t_9} = 1$)
t_{10}	finish of the production process, transport to final buffer ($\lambda_{t_{10}} = 4$)
t_{11}	removal of final goods ($\lambda_{t_{11}} = 1$)

Figure 4.9: A Petri net system modeling a manufacturing system (adapted from [RJS02]).

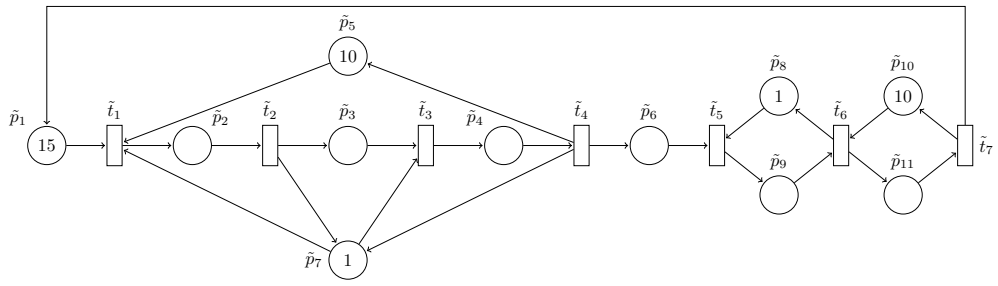

Figure 4.10: A reduced Petri net system to model the manufacturing system.

$\tilde{p}_7$ is needed in order to model the availability of both machines M_1 and M_2. For this reason, the transitions $\tilde{t}_2$ and $\tilde{t}_4$ have a common output place unlike their counterparts in the original net. Similarly, $\tilde{t}_1$ and $\tilde{t}_3$ are now in conflict relation. This shows that, in general, the new net is not simply a subnet of the original net which is obtained simply by removing (redundant) nodes and all their connecting arcs. No arc weights are altered by the reduction. Thus, all firing rates remain as in the original net as well.

4.3.7 Case Study II: The Role of Choices

Studying regions and firing rates of the reduced net, the main difficulties are due to choices. They arise when, by the reduction, places lose their property of being choices. The reason is that in this case weights of arcs from places to transitions change. These new arc weights directly affect the matrices Π_K and the regions as both are defined via Pre. Moreover, the weak condition of equation (4.11) only comes into play when there are transitions in CEQ relation whose input places are not equivalent.

The following example illustrates the entire reduction process. In order to incorporate the main issues discussed in this chapter, a purely academic example with an equal conflict is studied.

Let us consider the net in Figure 4.11(a). The corresponding symmetry group is

$$\Sigma^t_{\langle \mathcal{N},\lambda \rangle} = \{id, (p_1\, p_2), (t_2\, t_3), (p_1\, p_2)(t_2\, t_3)\}.$$

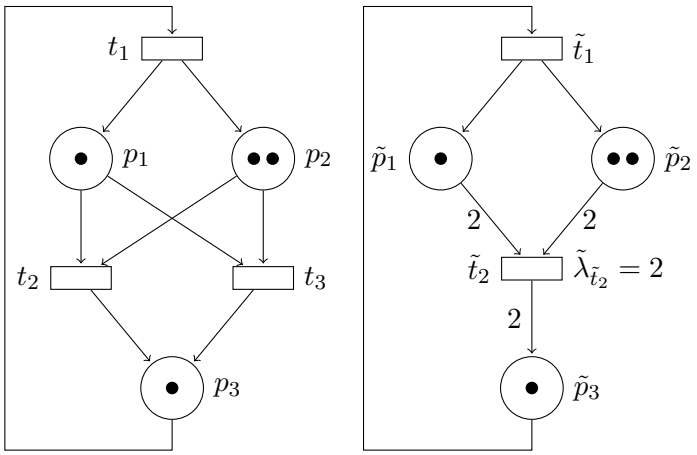

(a) The original net (b) The reduced net

Original Net		**Reduced Net**	
Configuration	Region	Configuration	Region
$K_1(t_2) = K_1(t_3) = p_1$	$m_{p_1} \leq m_{p_2}$	$\widetilde{K}_1(\tilde{t}_2) = \tilde{p}_1$	$\widetilde{m}_{\tilde{p}_1} \leq \widetilde{m}_{\tilde{p}_2}$
$K_2(t_2) = K_2(t_3) = p_2$	$m_{p_2} \leq m_{p_1}$	$\widetilde{K}_2(\tilde{t}_2) = \tilde{p}_2$	$\widetilde{m}_{\tilde{p}_2} \leq \widetilde{m}_{\tilde{p}_1}$
$K_3(t_2) = p_1,\ K_3(t_3) = p_2$	$m_{p_1} = m_{p_2}$		
$K_4(t_2) = p_2,\ K_4(t_3) = p_1$	$m_{p_1} = m_{p_2}$		

(c) Configurations

Figure 4.11: A reduction that resolves an equal conflict.

Its isotropy subgroup at the initial marking $m_0 = \begin{pmatrix} 1 & 2 & 1 \end{pmatrix}^T$ is $\Sigma_{m_0} = \{id, (t_2\, t_3)\}$. For this subgroup the net is RSC and we perform the reduction with respect to Σ_{m_0}.

The corresponding matrices are

$$Pre = \begin{pmatrix} 0 & 1 & 1 \\ 0 & 1 & 1 \\ 1 & 0 & 0 \end{pmatrix}, \qquad Post = \begin{pmatrix} 1 & 0 & 0 \\ 1 & 0 & 0 \\ 0 & 1 & 1 \end{pmatrix}, \qquad \phi = I_3,$$

$$\widetilde{Pre} = \begin{pmatrix} 0 & 2 \\ 0 & 2 \\ 1 & 0 \end{pmatrix}, \qquad \widetilde{Post} = \begin{pmatrix} 1 & 0 \\ 1 & 0 \\ 0 & 2 \end{pmatrix}, \qquad \theta = \begin{pmatrix} 1 & 0 \\ 0 & 1 \\ 0 & 1 \end{pmatrix}.$$

The reduced net is shown in Figure 4.11(b).

Let us compare the configurations of the two nets. Configurations K_3 and K_4 are not in $\mathcal{K}_{\mathcal{N}}^{\Sigma_{m_0}}$ as for $\sigma = (t_2\, t_3)$ we get $\mu(K_3(t_2)) = \tilde{p}_1 \neq \tilde{p}_2 = \mu(K_3(\sigma(t_2)))$ and $\mu(K_4(t_2)) = \tilde{p}_2 \neq \tilde{p}_1 = \mu(K_4(\sigma(t_2)))$. The regions corresponding to configurations K_1 and K_2 are described by means of

$$G_{K_1} = G_{K_1}\phi = \begin{pmatrix} 1 & -1 & 0 \\ 1 & -1 & 0 \end{pmatrix} = -G_{K_2} = -G_{K_2}\phi.$$

Their counterparts in the reduced net are

$$G_{\widetilde{K}_1} = \begin{pmatrix} \frac{1}{2} & -\frac{1}{2} & 0 \end{pmatrix} = -G_{\widetilde{K}_2}.$$

Due to the fact that the arc weights of the input arcs of $\tilde{t}_2$ differs from those of t_2 or t_3, the rows of the matrices $G_{K_1}\phi$ and $G_{\widetilde{K}_1}$ (or $G_{K_2}\phi$ and $G_{\widetilde{K}_2}$) do not coincide. However, they are identical up to multiplication by a positive scalar. That is, condition (4.11) holds and the regions coincide.

Finally, the firing rate of transition $\tilde{t}_2$ has to be adapted to

$$\tilde{\lambda}_{\tilde{t}_2} = \lambda_{t_2} \frac{\widetilde{Pre}_{\tilde{p}_1,\tilde{t}_2}}{Pre_{p_1,t_2}} = \lambda_{t_2} \frac{\widetilde{Pre}_{\tilde{p}_2,\tilde{t}_2}}{Pre_{p_2,t_2}} = 2\lambda_{t_2}$$

according to Equation (4.13) to complete the reduction procedure.

An alternative way to reduce the Petri net in this example is to remove place p_2 as it is implicit, i.e., it never constrains the flow of t_2 or t_3. The removal of implicit places is a well-known technique. Here, symmetries help us to identify the implicit place. As p_1 and p_2 are equivalent with respect to $\Sigma^t_{\langle\mathcal{N},\lambda\rangle}$ and as isotropy subgroups are constant along trajectories, the marking of the two places cannot become equal. Therefore, $m_{p_2}(\tau) > m_{p_1}(\tau)$ for all $\tau \geq 0$ which makes p_2 implicit. Such implicit places typically appear if two places are equivalent with respect to $\Sigma^t_{\langle\mathcal{N},\lambda\rangle}$ but not with respect to the chosen subgroup Σ.

4.3.8 Consolidation of Results

In nets with symmetry, the corresponding system of ODEs can always be reduced to an s-dimensional system, where s is the dimension of the fixed-point subspace induced by the symmetry. In contrast to this purely algebraic reduction given by system (4.6), the physical reduction of the net allows for easier interpretation and other reduction techniques can be applied afterwards to reduce the system even further.

The reduction is always performed with respect to a subgroup $\Sigma \subset \Sigma^t_{\langle\mathcal{N},\lambda\rangle}$ which is chosen such that the net is RSC with respect to this subgroup. The reduction is valid for any initial marking m_0 with $\Sigma \subset \Sigma_{m_0}$.

If the original net is choice-free or none of the output transitions of a choice are equivalent, then the firing rates in both nets are the same, otherwise they might have to be increased in the reduced net. If unequal conflicts are "resolved" by the reduction, then it is in general not possible to adjust the firing rates and the partitions of the marking spaces do not coincide.

We summarize our results on the evolution in the following theorem which follows from Equation (4.7) together with all the considerations on the configurations, regions, and firing speeds considered in this section.

Theorem 4.20. *Let $\langle\mathcal{N},\lambda\rangle$ be a Petri net and m_0 its initial marking. Let $\Sigma \subset \Sigma_{m_0} \subset \Sigma^t_{\langle\mathcal{N},\lambda\rangle}$ be a subgroup such that the net is RSC with respect to Σ. Let the reduced net be given as described above with the firing rates adapted accordingly and let $\phi^+ m_0$ be the initial marking of the reduced net. Suppose that $\widetilde{m}$ and $\tilde{f}$*

denote the marking evolution and the firing flow of the reduced net, respectively, then $m(\tau) = \phi\,\widetilde{m}(\tau)$ *and* $f(\widetilde{m}(\tau)) = \theta\tilde{f}(\widetilde{m}(\tau))$ *for all* $\tau \geq 0$.

The idea behind the procedure is based on fixed-point subspaces which typically appear for equivariant dynamical systems. Both the concept behind the reduction technique and the proof of its correctness are based on a reduction of the PWL system associated with the original continuous Petri net system. However, the implementation of the procedure does not require the intermediate step of the reduced PWL system. Instead it consists of the following steps:

1. Compute the isotropy subgroup at the initial marking Σ_{m_0}.
2. Choose a subgroup $\Sigma \subset \Sigma_{m_0}$ s.t. $\mathcal{N}$ is RSC with respect to Σ and define a mapping μ.
3. Compute $\widetilde{Pre}$ and $\widetilde{Post}$ using (4.8) and (4.9).
4. Compute firing rates with (4.13).

4.3.9 Net Morphisms

In this chapter, a reduction technique has been developed, that — given the TCPN is symmetric — transforms the original net $\mathcal{N} = \langle \mathcal{P}, \mathcal{T}, Pre, Post \rangle$ into the reduced net $\widetilde{\mathcal{N}} = \langle \widetilde{\mathcal{P}}, \widetilde{\mathcal{T}}, \phi^+ Pre\,\theta, \phi^+ Post\,\theta \rangle$. Each node of the new net represents an equivalence class of nodes of the original net. In the context of ordinary Petri nets, a map that relates a Petri net with a net composed of equivalence classes of nodes and arcs between them while preserving central structural properties is known as a quotient[3] [Des91]. They are special net morphisms. We therefore study in this section if the symmetry reduction method can be interpreted as a net morphism in order to check if results from general net theory, where morphisms between nets are considered instead of single nets, can be applied [Des91, GLT80].

Petri net morphisms are maps from Petri nets to Petri nets. They have been defined first for ordinary Petri nets [GLT80, Des91, GV03]. Extensions are known for place/transition nets [MMS94, EHP06] and even high-level nets [DHP91, Pra06].

[3] In the introduction to Section 4.3 it has been said that in the context of Coupled Cell Systems the result of a transformation of a net that merges equivalent nodes is called a quotient net. Analogously, we call $\widetilde{\mathcal{N}}$ a quotient net.

Net morphisms are fundamental for many operations on nets such as the composition of nets or refinements. They are used to define categories of Petri nets (e.g., safe Petri nets) and hence allow to study the relation between different such categories.

We start with the definition of net morphisms for ordinary Petri nets for which the term "quotient" is explicitly mentioned in the related literature (e.g., [GV03, DM91]). We consider ordinary Petri nets of the form $\mathcal{N} = \langle \mathcal{P}, \mathcal{T}, F \rangle$ where F denotes the set of arcs.[4]

Definition 4.21. *[GV03] Let $\mathcal{N}_1 = \langle \mathcal{P}_1, \mathcal{T}_1, F_1 \rangle$ and $\mathcal{N}_2 = \langle \mathcal{P}_2, \mathcal{T}_2, F_2 \rangle$ be two ordinary Petri nets. A mapping $\varphi : (\mathcal{P}_1 \cup \mathcal{T}_1) \to (\mathcal{P}_2 \cup \mathcal{T}_2)$ is a* net morphism *if*

- $(u, v) \in F_1 \cap (\mathcal{P}_1 \times \mathcal{T}_1) \Rightarrow (\varphi(u), \varphi(v)) \in F_2 \cap (\mathcal{P}_2 \times \mathcal{T}_2)$ *or* $\varphi(u) = \varphi(v)$ *and*
- $(u, v) \in F_1 \cap (\mathcal{T}_1 \times \mathcal{P}_1) \Rightarrow (\varphi(u), \varphi(v)) \in F_2 \cap (\mathcal{T}_2 \times \mathcal{P}_2)$ *or* $\varphi(u) = \varphi(v)$.

It is a folding *if it respects the type of nodes, i.e., $\varphi(\mathcal{P}_1) \subset \mathcal{P}_2$ and $\varphi(\mathcal{T}_1) \subset \mathcal{T}_2$. A morphism is a* quotient *if it is surjective and for all $(u', v') \in F_2$ there exists an arc $(u, v) \in F_1$ with $\varphi(u) = u'$ and $\varphi(v) = v'$.*

With this definition, morphisms can merge nodes but never delete any. In general, the node type does not have to be respected. In fact, such morphisms can be used to describe the fusion of subnets into a single node. An examples is given in Figure 4.12(a). In the case of our reduction technique, the mapping $\mu : (\mathcal{P} \cup \mathcal{T}) \to (\widetilde{\mathcal{P}} \cup \widetilde{\mathcal{T}})$ is a net morphism between the underlying net graphs. This can be deduced from Equation (4.10) on page 81. It furthermore respects the node type and is surjective by definition of $\widetilde{\mathcal{P}}$ and $\widetilde{\mathcal{T}}$. Again from Equation (4.10), it follows that every arc of the reduced net has at least one counterpart in the original net. Hence, μ is in fact a quotient. However, when arc weights come in, the situation is slightly more difficult.

For the weighted extension, i.e., for place/transition nets, definitions of a morphism are stated in [EHP06, Pra06]. In contrast to general net morphisms of ordinary nets, the definition is restricted to maps that respect the node type. The definition can be stated particularly conveniently if the net is given in the set-based algebraic notion. In this notation, a place/transition net $\mathcal{N} = \langle \mathcal{P}, \mathcal{T}, pre, post \rangle$ is given by a

[4] Cf. expression (2.1) for place/transition nets of which ordinary Petri nets can be seen as a subset. A weight function is not needed for ordinary nets. The dynamics (i.e., the firing rule) is defined as for any place/transition net.

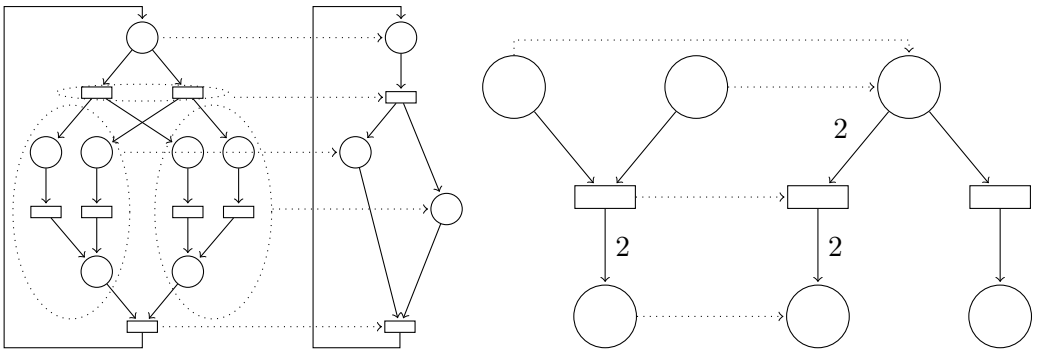

(a) A quotient [DM91] (b) A place/transition net morphism [Pad09]

Figure 4.12: Examples of net morphisms between Petri nets.

set $\mathcal{P}$ of places, a set $\mathcal{T}$ of transitions, as well as *pre*- and *post*-domain functions[5] $pre, post : \mathcal{T} \to \mathcal{P}^{\oplus}$, where $\mathcal{P}^{\oplus}$ is the free commutative monoid over P or, in other words, the set of finite multisets over $\mathcal{P}$. In this notation $pre(t_1) = 2p_1 \oplus p_3$ means that transition t_1 has two input places p_1 and p_3. The associated arc weights are 2 and 1, respectively. A marking of the net is given by $M = \sum_{p \in \mathcal{P}} m_p p$ where m_p denotes the number of tokens in place p. In this notation arc weights and markings are always assumed to take only nonnegative integer values. For a map $f_{\mathcal{P}} : \mathcal{P}_1 \to \mathcal{P}_2$ between two sets of places, we define the extension $f_{\mathcal{P}}^{\oplus} : \mathcal{P}_1^{\oplus} \to \mathcal{P}_2^{\oplus}$ of $f_{\mathcal{P}}$ such that every $w = \sum_{p \in \mathcal{P}_1} \lambda_p \, p \in \mathcal{P}_1^{\oplus}$ is mapped to $f_{\mathcal{P}}^{\oplus}(w) = \sum_{p \in \mathcal{P}_1} \lambda_p f_{\mathcal{P}}(p)$.

Definition 4.22. *[EHP06] A* place/transition net morphism $f : \mathcal{N}_1 \to \mathcal{N}_2$ *between two place/transition nets* $\mathcal{N}_1 = \langle \mathcal{P}_1, \mathcal{T}_1, pre_1, post_1 \rangle$ *and* $\mathcal{N}_2 = \langle \mathcal{P}_2, \mathcal{T}_1, pre_2, post_2 \rangle$ *is given by*

$$f = (f_{\mathcal{P}} : \mathcal{P}_1 \to \mathcal{P}_2, f_{\mathcal{T}} : \mathcal{T}_1 \to \mathcal{T}_2)$$

compatible with the pre- and post-domain functions, i.e.,

$$pre_2 \circ f_{\mathcal{T}} = f_{\mathcal{P}}^{\oplus} \circ pre_1 \text{ and } post_2 \circ f_{\mathcal{T}} = f_{\mathcal{P}}^{\oplus} \circ post_1.$$

This equation can be represented by the following diagram:

[5] Lower case letters are used to distinguish the set-based algebraic notation from the matrix notation with *Pre* and *Post*.

$$\begin{array}{ccc} \mathcal{T}_1 & \overset{pre_1}{\underset{post_1}{\rightrightarrows}} & \mathcal{P}_1^{\oplus} \\ \Big\downarrow{\scriptstyle f_{\mathcal{T}}} & & \Big\downarrow{\scriptstyle f_{\mathcal{P}}^{\oplus}} \\ \mathcal{T}_2 & \overset{pre_2}{\underset{post_2}{\rightrightarrows}} & \mathcal{P}_2^{\oplus} \end{array}$$

An important property of place/transition net morphisms is that they preserve the firing behavior in the sense that

$$m[t > m' \Rightarrow f_{\mathcal{P}}^{\oplus}(m)[f_{\mathcal{T}}(t) > f_{\mathcal{P}}^{\oplus}(m'). \tag{4.14}$$

This is shown in [Pad09, Theorem 2.20].

Examples of place/transition net morphisms are given in Figure 4.12(b) and in Figure 4.13 where they affect elementary conjunctions as introduced in Table 2.1. For these examples, let us consider the symmetric case $w_1 = w_2$. We can see that for those conjunctions related to alternatives (choices and attributions) the arc weights of the original and the transformed net are identical. Meanwhile, for conjunctions related to concurrency (forks and joins) they are summed up. This is contrary to the behavior of the symmetry reduction as presented in this thesis where arc weights increase when choices or attributions have less output or input arcs, respectively, after the reduction.

To the author's knowledge, quotients have not been defined for place/transition nets. It seems natural to require that μ should be a place/transition net morphism that also satisfies the definition of a quotient for ordinary Petri nets. In that sense the mapping μ is not a quotient between $\mathcal{N}$ and $\widetilde{\mathcal{N}}$. However, as it is a quotient for the underlying net graphs and as the nodes of the reduced net represent quotient sets of nodes of the original net, $\widetilde{\mathcal{N}}$ could well be called the quotient net of $\mathcal{N}$ with respect to the group Σ.

In addition, the matrices ϕ and θ can be used to construct a reduced net such that μ is in fact a place/transition net morphism. This can only be achieved if arc weights are computed in a way that is compatible with the transformation of elementary conjunctions as depicted in Figure 4.13. In fact, for a place/transition

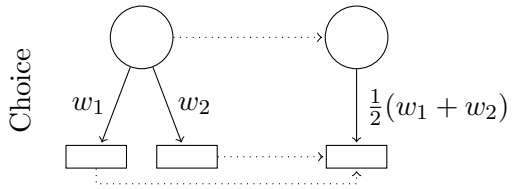

Figure 4.13: Place/transition net morphisms affecting elementary conjunctions. The dotted lines represent the morphisms.

net $\mathcal{N} = \langle \mathcal{P}, \mathcal{T}, Pre, Post \rangle$ and a group $\Sigma \subset \Sigma^s_{\mathcal{N}}$, the corresponding map $\mu = (\mu_{|\mathcal{T}}, \mu_{|\mathcal{P}})$ defines a place/transition net morphism between $\mathcal{N}$ and the smaller net $\langle \widetilde{\mathcal{P}}, \widetilde{\mathcal{T}}, \phi^T Pre\,(\theta^+)^T, \phi^T Post\,(\theta^+)^T \rangle$. This can be seen from

$$(\phi^T Pre\,(\theta^+)^T)_{\tilde{p},\tilde{t}} = \frac{1}{\langle \tilde{t} \rangle} \sum_{\substack{(p',t') \\ \in \mu^{-1}(\tilde{p}) \times \mu^{-1}(\tilde{t})}} Pre_{p,t} = \sum_{p \in \mu^{-1}(\tilde{p})} Pre_{p,t}$$

for an arbitrary $t \in \mu^{-1}(\tilde{t})$ and

$$(pre_2 \circ \mu)(t) = pre_2(\mu(t)) = \bigoplus_{\tilde{p} \in \widetilde{\mathcal{P}}} (\phi^T Pre (\theta^+)^T)_{\tilde{p},\mu(t)}\ \tilde{p} = \bigoplus_{\tilde{p} \in \widetilde{\mathcal{P}}} \left(\sum_{p \in \mu^{-1}(\tilde{p})} Pre_{p,t} \right) \tilde{p},$$

$$(\mu^{\oplus} \circ pre_1)(t) = \mu^{\oplus}(\bigoplus_{p \in \mathcal{P}} Pre_{p,t}\ p) = \bigoplus_{p \in \mathcal{P}} Pre_{p,t}\ \mu(p) = \bigoplus_{\tilde{p} \in \widetilde{\mathcal{P}}} \left(\sum_{p \in \mu^{-1}(\tilde{p})} Pre_{p,t} \right) \tilde{p}.$$

The computation for $Post$ is analogous.

To summarize, $\mu : \mathcal{P} \cup \mathcal{T} \to \widetilde{\mathcal{P}} \cup \widetilde{\mathcal{T}}$ defines a mapping from $\mathcal{N} = \langle \mathcal{P}, \mathcal{T}, Pre, Post \rangle$ to the reduced nets with s places and q transitions

$$\widetilde{\mathcal{N}} = \langle \widetilde{\mathcal{P}}, \widetilde{\mathcal{T}}, \phi^+ Pre\,\theta, \phi^+ Post\,\theta \rangle$$

and

$$\widetilde{\mathcal{N}}' = \langle \widetilde{\mathcal{P}}, \widetilde{\mathcal{T}}, \phi^T Pre\,(\theta^+)^T, \phi^T Post\,(\theta^+)^T \rangle.$$

Considering the pair $\mathcal{N}$ and $\widetilde{\mathcal{N}}$, i.e., the first case, μ is a quotient of the underlying net graphs. In general, it is not a place/transition net morphism. Equivalence of the dynamics of the original and the reduced net is in the sense of Theorem 4.20. Thus, the marking of a place $\tilde{p}$ is the same as the marking of each place $p \in \mu^{-1}(\tilde{p})$. Considering the pair $\mathcal{N}$ and $\widetilde{\mathcal{N}}'$, i.e., the second case, μ is a place/transition net morphism and the two place/transition nets have the same behavior in the sense of Equation (4.14).

4.3.10 Implications for Discrete Nets

The reduction of a Petri net $\langle \mathcal{N}, \lambda \rangle$ to a smaller timed net $\langle \widetilde{\mathcal{N}}, \tilde{\lambda} \rangle$ has been developed for TCPNs. One might ask if the procedure is also valid for discrete nets, in particular for place/transition nets and SPNs as a timed extension for which TCPNs can serve as an approximation. A comprehensive answer to this question is beyond the scope of this thesis, but we can make some observations.

For place/transition nets it has been illustrated by Example 3.14 that — in contrast to TCPNs — isotropy subgroups are not constant along occurrence sequences. However, comparing reachability graphs of original and reduced Petri nets from the previous sections, one observes that occurrence sequences of the reduced net correspond to occurrence sequences of the original system by merging the firing of equivalent transitions.

In order to prove this, we introduce the following concept. Let $\mathcal{T}' \subset \mathcal{T}$ be a set of transitions. We say that $\mathcal{T}'$ is firable in m if all transitions can fire simultaneously. This is equivalent to saying that $m \geq Pre\left(\sum_{t \in \mathcal{T}'} e_t\right)$. We write $m[\mathcal{T}' > m'$ where m' is the resulting marking.

Theorem 4.23. *Let $\mathcal{N}$ be a place/transition net with initial marking m_0. Let $\Sigma \subset \Sigma_{m_0} \subset \Sigma^s_{\mathcal{N}}$ be a subgroup and matrices ϕ, θ defined as before. Let $\widetilde{\mathcal{N}} = \langle \widetilde{\mathcal{P}}, \widetilde{\mathcal{T}}, \phi^+ Pre\,\theta, \phi^+ Post\,\theta \rangle$ be the reduced net with respect to Σ and $\widetilde{m}_0 = \phi^+ m_0$, then*

$$\widetilde{m} \in RS(\widetilde{\mathcal{N}}, \widetilde{m}_0) \Rightarrow \phi\widetilde{m} \in RS(\mathcal{N}, m_0).$$

In particular, let $\tilde{t}^{(1)}\tilde{t}^{(2)}\ldots\tilde{t}^{(j)}$ be a firing sequence of $\widetilde{\mathcal{N}}$ which is firable from $\widetilde{m}_0$ and let $\widetilde{m}_1, \ldots, \widetilde{m}_j$ be the markings reached, then

$$m_0 = \phi\widetilde{m}_0[\mu^{-1}(\tilde{t}^{(1)}) > \phi\widetilde{m}_1, \ldots, \phi\widetilde{m}_{j-1}[\mu^{-1}(\tilde{t}^{(j)}) > \phi\widetilde{m}_j.$$

Proof. 1. We first show that for $i = 1, \ldots, j$ the set $\mu^{-1}(\tilde{t}^{(i)})$ is firable from $\phi\widetilde{m}_{i-1}$. Firability in the reduced net implies $\widetilde{m}_{i-1} \geq \widetilde{Pre}\, e_{\tilde{t}^{(i)}}$ where $e_{\tilde{t}^{(i)}} \in \mathbb{R}^q$ is the corresponding unit vector. We need to show that $\phi\widetilde{m}_{i-1} \geq Pre(\sum_{t \in \mu^{-1}(\tilde{t}^{(i)})} e_t)$.

Let now $p \in \mathcal{P}$. Then,

$$\left(Pre \left(\sum_{t \in \mu^{-1}(\tilde{t}^{(i)})} e_t \right) \right)_p = \sum_{t \in \mu^{-1}(\tilde{t}^{(i)})} Pre_{p,t} = \widetilde{Pre}_{\mu(p),\tilde{t}^{(i)}}$$
$$\leq (\widetilde{m}_{i-1})_{\mu(p)} = (\phi \widetilde{m}_{i-1})_p.$$

2. As a second step we show that the sequence of markings is correct. Let m' be such that $\phi\widetilde{m}_{i-1}[\mu^{-1}(\tilde{t}^{(i)}) > m'$. We show that $m' = \phi\widetilde{m}_i$.

   For the original system we have

$$m' = \phi\widetilde{m}_{i-1} + C \left(\sum_{t \in \mu^{-1}(\tilde{t}^{(i)})} e_t \right) = \phi\widetilde{m}_{i-1} + C\theta e_{\tilde{t}^{(i)}}$$

   and for the reduced system

$$\widetilde{m}_i = \widetilde{m}_{i-1} + \widetilde{C} e_{\tilde{t}^{(i)}} = \widetilde{m}_{i-1} + \phi^+ C\theta e_{\tilde{t}^{(i)}} \Rightarrow \phi\widetilde{m}_i = \phi\widetilde{m}_{i-1} + \phi\phi^+ C\theta e_{\tilde{t}^{(i)}}.$$

   The equality $m' = \phi\widetilde{m}_i$ holds if $C\theta e_{\tilde{t}^{(i)}} \in Fix(\Sigma)$ since $\phi\phi^+$ is the identity on this set. As $\theta e_{\tilde{t}^{(i)}}$ is a column of θ, it is invariant towards multiplication with T_σ. Therefore,

$$C\theta e_{\tilde{t}^{(i)}} = CT_\sigma \theta e_{\tilde{t}^{(i)}} = S_\sigma C\theta e_{\tilde{t}^{(i)}}$$

   for all $\sigma \in \Sigma$. Hence, $C\theta e_{\tilde{t}^{(i)}} \in Fix(\Sigma)$.

□

In this way the reduced net exhibits the "symmetric part" of the net behavior. Special attention should be paid though to the resolution of conflicts that result in increased arc weights as in those cases when firing rates have to be adapted in TCPNs. The difference is that the $\mathcal{T}$-rule (cf. Figure 4.1(a)) does not hold for discrete nets and changes of the arc weight change the enabling. Therefore, the overall behavior of the system may change significantly. Consider the Petri net and its reduction in Figure 4.8 as an example where the weight of an input arc is changed. For the initial marking $\begin{pmatrix} 2 & 0 & 0 \end{pmatrix}^T$ deadlock markings are reachable in the original nets if t_1 or t_2 fire twice in a row. The reduced net, on the other hand,

that represents only "symmetric" occurrence sequences, is deadlock free. Therefore, the reduction of discrete Petri nets should be performed primarily with respect to subgroups of Σ_{m_0} such that transitions in conflict relation are not equivalent. It remains an open question if under this condition performance measures of SPNs are preserved by the reduction.

5

Parameter-Dependent Systems

This chapter analyzes the effect of the variation of a firing rate on the system's behavior. By linearity, there occurs no qualitative change of the dynamics if all firing rates are increased by the same factor as stated in Section 2.4. However, if only some of the firing rates are increased, the throughput in steady state can be nonmonotonic and even discontinuous. We show that the same dynamic effect also appears if the throughput is monotonic in the firing rate. The jump in the throughput is explained in terms of *discontinuity-induced bifurcations* which are bifurcations that occur at points where the vector field is nonsmooth. For TCPNs this means that a steady state hits a boundary between regions M_K when the bifurcation occurs. After an introduction to these bifurcations in Section 5.2, four TCPNs are analyzed with respect to such bifurcations. They occur when an equilibrium becomes nonhyperbolic at a boundary. It is conjectured in Section 5.4 that configurations which are not injective are crucial for these discontinuity-induced bifurcations in TCPNs since the corresponding regions can contain equilibria only for particular ratios of firing rates. Thereby, we focus on bifurcations in the class of mono-T-semiflow nets.

5.1 Motivation

In Example 2.14, the throughput vector of a TCPN under variation of the firing rate of a transition is studied. The throughput of its transitions in steady state, which is an important performance indicator, drops abruptly for a specific firing rate. This is highly undesirable. If, for example, in a manufacturing system a machine is replaced by a faster one, the performance of the system should not worsen (cf. [JRS05, MRS09]). Furthermore, thinking of robustness, a system should not be operated at rates close to the critical rate as these are sensitive towards perturbations. For applications it is thus important to know when such an effect occurs.

The throughput vector of a TCPN depends continuously on the steady state marking since f is a continuous function. This implies that a discontinuity in the throughput can only occur if for a small change of the firing rate the equilibrium that the system converges to is not close to the original steady state marking. In fact, for the TCPN studied in the previously mentioned Example 2.14 we will observe that for a specific value of the firing rate λ_{t_1} the equilibrium of one region disappears while an equilibrium in another region emerges. In the TCPN literature, jumps in the throughput are usually considered with respect to monotonicity [JRS05, MRS09, SJMV11]. In [MRS09], sufficient conditions for monotonicity are proved. In this contribution, the focus is on the continuity of the throughput vector or, equivalently, of the steady state marking the system converges to (if it exists).

We explain abrupt changes of the throughput in terms of *discontinuity-induced bifurcations*. They arise from the perturbation of piecewise smooth ODE systems that have an equilibrium exactly on the border between different regions [Sim10, BCBK08]. A study of this phenomenon can advance our understanding of the dynamics of TCPNs. In [VS11], for example, similar criteria to those relevant for bifurcations are studied in order to obtain results on timing and liveness. Furthermore, discontinuity-induced bifurcations often appear together with uncontrollable poles (cf. [MRRS08]). A profound knowledge of bifurcations may therefore lead to advances in control problems for TCPN systems.

Examples furthermore suggest that close to bifurcation points TCPNs do not provide a good approximation of the mean marking or throughput of the corresponding SPN. Thus, if we understand the appearance of discontinuity-induced bifurcations, this

may also help to develop criteria to decide when it is reasonable to use TCPNs as approximations of SPNs. This is one of the central open questions concerning TCPNs though a solution to this problem is beyond the scope of this thesis.

An interesting property of the discontinuity-induced bifurcations studied in this chapter is that they involve three regions while the theory traditionally deals with bifurcations involving only two regions. Furthermore, they violate the genericity condition that border equilibria are always isolated and hyperbolic on boundaries (cf. [BCBK08, p. 220]). Instead, we study systems where the steady state loses hyperbolicity exactly when it hits the boundary as a firing rate is changed. In a generic piecewise linear system this requires the variation of two parameters (codimension two, cf. [BCBK08]) while the topology of a Petri net induces a special structure in the corresponding dynamical system such that the bifurcations occur also under the variation of a single parameter.

In this chapter, we study TCPN systems under variation of a single firing rate as a bifurcation parameter. For this reason we slightly redefine the vector field F (cf. Equation (2.11)) such that for a variation of the rate of $t \in \mathcal{T}$ we write

$$F : \mathbb{R}_{\geq 0}^{|\mathcal{P}|} \times \mathbb{R}_{>0} \to \mathbb{R}^{|\mathcal{P}|},\ F(m, \lambda_t) = C\Lambda_{\lambda_t}\Pi_K m \text{ for } m \in M_K$$

where Λ_{λ_t} denotes the usual matrix of firing rates where λ_t is the rate of t.

In general, matrices $A_K = C\Lambda_{\lambda_t}\Pi_K$ $(K \in \mathcal{K})$ are singular due to the conservation laws induced by $\mathcal{P}$-invariants. This makes the application of the traditional theory on stability of fixed points and discontinuous bifurcations difficult. The problem does not occur if an equivalent but reduced form of the TCPN system as in Section 4.2.2 is studied. The reduction preserves the spectrum except for zero eigenvalues. Therefore, all examples in this chapter are studied in the reduced form.

5.2 Bifurcations in Piecewise Smooth Continuous Systems

5.2.1 Piecewise Smooth Systems and Their Equilibria

In many systems of physical interest, the defining equations depend on some parameters. Bifurcation theory studies the qualitative change in the character of solutions

that may occur when one or more of these parameters are varied [GH83]. Bifurcations of smooth vector fields have been studied for decades in the area of nonlinear systems. Interesting new bifurcation phenomena may arise if the system is only piecewise smooth. There are various types of systems which are typically modeled by a piecewise smooth flow. Examples are often found in mechanical or electrical systems with saturation, backlash, or relays. The article [Kow05] mentions switched electronic circuits and vibro-impacting machines as examples. They can also be found in mathematical biology to model genetic regulatory systems [Jon02] and even in the social and financial sciences [BCBK08].

Discontinuity-induced bifurcations arise from the perturbation of piecewise smooth dynamical systems that have an equilibrium exactly on the border between regions with smooth dynamics [Sim10, BCBK08]. Formally speaking, "a bifurcation occurs if an arbitrarily small perturbation produces a topologically nonequivalent system. The bifurcation is discontinuity-induced if it affects the state portrait in more than one region, [or in a switching manifold]" [CBHJ11].

Discontinuity-induced bifurcations can either be analogues of smooth bifurcations, e.g., discontinuous saddle-node bifurcations where two equilibria coexist, collide, and disappear at the bifurcation, or they can be unique to piecewise-smooth systems, e.g., discontinuous Hopf-saddle-node bifurcations which show properties of both Hopf- and saddle-node bifurcations. In the literature, discontinuity-induced bifurcations also appear as C bifurcations, boundary equilibrium bifurcations, border-collision bifurcations, or discontinuous bifurcations (cf. [Sim10]). In this section, relevant definitions and concepts in the area of discontinuity-induced bifurcations are summarized. It follows to a great extent the work of [BCBK08] where also numerous academic and applied examples can be found. The focus is on phenomena that have been observed in the context of TCPNs. In particular, we concentrate on nonsmooth but continuous systems and hence exclude interesting phenomena like pseudoequilibria or sliding.

We consider piecewise smooth continuous systems of the form $\dot{x} = G(x, \lambda)$ where $G : \mathbb{R}^n \times \mathbb{R} \to \mathbb{R}^n$ is a piecewise smooth continuous vector field, i.e., G is continuous in both x and λ and for some index set I there exist open sets X_i and smooth functions[1]

[1] Functions G_i are defined on $\mathbb{R}^n \times \mathbb{R}$ for simplicity. In fact, it is sufficient to consider some open set that contains the closure of X_i.

$G_i : \mathbb{R}^n \times \mathbb{R} \to \mathbb{R}^n$ such that $G(x, \lambda) = G_i(x, \lambda)$ for all $x \in X_i$. The regions X_i are separated by an $(n-1)$-dimensional set S which is known as the switching boundary. It consists of finitely many smooth manifolds intersecting transversely. In the case of TCPNs, S is built up from hyperplanes. Its piecewise linear dynamics are in particular piecewise smooth.

We distinguish between different types of equilibria.

Definition 5.1. *Let $\lambda \in \mathbb{R}$. We call $x \in \mathbb{R}^n$ an* admissible equilibrium *of X_i if $x \in X_i$ and $G_i(x, \lambda) = 0$. A point x is a* virtual equilibrium *of X_i if $G_i(x, \lambda) = 0$ but $x \notin X_i$. It is a* boundary equilibrium *if $x \in S$ and $G(x, \lambda) = 0$.*

It is important to notice that virtual equilibria may govern the dynamics of a region even though they lie outside of it. We illustrate these terms with a simple example which is a special case of the closed-loop control systems with saturation in [APÁ00].

Example 5.2. We study the piecewise affine system

$$\dot{x} = x - \lambda \operatorname{sat}(x)$$

where $\lambda > 0$ and $\operatorname{sat} : \mathbb{R} \to \mathbb{R}$, $\operatorname{sat}(x) = \operatorname{sgn}(x) \cdot \min(|x|, 1)$ is the normalized saturation. The system can alternatively be written as

$$\dot{x} = \begin{cases} x + \lambda, & \text{if } x \leq -1 \\ (1 - \lambda)x, & \text{if } |x| \leq 1 \\ x - \lambda, & \text{if } x \geq 1. \end{cases}$$

We now vary the parameter λ.

- If $\lambda < 1$, the left and the right region contain a virtual equilibrium each while 0 is an admissible unstable equilibrium of the middle region.
- For $\lambda = 1$ the middle region is a dead zone, i.e., all its elements are admissible equilibria. The points -1 and 1 are border equilibria of the saturated regions.
- For $\lambda > 1$ each region contains an isolated admissible equilibrium of which only the central one is stable.

For $\lambda = 1$ the system undergoes a *nonsmooth pitchfork bifurcation*, which means

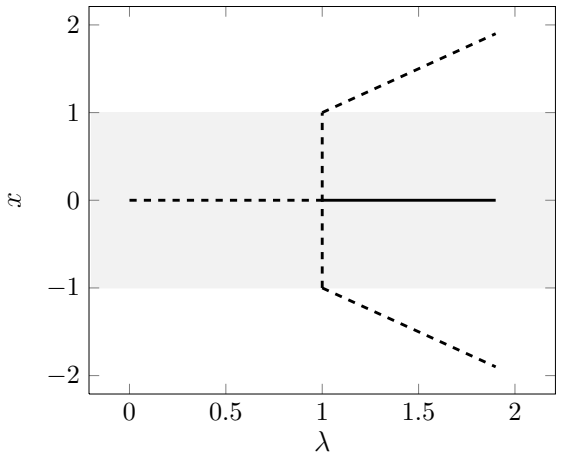

Figure 5.1: Bifurcation diagram of the system $\dot{x} = x - \lambda \operatorname{sat}(x)$.

that "an unstable invariant set is destroyed to create two invariant unstable sets separated by a stable set" [Gle02]. Figure 5.1 shows the bifurcation diagram. ♢

Let us see how to check for admissible equilibria of TCPNs. This can be done using the reduction of Section 4.2.2. It is straightforward if $\widetilde{A}_K$ is regular, i.e., the singularity of A_K is only due to $\mathcal{P}$-invariants. As the reduced system is equivalent to the original one, we look for an equilibrium marking in reduced space. Equation (4.5) then provides a system of linear inequalities to check if the result is contained in M_K. An equilibrium marking $\widetilde{m}^* \in \mathbb{R}^r$ of configuration K has to satisfy

$$\widetilde{A}_K \widetilde{m}^* + \widetilde{a}_K = 0 \Leftrightarrow \widetilde{m}^* = -\widetilde{A}_K^{-1} \widetilde{a}_K.$$

This reduced state is contained in $\widetilde{M_K}$ if and only if

$$\begin{bmatrix} -C_r \\ G_K C_r \end{bmatrix} \widetilde{m}^* + \begin{bmatrix} -m_0 \\ G_K m_0 \end{bmatrix} \leq 0.$$

With $\widetilde{a}_K = C_r^+ A_K m_0$ this is equivalent to

$$\begin{pmatrix} C_r \widetilde{A}_K^{-1} C_r^+ A_K m_0 - m_0 \\ -G_K C_r \widetilde{A}_K^{-1} C_r^+ A_K m_0 + G_K m_0 \end{pmatrix} \leq 0.$$

The following proposition summarizes this observation.

Proposition 5.3. *Let $\widetilde{A}_K$ be invertible. There exists $m \in M_K$ with $A_K m = 0$ and $m - m_0 \in \mathrm{im}(C)$ if and only if*

$$\begin{pmatrix} C_r \widetilde{A}_K^{-1} C_r^+ A_K - I_{|\mathcal{P}|} \\ G_K(I_{|\mathcal{P}|} - C_r \widetilde{A}_K^{-1} C_r^+ A_K) \end{pmatrix} m_0 \leq 0.$$

The marking is unique and given by $m = m_0 - C_r \widetilde{A}_K^{-1} \widetilde{a}_K$.

5.2.2 Boundary Equilibrium Bifurcations

Let us consider a generic discontinuity-induced bifurcation that occurs at a smooth point on a switching manifold upon variation of a single parameter of a piecewise smooth continuous system. Bifurcations at nonsmooth points of the switching manifold or at the intersection of switching manifolds are generic in systems with higher codimension only (cf. [Sim10, p. 8]). Locally, we can write the system as

$$\dot{x} = \begin{cases} G^{(L)}(x, \lambda) & \text{if } H(x, \lambda) \leq 0, \\ G^{(R)}(x, \lambda) & \text{if } H(x, \lambda) \geq 0, \end{cases} \tag{5.1}$$

where $G^{(L)}$, $G^{(R)} : \mathbb{R}^n \times \mathbb{R} \to \mathbb{R}^n$ and $H : \mathbb{R}^n \times \mathbb{R} \to \mathbb{R}$ are sufficiently smooth in all their arguments. H describes the switching boundary. By continuity $G^{(L)}(x, \lambda) = G^{(R)}(x, \lambda)$ whenever $H(x, \lambda) = 0$.

With this notation, x is an admissible equilibrium if either $G^{(L)}(x, \lambda) = 0$ and $H(x, \lambda) < 0$ or $G^{(R)}(x, \lambda) = 0$ and $H(x, \lambda) > 0$. Analogously, it is a virtual equilibrium if either $G^{(L)}(x, \lambda) = 0$ and $H(x, \lambda) > 0$ or $G^{(R)}(x, \lambda) = 0$ and $H(x, \lambda) < 0$. Finally, it is a boundary equilibrium if $G^{(L)}(x, \lambda) = G^{(R)}(x, \lambda) = 0$ and $H(x, \lambda) = 0$.

In [BCBK08, p. 220] boundary equilibrium bifurcations are defined:

Definition 5.4. *System* (5.1) *undergoes a* boundary equilibrium bifurcation *at $\lambda = \lambda^*$ if there exists $x^* \in \mathbb{R}^n$ such that*

(1) x^* is a boundary equilibrium for λ^*

(2) $G_x^{(L)}(x^*, \lambda^*)$ and $G_x^{(R)}(x^*, \lambda^*)$ are invertible, and

(3) $H_\lambda(x^*, \lambda^*) - H_x(x^*, \lambda^*) \left(G_x^{(i)}(x^*, \lambda^*)\right)^{-1} G_\lambda^{(i)}(x^*, \lambda^*) \neq 0$ for $i = L, R$.

With the second condition we require that this boundary equilibrium is isolated for both vector fields. This allows to apply the implicit function theorem, i.e., there exist neighborhoods U and V of λ^* and x^*, respectively, and unique functions $x^{(L)}, x^{(R)} : U \to V$ such that $x^{(L)}(\lambda^*) = x^{(R)}(\lambda^*) = x^*$ and $G^{(L)}(x^{(L)}(\lambda), \lambda) = G^{(R)}(x^{(R)}(\lambda), \lambda) = 0$ for all $\lambda \in U$. If this condition did not hold, an equilibrium would be nonhyperbolic when hitting the boundary which would be a codimension-two scenario (cf. [BCBK08, p. 222]). In the same book ([BCBK08, p. 449]), this is interpreted as a smooth and nonsmooth bifurcation occurring simultaneously, i.e., for the same value of the bifurcation parameter.

Condition (3) is a nondegeneracy condition with respect to λ. It ensures that curves of equilibria $x^{(L)}$ and $x^{(R)}$ cross through the bifurcation point at λ^*. A curve on the switching manifold along which an equilibrium lies would correspond to a codimension-two scenario (cf. [Sim10, p. 53]).

Generic boundary equilibrium bifurcations can be classified into two scenarios where the equilibrium can either persist or disappear in a fold-like scenario as it collides with the discontinuity boundary (cf. [BCBK08, p. 221], [BBC$^+$08, p. 640], [Sim10, p. 13]). The system exhibits a *persistence* (or border-crossing) for $\lambda = \lambda^*$ if a branch of admissible equilibria and a branch of virtual equilibria cross at the bifurcation point and exchange their properties. Examples of persistence are discontinuous Hopf bifurcations, where a single equilibrium persists but turns from a node into a focus with opposing stability encircled by a periodic orbit, and stability switching bifurcations, where an attracting node changes to a repelling node.

A boundary equilibrium bifurcation is associated with a *nonsmooth fold* if branches of admissible equilibria collide and annihilate at the bifurcation point.[2] This is observed, e.g., at discontinuous saddle-node bifurcations. Figure 5.2 illustrates the different scenarios. Conditions for their existence for systems in a canonical form can be found in [BCBK08, Sim10]. For the planar case a classification of possible discontinuity-induced bifurcations is given in [Sim10, pp. 46–49].

The definition of boundary equilibrium bifurcations by [BCBK08] as stated above does not involve any requirements on eigenvalues or stability. Hence, persistence also includes the case that a single hyperbolic equilibrium crosses the switching manifold

[2] This definition slightly differs from the definition of persistence and nonsmooth folds in discontinuous systems where they appear together with pseudoequilibria [DDCK11, CBHJ11].

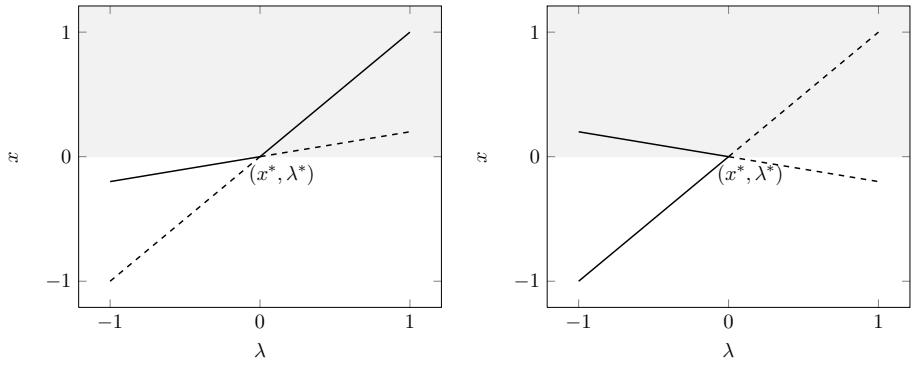

(a) Persistence (b) Nonsmooth fold

Figure 5.2: Boundary equilibria in nonsmooth continuous systems (modified from [BCBK08, p. 224]). Solid (dashed) lines represent admissible (virtual) equilibria. In each case the boundary between the two regions is at $x = 0$ and the bifurcation occurs at $(0, 0)$.

and neither of its associated eigenvalues cross the imaginary axis. The number of invariant sets remains constant and their stability does not change. So, strictly speaking, this is no bifurcation [Sim10, p. 46].

In the next section, four timed continuous Petri nets are studied with respect to the variation of one firing rate as a bifurcation parameter. In one of these examples, we observe border-crossing as defined above (cf. Section 5.3.2). However, since the respective admissible equilibria are stable on both sides, this is not a bifurcation in the sense of [Sim10]. Nonsmooth folds are not observed since the dynamics in each region is linear which excludes the chance of two equilibria existing on exactly one side of the switching hyperplane.

In the upcoming examples of TCPNs, we observe that jumps in the throughput vector are due to a special type of discontinuity-induced bifurcations where an admissible equilibrium loses hyperbolicity as it hits a boundary. This violates the nondegeneracy condition (2) and is not part of the standard literature on the topic. Furthermore, more than one switching manifold participates in the bifurcation.

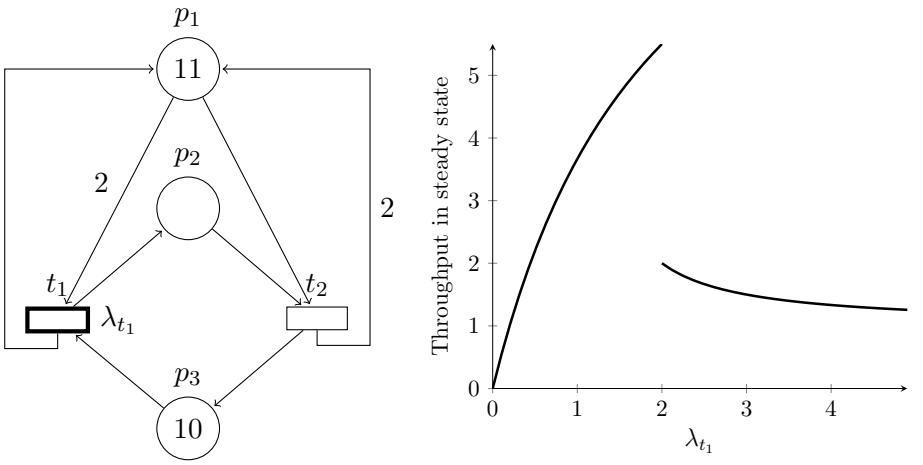

(a) The TCPN system

(b) The throughput of t_1 under variation of the firing rate λ_{t_1}

Figure 5.3: Example of a TCPN system whose throughput is not monotonic under variation of the firing rate λ_{t_1}.

5.3 Four Examples of Discontinuity-Induced Bifurcations in TCPNs

5.3.1 Example I

We reconsider the TCPN system in Figure 5.3(a) which has already appeared several times in this thesis. In Example 2.5, the corresponding PWL system is set up and Example 2.14 presents the nonmonotonicity of its throughput. In Section 4.2.2 an alternative formulation of the corresponding PWL system in reduced space has been obtained. This reduced formulation is also used here. In fact, all examples of the chapter are studied in the reduced formulation. This is done, on the one hand, in order to obtain systems of small dimension and, on the other hand, to remove zero eigenvalues that complicate the analysis. The analysis of the first three examples has already been published in [Mey12].

The partition of the one-dimensional phase space can be taken from Example 4.4 as it does not depend on the firing rates. The matrices A_K and $\widetilde{A}_K$ ($K \in \mathcal{K}_\mathcal{N}$)

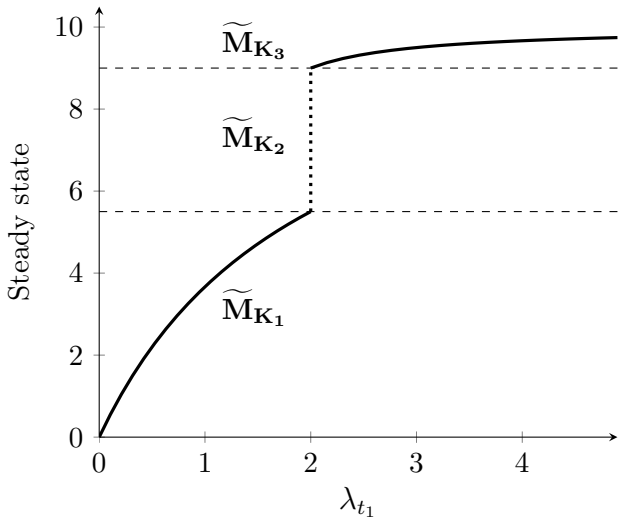

Figure 5.4: The steady states of the reduced system for different firing rates λ_{t_1}. The dotted line represents infinitely many unstable equilibria that coexist for $\lambda_{t_1} = 2$.

accordingly are computed with $\lambda = \begin{pmatrix} \lambda_{t_1} & 1 \end{pmatrix}^T$ leading to the dynamics

$$\dot{\widetilde{m}} = \begin{cases} -\left(1 + \frac{\lambda_{t_1}}{2}\right)\widetilde{m} + \frac{11}{2}\lambda_{t_1} & \text{if } \widetilde{m} \in \widetilde{M}_{K_1}, \\ \left(1 - \frac{\lambda_{t_1}}{2}\right)\widetilde{m} + \frac{11}{2}\lambda_{t_1} - 11 & \text{if } \widetilde{m} \in \widetilde{M}_{K_2}, \\ (1 - \lambda_{t_1})\widetilde{m} + 10\lambda_{t_1} - 11 & \text{if } \widetilde{m} \in \widetilde{M}_{K_3}. \end{cases}$$

The initial value is $\widetilde{m}(0) = 0$, which is in $\widetilde{M}_{K_1}$. From there, $\widetilde{m}$ increases monotonically in time. The region contains an admissible steady state if $0 \leq \frac{11\lambda_{t_1}}{\lambda_{t_1}+2} < \frac{11}{2}$, that is, for $\lambda_{t_1} < 2$. For $\lambda_{t_1} = 2$, this equilibrium becomes a boundary equilibrium and $\widetilde{M}_{K_2}$ is a dead region ($\dot{\widetilde{m}} = 0$). If the value is further increased, the boundary equilibrium becomes a virtual equilibrium. For $\lambda_{t_1} > 2$, the marking trajectory leaves region $\widetilde{M}_{K_1}$ towards $\widetilde{M}_{K_2}$ where $\widetilde{m}$ is monotonically increasing. This region does not contain a steady state and is thus left towards $\widetilde{M}_{K_3}$. $\widetilde{M}_{K_3}$ contains the admissible steady state $\frac{10\lambda_{t_1}-11}{\lambda_{t_1}-1}$ whenever $\lambda_{t_1} > 2$. It is reached as $\widetilde{m}$ increases monotonically in this interval.

As λ_{t_1} is being increased, the position of the steady state in region $\widetilde{M}_{K_1}$ moves

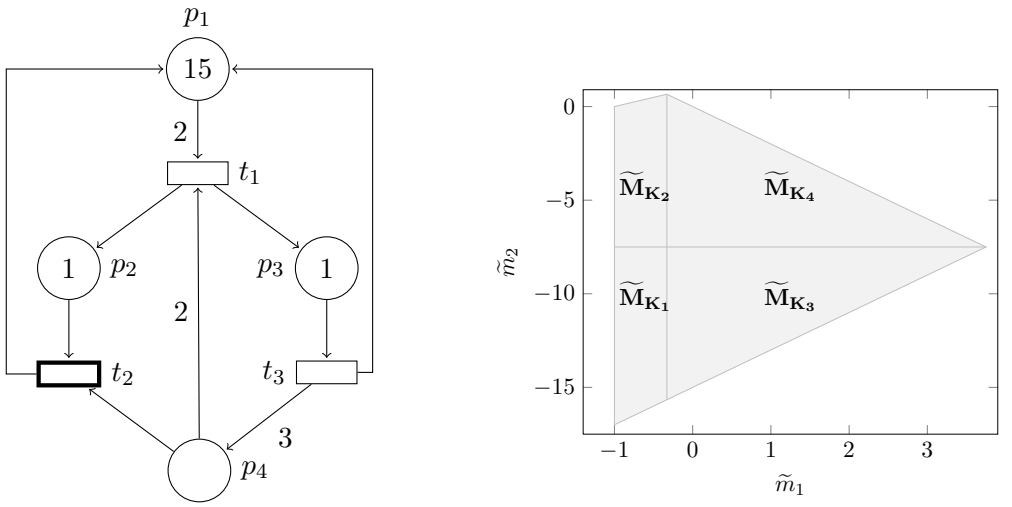

(a) The TCPN system with variable firing rate λ_{t_2}

(b) The partition of the phase space after the reduction

Figure 5.5: This TCPN system exhibits a discontinuity-induced bifurcation.

towards the neighboring region $\widetilde{M}_{K_2}$. The discontinuity-induced bifurcation occurs for $\lambda_{t_1} = 2$ when it hits the boundary between the regions. Figure 5.4 shows the corresponding bifurcation diagram.

The Petri net is of type mono-T-semiflow, i.e., a conservative and consistent net with a unique minimal $\mathcal{T}$-semiflow $x = \begin{pmatrix} 1 & 1 \end{pmatrix}^T$. The throughput vector depends continuously on the steady state and is given by

$$\begin{cases} \frac{11\lambda_{t_1}}{\lambda_{t_1}+2}x & \text{if } \lambda_{t_1} \in (0, 2], \\ \frac{\lambda_{t_1}}{\lambda_{t_1}-1}x & \text{if } \lambda_{t_1} > 2. \end{cases}$$

Its first component is shown in Figure 5.3(b).

5.3.2 Example II

This example is taken from [MRS09] where it illustrates nonmonotonicity of the throughput. The net is shown in Figure 5.5(a). We consider variations of the firing rate λ_{t_2}, i.e., the system is studied for $\lambda = \begin{pmatrix} 1 & \lambda_{t_2} & 1 \end{pmatrix}^T$.

There are four configurations given by the table

	t_1	t_2	t_3
K_1	p_1	p_2	p_3
K_2	p_4	p_2	p_3
K_3	p_1	p_4	p_3
K_4	p_4	p_4	p_3.

We reduce the system with respect to the initial marking $m_0 = \begin{pmatrix} 15 & 1 & 1 & 0 \end{pmatrix}^T$ using the matrix

$$C_r = \begin{pmatrix} -2 & 1 \\ 1 & -1 \\ 1 & 0 \\ -2 & -1 \end{pmatrix}.$$

The resulting system is in $\mathbb{R}^2$ with a partition into regions as shown in Figure 5.5(b). The dynamics of the reduced system is given by

$$\widetilde{A}_{K_1} = \begin{pmatrix} -2 & \frac{1}{2} \\ -1+\lambda_{t_2} & -\lambda_{t_2} \end{pmatrix}, \qquad \widetilde{a}_{K_1} = \begin{pmatrix} \frac{13}{2} \\ -1+\lambda_{t_2} \end{pmatrix},$$
$$\widetilde{A}_{K_2} = \begin{pmatrix} -2 & -\frac{1}{2} \\ -1+\lambda_{t_2} & -\lambda_{t_2} \end{pmatrix}, \qquad \widetilde{a}_{K_2} = \begin{pmatrix} -1 \\ -1+\lambda_{t_2} \end{pmatrix},$$
$$\widetilde{A}_{K_3} = \begin{pmatrix} -2 & \frac{1}{2} \\ -1-2\,\lambda_{t_2} & -\lambda_{t_2} \end{pmatrix}, \qquad \widetilde{a}_{K_3} = \begin{pmatrix} \frac{13}{2} \\ -1 \end{pmatrix},$$
$$\widetilde{A}_{K_4} = \begin{pmatrix} -2 & -\frac{1}{2} \\ -1-2\,\lambda_{t_2} & -\lambda_{t_2} \end{pmatrix}, \qquad \widetilde{a}_{K_4} = \begin{pmatrix} -1 \\ -1 \end{pmatrix}.$$

Possible fixed points are computed by solving the linear system of equations

$$\widetilde{A}_K \widetilde{m}^* = -\widetilde{a}_K \tag{5.2}$$

for every configuration.

- Configurations K_1 and K_3: $\widetilde{A}_{K_1}$ and $\widetilde{A}_{K_3}$ are regular for any value of λ_{t_2} leading to unique solutions of System (5.2). For $\lambda_{t_2} \in \left[0, \frac{2}{45}\right)$ the region $\widetilde{M}_{K_1}$ contains one admissible steady state and so does $\widetilde{M}_{K_3}$ for $\lambda_{t_2} \in \left(\frac{2}{45}, \frac{1}{2}\right)$.

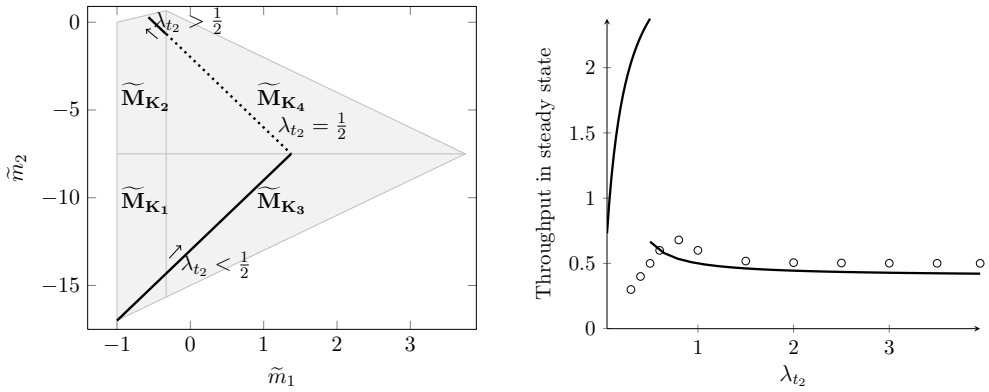

(a) The steady states of the reduced system for different firing rates λ_{t_2}.

(b) The throughput under variation of λ_{t_2}. The dots represent the throughput of the corresponding SPN.

Figure 5.6: A discontinuity-induced bifurcation and its effect on the throughput of the TCPN system in Example II.

- Configuration K_2: For $\lambda_{t_2} > \frac{1}{2}$, region $\widetilde{M}_{K_2}$ contains an admissible equilibrium. If $\lambda_{t_2} = \frac{1}{5}$, $\widetilde{A}_{K_2}$ is singular while $\operatorname{rank}(A_{K_2}) = r$. However, since there exists no $\widetilde{m}^*$ for this value of λ_{t_2} such that $\widetilde{A}_{K_2}\widetilde{m}^* + \widetilde{a}_{K_2} = 0$, the singularity results in no additional fixed points.
- Configuration K_4: For $\lambda_{t_2} \neq \frac{1}{2}$, the above linear system of equations has the single solution $\widetilde{m}^* = \begin{pmatrix} -1 & 2 \end{pmatrix}^T$ which is not contained in the phase space since $m_0 + C_r\widetilde{m}^*$ contains negative components. If $\lambda_{t_2} = \frac{1}{2}$, the system is underdetermined with solution set

$$\left\{ \begin{pmatrix} \frac{11}{8} - \frac{41}{24}a \\ -\frac{15}{2} + \frac{41}{6}a \end{pmatrix} : \; a \in [0,1] \right\}.$$

  This includes the border equilibrium $\begin{pmatrix} -\frac{1}{3} & -\frac{2}{3} \end{pmatrix}^T \in \widetilde{M}_{K_2} \cap \widetilde{M}_{K_4}$ and the border equilibrium $\begin{pmatrix} \frac{11}{8} & -\frac{15}{2} \end{pmatrix}^T \in \widetilde{M}_{K_3} \cap \widetilde{M}_{K_4}$. Both border equilibria are connected via the infinitely many equilibria in $\widetilde{M}_{K_4}$ that exist if $\lambda_{t_2} = \frac{1}{2}$ (see dotted line in Figure 5.6(a)).

This results in the following dynamic behavior of the original system. In all simulations that have been carried out for different values of λ_{t_2} the trajectory approaches

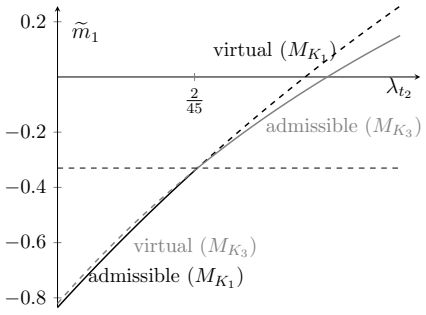

Figure 5.7: Persistence at the switching boundary $\widetilde{M}_{K_1} \cap \widetilde{M}_{K_3}$. The figure shows the first component of the equilibria in dependence on λ_{t_2}. For $\lambda_{t_2} = \frac{2}{45}$, there is a boundary equilibrium at which admissible and virtual equilibria exchange their roles.

a steady state m^* eventually. For $\lambda_{t_2} \in (0, \frac{2}{45}]$ convergence against a steady state $m^* \in M_{K_1}$ can be observed. For $\lambda_{t_2} \in [\frac{2}{45}, \frac{1}{2}]$ the steady state is in M_{K_3}. If $\lambda_{t_2} = \frac{2}{45}$, the steady state is on the boundary of both regions. Virtual and admissible equilibria of M_{K_1} and M_{K_3} meet at this value of λ_{t_2} and the branch of virtual equilibria becomes admissible and vice versa. This is an example of persistence (or border-crossing) in TCPNs and is illustrated in Figure 5.7. The steady state changes continuously with λ_{t_2}.

A different scenario is observed when $\lambda_{t_2} = \frac{1}{2}$. The steady state that was formerly in M_{K_3} hits the boundary $M_{K_3} \cap M_{K_4}$ and becomes nonhyperbolic. It jumps from the border $M_{K_3} \cap M_{K_4}$ to $M_{K_2} \cap M_{K_4}$. The throughput drops significantly.

The resulting throughput vector in steady state depends discontinuously on λ_{t_2} and is given by

$$\begin{cases} \frac{17\lambda_{t_2}}{1+3\lambda_{t_2}} x & \text{if } \lambda_{t_2} \leq \frac{2}{45}, \\ \frac{19\lambda_{t_2}}{1+6\lambda_{t_2}} x & \text{if } \lambda_{t_2} \in \left[\frac{2}{45}, \frac{1}{2}\right), \\ \frac{2\lambda_{t_2}}{-1+5\lambda_{t_2}} x & \text{if } \lambda_{t_2} \geq \frac{1}{2}. \end{cases}$$

where $x = \begin{pmatrix} 1 & 1 & 1 \end{pmatrix}^T$ is the minimal $\mathcal{T}$-semiflow of this mono-T-semiflow Petri net. The corresponding graph is shown in Figure 5.6(b) where in addition the throughput of the corresponding SPN is drawn. These values have been obtained

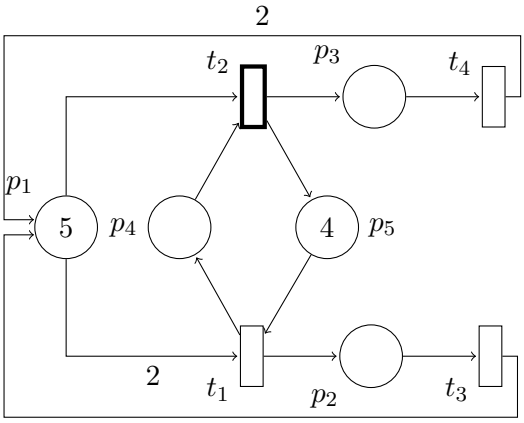

Figure 5.8: A TCPN system with an unsatisfactory approximation of the steady state of the underlying SPN.

with PIPE 2.5.[3] It can be seen that close to $\lambda_{t_2} = \frac{1}{2}$ the throughput of the SPN is not well approximated by the TCPN.

5.3.3 Example III

In the previous example, the approximation of the SPN's throughput is particularly inadequate close to the bifurcation point. Furthermore, it is pointed out in [LL11] that the approximation of SPNs by TCPNs is particularly unsatisfactory in regions where a place constrains the flow of more than one transition. In the previous two examples the jump in the throughput was evoked by the singularity of $\widetilde{A}_K$ in regions with exactly that property. This raises the question of how these two aspects are related and if the example studied in [LL11] has similar properties as the two previous ones.

The TCPN is depicted in Figure 5.8. For the initial marking $m_0 = \begin{pmatrix} 5 & 0 & 0 & 0 & 4 \end{pmatrix}^T$ the approximation of the mean marking of the corresponding SPN is reported to be particularly poor for $\lambda = \begin{pmatrix} 6 & 2 & 3 & \frac{1}{2} \end{pmatrix}^T$. We study the system under variation of λ_{t_2}, i.e., with $\lambda = \begin{pmatrix} 6 & \lambda_{t_2} & 3 & \frac{1}{2} \end{pmatrix}^T$.

[3] http://pipe2.sourceforge.net/

The net has four configurations

	t_1	t_2	t_3	t_4
K_1	p_1	p_1	p_2	p_3
K_2	p_1	p_4	p_2	p_3
K_3	p_5	p_1	p_2	p_3
K_4	p_5	p_4	p_2	p_3

of which K_4 cannot be active due to the conservation laws imposed by the $\mathcal{P}$-invariants. As $\operatorname{rank}(C) = 3$, the originally 5-dimensional system can be transformed to a 3-dimensional system. An appropriate matrix C_r is obtained from C by removing its last column.

As in the previous examples, we compute the steady states of all admissible regions.

- Configuration K_1: Matrix $\widetilde{A}_{K_1}$ is singular if $\lambda_{t_2} = \frac{1}{2}\lambda_{t_1}$ (here $\lambda_{t_2} = 3$). For this value there is a line segment

$$\left\{ \begin{pmatrix} 0 \\ \frac{15}{4} \\ -\frac{5}{8} \end{pmatrix} + \alpha \begin{pmatrix} 1 \\ -\frac{3}{4} \\ \frac{9}{8} \end{pmatrix} : \alpha \in \mathbb{R} \right\} \cap \widetilde{M}_{K_1}$$

  of steady states in the region. For $\lambda_{t_2} \neq 3$ the linear solution of $\widetilde{A}_{K_1}\widetilde{m} = -\widetilde{a}_{K_1}$ does not lie in the reduced phase space, i.e., the corresponding vector in original coordinates has negative entries.

- Configurations K_2 and K_3: Matrices $\widetilde{A}_{K_2}$ and $\widetilde{A}_{K_3}$ are regular for any positive choice of λ_{t_2}. There exists a unique steady state in $\widetilde{M}_{K_2}$ if $\lambda_{t_2} \geq 3$ and a unique steady state in $\widetilde{M}_{K_3}$ if $0 < \lambda_{t_2} \leq 3$. For $\lambda_{t_2} = 3$ these steady states are border equilibria as they are equilibria for both $\widetilde{M}_{K_1}$ and $\widetilde{M}_{K_2}$ or $\widetilde{M}_{K_3}$, respectively. They are connected via the steady states in region $\widetilde{M}_{K_1}$. In simulations we also observe that for firing rates just slightly smaller than 3, convergence is relatively slow.

The net is mono-T-semiflow with minimal $\mathcal{T}$-semiflow $x = \begin{pmatrix} 1 & 1 & 1 & 1 \end{pmatrix}^T$ and the

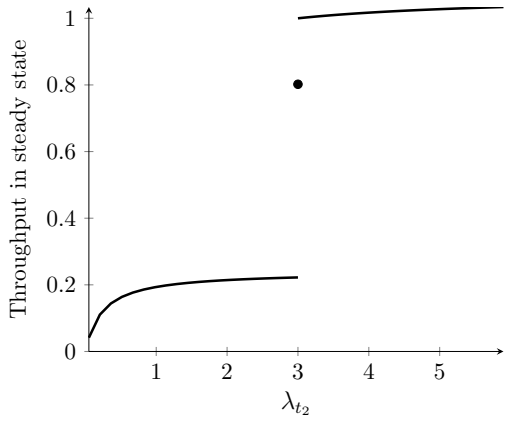

Figure 5.9: The throughput under variation of λ_{t_2}.

throughput for different values of λ_{t_2} is given by[4]

$$\begin{cases} \frac{6\lambda_{t_2}}{25\lambda_{t_2}+6}x & \text{if } \lambda_{t_2} < 3, \\ \frac{2175072511}{2711943423}x & \text{if } \lambda_{t_2} = 3, \\ \frac{15\lambda_{t_2}}{14\lambda_{t_2}+3}x & \text{if } \lambda_{t_2} > 3. \end{cases}$$

Figure 5.9 contains a plot of this function. We see (and can confirm by inspecting derivatives) that the throughput is monotonic though not continuous. Therefore, this phenomenon should not just be considered with respect to monotonicity as in [JRS05, MRS09] but also with respect to continuity.

A similar behavior is observed when considering the variation of λ_{t_1}, namely for $\lambda = \begin{pmatrix} \lambda_{t_1} & 2 & 3 & \frac{1}{2} \end{pmatrix}^T$. For $\lambda_{t_1} \leq 4$ the solution approaches an equilibrium in region $\widetilde{M}_{K_2}$. For $\lambda_{t_1} \geq 4$, region $\widetilde{M}_{K_3}$ contains a steady state. If $\lambda_{t_1} = 4$, then $\widetilde{A}_{K_1}$ is singular and region $\widetilde{M}_{K_1}$ contains infinitely many fixed points. If $\lambda_{t_1} = \frac{6}{29}$, then $\widetilde{A}_{K_3}$ is singular. However, this does not result in additional fixed points as for this value $\widetilde{A}_{K_3}\widetilde{m} + \widetilde{a}_{K_3} = 0$ has no solution.

[4]The value for $\lambda_{t_2} = 3$ has been obtained with Maple 15 using matrix exponentials.

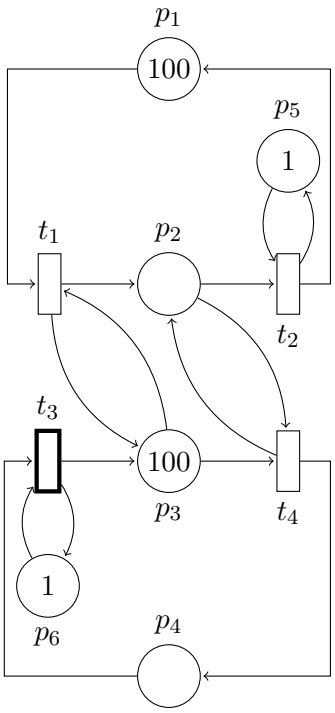

Figure 5.10: A net with periodic orbits for certain values of λ_{t_3}.

5.3.4 Example IV

We consider the TCPN system in Figure 5.10 which has been reported in [MRRS08] to exhibit oscillatory behavior for $\lambda = \begin{pmatrix} 1 & 12 & 10 & 1 \end{pmatrix}^T$. This net is not of type mono-T-semiflow and we can identify new discontinuity-induced bifurcation involving a center. We consider this system under the variation of λ_{t_3}. Bifurcations occur for λ_{t_3} equal to 1, 12, and 88.

The net has 16 configurations. These are defined in Table 5.1. Since $\text{rank}(C) = 2$, the system can be transformed to an equivalent two-dimensional system. When performing the reduction with respect to the initial marking $\begin{pmatrix} 100 & 0 & 100 & 0 & 1 & 1 \end{pmatrix}^T$, only 10 regions remain to be considered. Four configurations (K_9, K_{10}, K_{12}, K_{13}) cannot be active due to the conservation laws imposed by the $\mathcal{P}$-invariants and two regions, namely M_{K_4} and M_{K_5}, appear as a single point in the reduced phase space

Config.	t_1	t_2	t_3	t_4	Remarks
K_1	p_1	p_2	p_4	p_2	
K_2	p_3	p_2	p_4	p_2	
K_3	p_1	p_5	p_4	p_2	
K_4	p_3	p_5	p_4	p_2	$\widetilde{M}_{K_4} = (1\ 1)^T$
K_5	p_1	p_2	p_6	p_2	$\widetilde{M}_{K_5} = (1\ 1)^T$, $\widetilde{A}_{K_5}$ singular
K_6	p_3	p_2	p_6	p_2	
K_7	p_1	p_5	p_6	p_2	$\widetilde{A}_{K_7}$ singular
K_8	p_3	p_5	p_6	p_2	
K_9	p_1	p_2	p_4	p_3	$\widetilde{M}_{K_9} = \emptyset$
K_{10}	p_3	p_2	p_4	p_3	$\widetilde{M}_{K_{10}} = \emptyset$
K_{11}	p_1	p_5	p_4	p_3	
K_{12}	p_3	p_5	p_4	p_3	$\widetilde{M}_{K_{12}} = \emptyset$, $\widetilde{A}_{K_{12}}$ singular
K_{13}	p_1	p_2	p_6	p_3	$\widetilde{M}_{K_{13}} = \emptyset$
K_{14}	p_3	p_2	p_6	p_3	
K_{15}	p_1	p_5	p_6	p_3	
K_{16}	p_3	p_5	p_6	p_3	$\widetilde{A}_{K_{16}}$ singular

Table 5.1: Configurations of the Petri net of Example IV. In this example, singularity of a system matrix is always independent of the particular choice of λ_{t_3}.

and can therefore be neglected. For the choice

$$C_r = \begin{pmatrix} -1 & 0 \\ 1 & 0 \\ 0 & -1 \\ 0 & 1 \\ 0 & 0 \\ 0 & 0 \end{pmatrix}$$

the corresponding partition of the reduced phase space is shown in Figure 5.11.

The net exhibits discontinuity-induced bifurcations at three different values of λ_{t_3}. For $\lambda_{t_3} \in (0, 1]$ there is a stable node in region $\widetilde{M}_{K_6}$. At $\lambda_{t_3} = 1$ this equilibrium collides with the border $\widetilde{M}_{K_6} \cap \widetilde{M}_{K_8}$ where it remains asymptotically stable. Since the eigenvalues of $\widetilde{A}_{K_8}$ are $\pm i$, the node becomes a center for $\lambda_{t_3} > 1$ and is therefore non-hyperbolic. It remains stable but not asymptotically stable. When the bifurcation

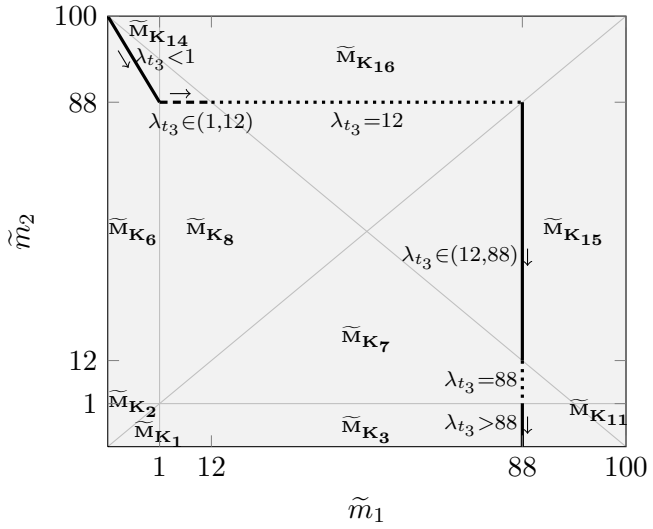

Figure 5.11: The bifurcation diagram for Example IV. Solid lines represent stable nodes, dotted lines represent line segments of nodes and the dashed line for $\lambda_{t_3} \in (1, 12)$ represents centers. In order to improve the readability the figure is not to scale.

value is further increased, the center moves towards the region $\widetilde{M}_{K_{16}}$ whose boundary is hit for $\lambda_{t_3} = 12$. Since $\widetilde{A}_{K_{16}}$ is singular, the equilibrium remains nonhyperbolic. As in previous examples, there exists a line segment of equilibria which connects to the region $\widetilde{M}_{K_{15}}$. This region contains an admissible node for $\lambda_{t_3} \in (12, 88)$.

Another bifurcation occurs at $\lambda_{t_3} = 88$. This time, the bifurcation resembles those observed in the Examples I-III. The matrix $\widetilde{A}_{K_7}$ is singular for any value of the firing rate λ_{t_3}. The stable node of K_{15} remains admissible till it hits the boundary of $\widetilde{M}_{K_7}$ at $\lambda_{t_3} = 88$. This region contains infinitely many equilibria connecting to region $\widetilde{M}_{K_3}$ which contains an admissible stable node for $\lambda_{t_3} > 88$. Figure 5.11 shows the bifurcation diagram.

5.4 The Role of Critical Regions

In the examples of the previous section, bifurcations occur at the boundary of regions where $\widetilde{A}_K$ becomes singular. In Examples I-III, these regions share the property, that

they belong to configurations where one place constrains the flow of more than one transition in unequal conflict relation. In [LL11], such regions are termed *critical*. In analogy we define critical configurations.

Definition 5.5. *A configuration $K \in \mathcal{K}_\mathcal{N}$ is* critical *if it is not injective.*

The following lemma states that only in critical regions $\operatorname{rank}(A_K) < r$.

Lemma 5.6. *If K is injective, then* $\operatorname{rank}(A_K) = r$.

Proof. Each row of Π_K contains a single nonzero entry. As K is not critical, these entries appear in different columns and $\operatorname{rank}(\Pi_K) = |\mathcal{T}|$. $\Lambda \in \mathbb{R}^{|\mathcal{T}|\times|\mathcal{T}|}$ is always invertible and $\operatorname{rank}(C) = r$.

By Sylvester's rank inequality,

$$r \geq \operatorname{rank}(A_K) = \operatorname{rank}(C\Lambda\Pi_K) \geq \operatorname{rank}(C\Lambda) + \operatorname{rank}(\Pi_K) - |\mathcal{T}| = r + |\mathcal{T}| - |\mathcal{T}| = r.$$

□

Note that $\widetilde{A}_K$ may be singular even if $\operatorname{rank}(A_K) = r$. This happens only if 0 is an eigenvalue of A_K with geometric multiplicity smaller than its algebraic multiplicity. This can be seen, for instance, for K_2 in Example II and K_7 in Example IV. The identification of necessary conditions for singularity of $\widetilde{A}_K$ is still a topic of research.

Now, let us consider the problem from a slightly different perspective. For a flow f^* to be a steady state flow, it has to satisfy $Cf^* = 0$. Furthermore, for a configuration K such a steady state flow can only appear if $f^* \in \operatorname{im}(\Lambda\Pi_K)$. Thus, for a steady state to exist in M_K, there has to exist $f^* \in \mathbb{R}^{|\mathcal{T}|}_{\geq 0} \cap \ker(C) \cap \operatorname{im}(\Lambda\Pi_K)$. If K is uncritical, then $\operatorname{im}(\Lambda\Pi_K) = \mathbb{R}^{|\mathcal{T}|}$ and $\ker(C) \cap \operatorname{im}(\Lambda\Pi_K) = \ker(C)$. If K is critical, then there are fewer possible steady state flows as $\operatorname{im}(\Lambda\Pi_K) \cap \ker(C) \subsetneq \ker(C)$. This effect can be observed in Example II.

Example 5.7. The Petri net in Example II has a $\mathcal{T}$-invariant $x = \begin{pmatrix} 1 & 1 & 1 \end{pmatrix}^T$ that spans $\ker(C)$. Meanwhile $\operatorname{im}(\Lambda\Pi_{K_4})$ is spanned by the columns of

$$\Lambda\Pi_{K_4} = \begin{pmatrix} 0 & 0 & 0 & \frac{1}{2}\lambda_{t_1} \\ 0 & 0 & 0 & \lambda_{t_2} \\ 0 & 0 & \lambda_{t_3} & 0 \end{pmatrix}.$$

A nontrivial intersection of the two sets exists only if $\lambda_{t_1} = 2\lambda_{t_2}$, i.e., exactly for the bifurcation value. ♢

For mono-T-semiflow nets, this observation can be refined. Let

$$v = \begin{pmatrix} v_{t_1} \\ \vdots \\ v_{t_{|\mathcal{T}|}} \end{pmatrix} > 0$$

be a $\mathcal{T}$-invariant. Such a vector always exists since mono-T-semiflow nets are consistent. If $m^* \in M_K$ is a live steady state, there exists $\chi > 0$ with $\Lambda\Pi_K m^* = \chi v$. By components, this yields

$$\lambda_t \frac{m^*_{K(t)}}{Pre_{K(t),t}} = \chi v_t \Leftrightarrow m^*_{K(t)} = \chi v_t \, \frac{Pre_{K(t),t}}{\lambda_t}$$

for all $t \in \mathcal{T}$. If K is critical, then there exist $t, t' \in \mathcal{T}$ with $t \neq t'$ and $K(t) = K(t')$. From $m^*_{K(t)} = m^*_{K(t')}$ it follows that

$$\chi v_t \, \frac{Pre_{K(t),t}}{\lambda_t} = \chi v_{t'} \, \frac{Pre_{K(t'),t'}}{\lambda_{t'}} \Leftrightarrow \frac{\lambda_{t'}}{\lambda_t} = \frac{v_{t'}}{v_t} \cdot \frac{Pre_{K(t'),t'}}{Pre_{K(t),t}}. \tag{5.3}$$

Only for this ratio of λ_t and $\lambda_{t'}$, which depends purely on the net structure, there exist equilibrium markings with nonzero throughput in M_K. This is exactly the ratio when the bifurcation occurs in the Examples I-III, in Example II both with respect to λ_{t_1} and λ_{t_2}.

We have shown that critical regions of mono-T-semiflow nets may contain equilibria only if the firing rates of the respective transitions in conflict relation are in a special ratio. We may use this ratio to compute candidate values for bifurcations. It remains a question of future research if this ratio always implies the occurrence of a discontinuity-induced bifurcation for this net class and if other bifurcation values can exist. The net in Example IV is not mono-T-semiflow and bifurcations occur even though t_3 is not in conflict relation.

6

Conclusion and Outlook

In this thesis, the dynamics of timed continuous Petri nets with infinite server semantics has been studied with respect to the relation with the underlying net structure. A special focus has been on the study of symmetries and bifurcations. This last chapter comments on the contributions of this work and discusses future research questions.

Altogether, this thesis makes four major contributions to the current research in the dynamics of timed continuous Petri nets with infinite server semantics:

1. The definition of symmetries in TCPNs and proof of an equivariance condition,
2. a reduction technique that results in a piecewise (affine) system of smaller dimension,
3. a reduction technique that transforms the TCPN into a smaller one with fewer nodes,
4. the identification of discontinuity-induced bifurcations in TCPNs and of special ratios of firing rates.

Symmetries in TCPNs have been defined as a natural extension to the notion of symmetry in place/transition nets. To the best of the author's knowledge, this is the first time that symmetries in TCPNs have been considered. It has been shown that these symmetries are reflected in the associated dynamical system in the way that the piecewise linear vector field is equivariant with respect to the group action of any subgroup of the initial markings isotropy subgroup. This allows to apply standard results from equivariant systems theory, e.g., it follows the existence of flow-invariant fixed-point sets. It has furthermore been proved that equivariant dynamics in piecewise linear systems always come along with a permutation of the underlying polyhedral partition and similar system matrices just as observed for TCPNs.

A comparison with the effect of symmetries in place/transition nets, where isotropy subgroups are not constant along paths in the reachability graph, has been made. However, algorithms developed for the computation of symmetries in discrete Petri nets can also be used in continuous nets.

Two reductions have been proposed for TCPNs with symmetries. The first one is an algebraic reduction resulting in a dynamical system of smaller dimension. Instead of being $|\mathcal{P}|$-dimensional the reduced dimension is given by the number of equivalence classes of places with respect to the isotropy subgroup of the initial marking. This reduction is then combined with a related reduction with respect to $\mathcal{P}$-invariants in the net. The original and reduced system are equivalent in the sense that the solution to one system can be obtained from the solution to the other system by a simple linear transformation.

Taking the idea of this reduction with respect to fixed-point sets a step further, it has been demonstrated how to reduce the Petri net itself rather than the associated dynamical system only. Every node of the reduced system represents one equivalence class of nodes of the original system. The marking of a place in the reduced net is the same as a marking of one of its counterparts in the original net. Unlike in the first reduction, this procedure is valid only under restrictions on the net structure, in particular, on the resolution of choices. For this reason the RSC property has been introduced. The correctness of the procedure has been proved by showing that the dynamical system of the original system after a reduction with the first method and the associated dynamical system of the smaller TCPN system are identical.

The advantage of the second reduction over the first one lies in the fact that the smaller net is easier to handle for a human modeler and that it allows to subsequently apply further reduction or transformation rules which are known for Petri nets.

The second reduction technique extends known techniques (e.g., [ADFN99]) in three ways. First, the reduction is performed by simple matrix multiplications and can therefore be performed automatically. An algorithm for the necessary computation of symmetries is known and implemented in some Petri net tools. Second, its restrictions on the net structure are a lot milder. In particular, there is no restriction to ordinary state machines for the equivalent subnets and an adaption of arc weights is possible. Third, the reduced net does not have to be a subnet of the original net as illustrated in the example of a manufacturing system in Section 4.3.6. In Section 4.3.10 it is discussed how this technique for continuous Petri nets might be applied to discrete nets. Since the $\mathcal{T}$-rule is not applicable in discrete nets, it is in general not allowed to increase the weight of input arcs to transitions. Therefore, for discrete nets, the restriction on conflicts have to be stricter.

In the literature on discrete Petri nets, symmetries are likely to be encountered in colored Petri nets (cf. [JK09]). These are high-level Petri nets which combine the capabilities of low-level Petri nets such as place/transition nets with the capabilities of a high-level programming language. Symmetries may appear in a natural way since components with identical dynamical behavior are modeled only once and the different entities are represented by colors [Jen96]. This is particularly true for the subclass of symmetric Petri nets, formerly known as stochastic well-formed nets [ŽS10], which can be understood as a colored extension of generalized stochastic Petri nets. Due to restrictions on the definition of color classes and functions, symmetries appear. [ŽS10] deals with the question how such nets can be fluidified. The MCPLC-example from Section 4.3 is actually a result of this approach. Theoretically, colored Petri nets can always be transformed into uncolored nets. As the idea behind fluidization is the approximation of largely populated nets, we do not want to separate the differently colored markings into different places. Instead, the marking of one place should be considered as a whole whenever this makes sense, even if different colors appear. Continuous counterparts of colored Petri nets are still a very young area of research. A future challenge is to incorporate the considerations on symmetries of this thesis into the transformation into continuous systems.

In Chapter 5, the dynamics of TCPNs depending on the firing rate of one transition has been studied. In four examples from the literature, discontinuity-induced bifurcations have been detected. In the case of Examples I and II, we can now explain the qualitative changes in the system's dynamics that lead to the jumps in the throughput that had been reported previously. The third example shows that not only monotonicity, which jumps in the throughput are traditionally associated with, but also continuity should be taken into account. The last example exhibits a bifurcation to a center.

The discontinuity-induced bifurcations observed are degenerate in the sense that, on the one hand, they need at least three regions to occur and, on the other hand, a fixed point loses hyperbolicity as it hits the boundary of a polyhedral region. For mono-T-semiflow nets it is shown that critical regions may contain a steady state only if the firing rates of the transitions in conflict relation have a special ratio.

To the best of the author's knowledge, discontinuity-induced bifurcations in TCPNs have never been studied before. So this area is still in its infancy and several open questions remain:

- Are jumps in the steady state or throughput always due to discontinuity-induced bifurcations of the type described in this thesis?
- Does the special ratio of firing rates of Equation (5.3) imply singularity of $\widetilde{A}_K$?
- Is it possible that for one choice of firing rates there are steady states in the interior of more than one region and what are necessary conditions for the existence of a single equilibrium?
- How can we predict bifurcations? In other words, what are necessary and sufficient conditions for the appearance of discontinuity-induced bifurcations in TCPNs?
- Do there exist more types of bifurcations in TCPNs (discontinuity-induced or not) than those observed in the examples presented in this thesis? Can new phenomena be observed if more than one firing rate is considered as a bifurcation parameter?
- How are the results of Chapter 5 related to the results on monotonicity in [MRS09]? We have seen in Example III that jumps in the throughput can

appear in monotonic system. Does nonmonotonicity imply discontinuity? To which extend do the sufficient conditions for monotonicity proved in [MRS09] prevent a TCPN from exhibiting discontinuity-induced bifurcations?

- How are the discontinuity-induced bifurcations related to the quality of the approximation of Markovian Petri nets by TCPNs?

This thesis contributes to the research on nonmonotonicities and discontinuities in timed continuous Petri nets under variation of a parameter by introducing the concept of bifurcations. Doing this, it provides a new angle of looking at this phenomenon and can therefore be a starting point for further research in the field.

Bibliography

[ABC+95] M. Ajmone Marsan, G. Balbo, G. Conte, S. Donatelli, and G. Franceschinis. *Modelling with Generalized Stochastic Petri Nets*. Wiley Series in Parallel Computing. John Wiley & Sons, London, 1995.

[Abe90] D. Abel. *Petri-Netze für Ingenieure - Modellbildung und Analyse diskret gesteuerter Systeme*. Springer, Berlin, 1990.

[ACB84] M. Ajmone Marsan, G. Conte, and G. Balbo. A class of generalized stochastic Petri nets for the performance evaluation of multiprocessor systems. *ACM Transactions on Computer Systems*, 2(2):93–122, 1984.

[ADFN99] M. Ajmone Marsan, S. Donatelli, G. Franceschinis, and F. Neri. Reductions in GSPN and SWN: an overview and an example of application. In *Network performance modeling and simulation*, pages 59–103. Gordon and Breach Science Publishers, Newark, 1999.

[AMP95] E. Asarin, O. Maler, and A. Pnueli. Reachability analysis of dynamical systems having piecewise-constant derivatives. *Theoretical Computer Science*, 138(1):35–65, 1995.

[APÁ00] J. Aracil, E. Ponce, and T. Álamo. A frequency-domain approach to bifurcations in control systems with saturation. *International Journal of Systems Science*, 31(10):1261–1271, 2000.

[Bal07] G. Balbo. Introduction to Generalized Stochastic Petri Nets. In *Formal Methods for Performance Evaluation*, LNCS 4486, pages 83–131. Springer, Berlin, 2007.

[BBC+08] M. di Bernardo, C. J. Budd, A. R. Champneys, P. Kowalczyk, A. B. Nordmark, G. Olivar, and P. T. Piiroinen. Bifurcations in nonsmooth dynamical systems. *SIAM Review*, 50(4):629–701, 2008.

[BCBK08] M. di Bernardo, A. R. Champneys, C. J. Budd, and P. Kowalczyk. *Piecewise-smooth Dynamical Systems, Theory and Applications*, volume 163 of *Applied Mathematical Sciences*. Springer, London, 2008.

[Ber86] G. Berthelot. Checking properties of nets using transformations. In *Advances in Petri Nets 1985*, LNCS 222, pages 19–40. Springer, Berlin, 1986.

[Ber87] G. Berthelot. Transformations and decompositions of nets. In *Petri Nets: Central Models and Their Properties*, LNCS 254, pages 359–376. Springer, Berlin, 1987.

[BG74] A. Ben-Israel and T. N. E. Greville. *Generalized Inverses: Theory and Applications*. John Wiley & Sons, New York, 1974.

[BK02] F. Bause and P. S. Kritzinger. *Stochastic Petri Nets – An Introduction to the Theory*. Vieweg, second edition, 2002.

[CBHJ11] A. Colombo, M. di Bernardo, S. J. Hogan, and M. R. Jeffrey. Bifurcations of piecewise smooth flows: Perspectives, methodologies and open problems. *Physica D: Nonlinear Phenomena*, In press, 2011.

[CCS91] J. Campos, G. Chiola, and M. Silva. Ergodicity and throughput bounds of Petri nets with unique consistent firing count vector. *IEEE Transactions on Software Engineering*, 17(2):117–125, 1991.

[CFPT04] V. Carmona, E. Freire, E. Ponce, and F. Torres. Invariant manifolds of periodic orbits for piecewise linear three-dimensional systems. *IMA Journal of Applied Mathematics*, 69(1):71–91, 2004.

[Chi98] G. Chiola. Timed Petri nets. In *Performance Models for Discrete Event Systems with Synchronisations: Formalism and Analysis Techniques*, pages 77–120. Editorial Kronos, 1998.

[Cli79] R. E. Cline. *Elements of the Theory of Generalized Inverses for Matrices*. Education Development Center, 1979.

[CM79] S. L. Campbell and D. D. Meyer. *Generalized Inverses of Linear Transformations*. Pitman, London, 1979.

[DA87] R. David and H. Alla. Continuous Petri nets. In *8th European Workshop on Applications and Theory of Petri Nets, Zaragoza, Spain*, 1987.

[DA93] R. David and H. Alla. Autonomous and timed continuous Petri nets. In *Advances in Petri Nets 1993*, LNCS 674, pages 71–90. Springer, 1993.

[DA05] R. David and H. Alla. *Discrete, Continuous, and Hybrid Petri Nets*. Springer, Berlin, 2005.

[DDCK11] F. Dercole, F. Della Rossa, A. Colombo, and Y. A. Kuznetsov. Two degenerate boundary equilibrium bifurcations in planar Filippov systems. *SIAM Journal on Applied Dynamical Systems*, 10(4):1525–1553, 2011.

[Des91] J. Desel. On abstractions of nets. In *Advances in Petri Nets 1991*, LNCS 524, pages 78–92. Springer, Berlin, 1991.

[DFGS08a] M. Dotoli, M. P. Fanti, A. Giua, and C. Seatzu. First-order hybrid Petri nets. An application to distributed manufacturing systems. *Nonlinear Analysis: Hybrid Systems*, 2(2):408–430, 2008.

[DFGS08b] M. Dotoli, M. P. Fanti, A. Giua, and C. Seatzu. Modelling systems by hybrid Petri nets: an application to supply chains. In *Petri Nets, Theory and Application*. InTech, 2008.

[DHP91] C. Dimitrovici, U. Hummert, and L. Petrucci. Semantics, composition and net properties of algebraic high-level nets. In *Advances in Petri Nets 1991*, LNCS 524, pages 93–117. Springer, Berlin, 1991.

[DJ01] J. Desel and G. Juhás. "What is a Petri net?" Informal answers for the informed reader. In *Unifying Petri Nets*, LNCS 2128, pages 1–25. Springer, Berlin, 2001.

[DM91] J. Desel and A. Merceron. Vicinity respecting net morphisms. In *Advances in Petri Nets 1990*, LNCS 483, pages 165–185. Springer, Berlin, 1991.

[EHP06] H. Ehrig, K. Hoffmann, and J. Padberg. Transformations of Petri nets. *Electronic Notes in Theoretical Computer Science*, 148(1):151–172, 2006.

[EJPR01] H. Ehrig, G. Juhás, J. Padberg, and G. Rozenberg, editors. *Unifying Petri Nets: Advances in Petri Nets*. Springer, Berlin, 2001.

[ES91] J. Esparza and M. Silva. On the analysis and synthesis of free choice systems. In *Advances in Petri Nets 1990*, LNCS 483, pages 243–286. Springer, Berlin, 1991.

[Fie96] M. Field. *Lectures on bifurcations, dynamics and symmetry*, volume 356 of *Pitman Research Notes in Mathematics*. Addison Wesley Longman, 1996.

[FR00] L. Farina and S. Rinaldi. *Positive linear systems: theory and applications*. John Wiley & Sons, New York, 2000.

[GG04] B. Gaujal and A. Giua. Optimal stationary behavior for a class of timed continuous Petri nets. *Automatica*, 40(9):1505–1516, 2004.

[GH83] J. Guckenheimer and P. Holmes. *Nonlinear Oscillations, Dynamical Systems, and Bifurcations of Vector Fields*. Springer, New York, 1983.

[Gle02] P. Glendinning. The non-smooth pitchfork bifurcation. *Discrete and Continuous Dynamical Systems – Series B*, 6(4):1–7, 2002.

[GLT80] H. Genrich, K. Lautenbach, and P. Thiagarajan. Elements of general net theory. In *Net Theory and Applications*, LNCS 84, pages 21–163. Springer, Berlin, 1980.

[GS03] M. Golubitsky and I. Stewart. *The Symmetry Perspective: From Equilibrium to Chaos in Phase Space and Physical Space*. Birkhäuser, Basel, 2003.

[GSS88] M. Golubitsky, I. Stewart, and D. G. Schaeffer. *Singularities and Groups in Bifurcation Theory*. Springer, New York, 1988.

[GST05] M. Golubitsky, I. Stewart, and A. Török. Patterns of synchrony in coupled cell networks with multiple arrows. *SIAM Journal on Applied Dynamical Systems*, 4(1):78–100, 2005.

[GTM08] T. Geyer, F. D. Torrisi, and M. Morari. Optimal complexity reduction of polyhedral piecewise affine systems. *Automatica*, 44(7):1728–1740, 2008.

[GV03] C. Girault and R. Valk, editors. *Petri Nets for Systems Engineering — A Guide to Modeling, Verification, and Applications.* Springer, Berlin, 2003.

[HD11] S. Hage-Packhäuser and M. Dellnitz. Stabilization via symmetry switching in hybrid dynamical systems. *Discrete and Continuous Dynamical Systems Series B*, 16(1):239–263, 2011.

[HJ99a] S. Hedlund and M. Johansson. PWLTool – A Matlab toolbox for analysis of piecewise linear systems. Technical report, TFRT7582. Department of Automatic Control, Lund Institute of Technology, Lund, Sweden, 1999.

[HJ99b] S. Hedlund and M. Johansson. A toolbox for computational analysis of piecewise linear systems. In *European Control Conference, Karlsruhe, Germany*, 1999.

[HJC05] H. J. Huang, L. Jiaob, and T. Y. Cheung. Property-preserving subnet reductions for designing manufacturing systems with shared resources. *Theoretical Computer Science*, 332(1–3):461–485, 2005.

[HJJJ85] P. Huber, A. M. Jensen, L. O. Jepsen, and K. Jensen. Towards reachability trees for high-level Petri nets. In *Advances in Petri Nets 1984*, LNCS 188, pages 215–233. Springer, Berlin, 1985.

[Hyd00] P. E. Hydon. *Symmetry methods for differential equations.* Cambridge Texts in Applied Mathematics. Cambridge University Press, 2000.

[IS00] J. Imura and A. van der Schaft. Characterization of well-posedness of piecewise-linear systems. *IEEE Transactions on Automatic Control*, 45(9):1600–1619, 2000.

[ISO04] ISO/IEC 15909-1:2004. *Software and system engineering – High-level Petri nets – Part 1: Concepts, definitions and graphical notation.* ISO, Geneva, Switzerland, 2004.

[JD93] M. D. Jeng and F. DiCesare. A review of synthesis techniques for Petri nets with applications to automated manufacturing systems. *IEEE Transactions on Systems, Man, and Cybernetics*, 23(1):301–312, 1993.

[Jen96] K. Jensen. Condensed state spaces for symmetrical coloured Petri nets. *Formal Methods in System Design*, 9(1-2):7–40, 1996.

[JJRS04] E. Jiménez, J. Júlvez, L. Recalde, and M. Silva. Relaxed continuous views of discrete event systems: considerations on Forrester diagrams and Petri nets. In *IEEE International Conference on Systems, Man and Cybernetics, The Hague, The Netherlands*, 2004.

[JJS05] E. Jiménez, J. Júlvez, and M. Silva. On controllability of timed contiuous Petri net systems: the join free case. In *44th IEEE Conference on Decision and Control, and the European Control Conference, Seville, Spain*, 2005.

[JK09] K. Jensen and L. M. Kristensen. *Coloured Petri Nets - Modelling and Validation of Concurrent Systems*. Springer, Berlin, 2009.

[JMV12] J. Júlvez, C. Mahulea, and C. R. Vázquez. SimHPN: A MATLAB toolbox for simulation, analysis and design with hybrid Petri nets. *Nonlinear Analysis: Hybrid Systems*, 6(2):806–817, 2012.

[Joh03] M. Johansson. *Piecewise linear control systems*, volume 284 of *Lecture Notes in Control and Information Sciences*. Springer, Berlin, 2003.

[Jon02] H. de Jong. Modeling and simulation of genetic regulatory systems: A literature review. *Journal of Computational Biology*, 9(1):67–103, 2002.

[JRS03] J. Júlvez, L. Recalde, and M. Silva. On reachability in autonomous continuous Petri net systems. In *Applications and Theory of Petri Nets 2003*, LNCS 2679, pages 221–240. Springer, Berlin, 2003.

[JRS05] J. Júlvez, L. Recalde, and M. Silva. Steady-state performance evaluation of continuous mono-T-semiflow Petri nets. *Automatica*, 41(4):605–616, 2005.

[JTMZ01] E. Y. T. Juan, J. J. P. Tsai, T. Murata, and Y. Zhou. Reduction methods for real-time systems using delay time Petri nets. *IEEE Transactions on Software Engineering*, 27(5):422–448, 2001.

[Jun03] T. Junttila. *On the Symmetry Reduction Method for Petri Nets and Similar Formalisms*. PhD thesis, Helsinki University of Technology, Laboratory for Theoretical Computer Science, Research Reports 80, 2003.

[KALD09] R. Kara, M. Ahmane, J. J. Loiseau, and S. Djennoune. Contstrained regulation of continuous Petri nets. *Nonlinear Analysis: Hybrid Systems*, 3(4):738–748, 2009.

[KD91] I. Koh and F. DiCesare. Modular transformation methods for generalized Petri nets and their application to automated manufacturing systems. *IEEE Transactions on Systems, Man, and Cybernetics*, 21(6):1512–1522, 1991.

[KMB+08] M. Kloetzer, C. Mahulea, C. Belta, L. Recalde, and M. Silva. Formal analysis of timed continuous Petri nets. In *47th IEEE Conference on Decision and Control, Cancun, Mexico*, 2008.

[Kow05] P. Kowalczyk. Robust chaos and border-collision bifurcations in non-invertible piecewise-linear maps. *Nonlinearity*, 18:485–504, 2005.

[Lef11] D. Lefebvre. About the stochastic and continuous Petri nets equivalence in the long run. *Nonlinear Analysis: Hybrid Systems*, 5(3):394–406, 2011.

[LFB87] H. Lee-Kwang, J. Favrel, and P. Baptiste. Generalized Petri net reduction method. *IEEE Transactions on Systems, Man, and Cybernetics*, 17(2):297–303, 1987.

[LL11] D. Lefebvre and E. Leclercq. Piecewise constant timed continuous PNs for the steady state estimation of stochastic PNs. *Discrete Event Dynamic Systems*, 22(2):179–196, 2011.

[MD09] A. Meyer and M. Dellnitz. Symmetries in timed continuous Petri nets. In *3rd IFAC Conference on Analysis and Design of Hybrid Systems, Zaragoza, Spain*, 2009.

[MDH11] A. Meyer, M. Dellnitz, and M. Hessel-von Molo. Symmetries in timed continuous Petri nets. *Nonlinear Analysis: Hybrid Systems*, 5(2):125–135, 2011.

[Mey12] A. Meyer. Discontinuity induced bifurcations in timed continuous Petri nets. Accepted for the 11th International Workshop on Discrete Event Systems, Guadalajara, Mexico, 2012.

[MF76] P. Merlin and D. Farber. Recoverability of communication protocols – implications of a theoretical study. *IEEE Transactions on Communications*, 24(9):1036–1043, 1976.

[Mit08] W. Mitkowski. Dynamical properties of Metzler systems. *Bulletin of the Polish Academy of Sciences*, 56:309–312, 2008.

[MMS94] J. Meseguer, U. Montanari, and V. Sassone. On the model of computation of place/transition Petri nets. In *Application and Theory of Petri Nets 1994*, LNCS 815, pages 16–38. Springer, Berlin, 1994.

[Mol82] M. K. Molloy. Performance analysis using stochastic Petri nets. *IEEE Transactions on Computers*, C-31(9):913–917, 1982.

[MP05] M.-H. Matcovschi and O. Pastravanu. Flow-invariant sets with respect to the markings of timed continuous Petri nets. In *44th IEEE Conference on Decision and Control, and the European Control Conference, Seville, Spain*, pages 7726–7731, 2005.

[MRRS08] C. Mahulea, A. Ramírez-Treviño, L. Recalde, and M. Silva. Steady-state control reference and token conservation laws in continuous Petri net systems. *IEEE Transactions on Automation Science and Engineering*, 5(2):307–320, 2008.

[MRS06] C. Mahulea, L. Recalde, and M. Silva. On performance monotonicity and basic servers semantics of continuous Petri nets. In *8th International Workshop on Discrete Event Systems, Ann Arbor, Michigan, USA*, 2006.

[MRS08] C. Mahulea, L. Recalde, and M. Silva. Observability of timed continuous Petri nets: A class of hybrid systems. In *17th IFAC World Congress, Seoul, Korea*, 2008.

[MRS09] C. Mahulea, L. Recalde, and M. Silva. Basic server semantics and performance monotonicity of continuous Petri nets. *Discrete Event Dynamic Systems*, 19(2):189–212, 2009.

[MS12] A. Meyer and M. Silva. Symmetry reductions in timed continuous Petri nets under infinite server semantics. In *4th IFAC Conference on Analysis and Design of Hybrid Systems, Eindhoven, The Netherlands*, 2012.

[Mur89] T. Murata. Petri nets: Properties, analysis and applications. *Proceedings of the IEEE*, 77(4):541–580, 1989.

[Pad09] J. Padberg. Skript Theoretische Informatik 1: Petrinetze. Hochschule für Angewandte Wissenschaften Hamburg, March 2009.

[PE01] J. Padberg and H. Ehrig. Parameterized net classes: A uniform approach to Petri net classes. In *Unifying Petri Nets*, LNCS 2128, pages 173–329. Springer, Berlin, 2001.

[Pet62] C. A. Petri. *Kommunikation mit Automaten*. PhD thesis, Technische Hochschule Darmstadt, 1962.

[Pra06] U. Prange. Algebraic high-level nets as weak adhesive HLR categories. *Electronic Communications of the EASST*, 2:1–13, 2006.

[RHS07] L. Recalde, S. Haddad, and M. Silva. Continuous Petri nets: Expressive power and decidability issues. In *Automated Technology for Verification and Analysis*, LNCS 4762, pages 362–377. Springer, Berlin, 2007.

[RHS10] L. Recalde, S. Haddad, and M Silva. Continuous Petri nets: Expressive power and decidability issues. *International Journal of Foundations of Computer Science*, 21(2):235–256, 2010.

[RJS02] L. Recalde, J. Júlvez, and M. Silva. Steady state performance evaluation for some continuous Petri nets. In *15th IFAC World Congress, Barcelona, Spain*, 2002.

[RMS06] L. Recalde, C. Mahulea, and M. Silva. Improving analysis and simulation of continuous Petri nets. In *IEEE International Conference on Automation Science and Engineering, Shanghai, China*, pages 7–12, 2006.

[RTS99] L. Recalde, E. Teruel, and M. Silva. Autonomous continuous P/T systems. In *Application and Theory of Petri Nets 1999*, LNCS 1639, pages 107–126. Springer, Berlin, 1999.

[SA92] C. Simone and M. Ajmone Marsan. The application of EB-equivalence rules to the structural reduction of GSPN models. *Journal of Parallel and Distributed Computing*, 15(3):296–302, 1992.

[SB96] R. H. Sloan and U. A. Buy. Reduction rules for time Petri nets. *Acta Informatica*, 33(7):687–706, 1996.

[Sch00a] K. Schmidt. How to calculate symmetries of Petri nets. *Acta Informatica*, 36(7):545–590, 2000.

[Sch00b] K. Schmidt. Integrating low level symmetries into reachability analysis. In *Tools and Algorithms for the Construction and Analysis of Systems*, LNCS 1785, pages 315–330. Springer, Berlin, 2000.

[Sch03] K. Schmidt. Using Petri net invariants in state space construction. In *Tools and Algorithms for the Construction and Analysis of Systems*, LNCS 2619, pages 473–488. Springer, Berlin, 2003.

[Sed88] R. Sedgewick. *Algorithms*. Addison-Wesley, Reading, Massachusetts, 1988.

[Sim10] D. J. W. Simpson. *Bifurcations in Piecewise-Smooth Continuous Systems*, volume 70 of *Nonlinear Science*. World Scientific, New Jersey, 2010.

[SJMV11] M. Silva, J. Júlvez, C. Mahulea, and C. R. Vázquez. On fluidization of discrete event models: observation and control of continuous Petri nets. *Discrete Event Dynamic Systems*, 21(4):427–497, 2011.

[SR02] M. Silva and L. Recalde. Petri nets and integrality relaxations: A view of continuous Petri net models. *IEEE Transactions on Systems, Man, and Cybernetics, Part C*, 32(4):314–327, 2002.

[SR04] M. Silva and L. Recalde. On fluidification of Petri nets: from discrete to hybrid and continuous models. *Annual Reviews in Control*, 28(2):253–266, 2004.

[SR05] M. Silva and L. Recalde. Continuization of timed Petri nets: From performance evaluation to observation and control. In *Applications and Theory of Petri Nets*, LNCS 3536, pages 26–47. Springer, Berlin, 2005.

[SR07] M. Silva and L. Recalde. Redes de Petri continuas: Expresividad, análisis y control de una clase de sistemas lineales conmutados. *Revista iberoamericana de automática e informática industrial*, 4(3):5–33, 2007.

[Sta90] P. H. Starke. *Analyse von Petri-Netz-Modellen.* Teubner, Stuttgart, 1990.

[Sta91] P. H. Starke. Reachability analysis of Petri nets using symmetries. *Systems Analysis Modelling Simulation*, 8(4–5):293–303, 1991.

[STC98] M. Silva, E. Teruel, and J. M. Colom. Linear algebraic and linear programming techniques for the analysis of place/transition net systems. In *Lectures on Petri Nets I: Basic Models*, LNCS 1491, pages 309–373. Springer, Berlin, 1998.

[Val94] A. Valmari. Compositional analysis with place-bordered subnets. In *Application and Theory of Petri Nets 1994*, LNCS 815, pages 531–547. Springer, Berlin, 1994.

[Val98] A. Valmari. The state explosion problem. In *Lectures on Petri Nets I: Basic Models*, LNCS 1491, pages 429–528. Springer, Berlin, 1998.

[VMM+08] C. R. Vázquez, A. M. Mangini, A. M. Mihalache, L. Recalde, and M. Silva. Timing and deadlock-freeness in continuous Petri nets. In *17th IFAC World Congress, Seoul, Korea*, 2008.

[VRS08] C. R. Vázquez, L. Recalde, and M. Silva. Stochastic continuous-state approximation of Markovian Petri net systems. In *47th IEEE Conference on Decision and Control, Cancun, Mexico*, pages 901–906, 2008.

[VS09] C. R. Vázquez and M. Silva. Hybrid approximations of Markovian Petri nets. In *3rd IFAC Conference on Analysis and Design of Hybrid Systems, Zaragoza, Spain*, 2009.

[VS11] C. R. Vázquez and M. Silva. Timing and liveness in continuous Petri nets. *Automatica*, 47(2):283–290, 2011.

[Wig90] S. Wiggins. *Introduction to Applied Nonlinear Dynamical Systems and Chaos.* Springer, New York, 1990.

[ŽS10] M. Žarnay and M. Silva. From coloured Petri nets to continuous P/T net models. Technical report, DISC: Distributed Supervisory Control of Large Plants, Zaragoza, 2010.

[ZZ94] R. Zurawski and M. Zhou. Petri nets and industrial applications: A tutorial. *IEEE Transactions on Industrial Electronics*, 41(6):567–583, 1994.